Journal of the OPTICAL SOCIETY *of* AMERICA

VOLUME 33
No. 2

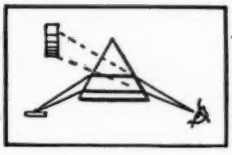

FEBRUARY
1943

Activating Light Sources for Luminescent Materials . . . . . E. W. BEGGS 61

Flux Calculations in Optical Systems . . . . . ARTHUR C. HARDY 71

Analysis of Errors in a Reflecting Prism . . . . . PAUL W. STEVENS 74

Absorption Tube for the Investigation of Gases at Low Pressures . . . . . PHILIP A. LEIGHTON AND DAVID H. VOLMAN 79

Solarization with X-Rays and Visible Light . . . . . ALBERT MAY 81

Analytical Representation of Standard Response Curves . . . . . PARRY MOON AND DOMINA EBERLE SPENCER 89

Mercury Arc Lamps: Effect of Electrode on Energy Distribution . . . . . WILLIAM THEODORE ANDERSON, JR. 104

Some Observations on the Use of Powders in Spectrochemical Analysis . . . . . A. E. RUEHLE AND E. K. JAYCOX 109

Light-and-Shadow Box as a Visual Aid in Measuring Spectra . . . . . JOHN J. HOPFIELD 113

New Methods of Calculating Illumination . . . . . PARRY MOON 115

Published monthly
at Prince and Lemon Sts., Lancaster, Pa.
by the
AMERICAN INSTITUTE OF PHYSICS
Incorporated
175 Fifth Avenue, New York, N. Y.
FOR AND UNDER THE EDITORIAL SUPERVISION OF THE
OPTICAL SOCIETY OF AMERICA

BOSTON UNIVERSITY
COLLEGE OF LIBERAL ARTS
LIBRARY

THE OPTICAL SOCIETY OF AMERICA

Officers of the Society

A. G. WORTHING, *President*
University of Pittsburgh
Pittsburgh, Pennsylvania

A. H. PFUND, *Vice President*
Johns Hopkins University
Baltimore, Maryland

ARTHUR C. HARDY, *Secretary*
Massachusetts Institute of Technology
Cambridge, Massachusetts

W. W. GRAEPER, *Treasurer*
Bausch & Lomb Optical Company
Rochester, New York

The Board of Directors consists of the above officers; the Editor of the Journal; the Past President; and five directors-at-large.

K. S. GIBSON, *Past President*
National Bureau of Standards
Washington, D. C.

GEORGE R. HARRISON, *Editor*
Massachusetts Institute of Technology
Cambridge, Massachusetts

Directors-at-Large

J. W. BEAMS
University of Virginia
Charlottesville, Virginia

D. B. JUDD
National Bureau of Standards
Washington, D. C.

RUDOLF KINGSLAKE
Eastman Kodak Company
Rochester, New York

D. L. MACADAM
Eastman Kodak Company
Rochester, New York

R. A. SAWYER
University of Michigan
Ann Arbor, Michigan

Rochester, New York, Section

J. H. WEBB, *President*
G. H. AKLIN, *Vice President*
A. F. TURNER, *Secretary*
F. H. PERRIN, *Treasurer*

Councillors:

F. E. ALTMAN
J. W. FORREST
F. M. E. HOLMES
V. L. PARKS
R. B. HORSFALL (*ex officio*)

Patrons

AMERICAN OPTICAL COMPANY BAUSCH & LOMB OPTICAL COMPANY
EASTMAN KODAK COMPANY

Corporation Members

AMERICAN CYSTOSCOPE MAKERS, INC., New York, New York
AMERICAN OPTICAL COMPANY, Southbridge, Massachusetts
BAUSCH & LOMB OPTICAL COMPANY, Rochester, New York
BELL & HOWELL COMPANY, Chicago, Illinois
BELL TELEPHONE LABORATORIES, INC., New York, New York
BENDIX AVIATION CORPORATION, New York, New York
CORNING GLASS WORKS, Corning, New York
E. I. DUPONT DE NEMOURS & COMPANY, INC., Chemical Department, Experimental Station, Wilmington, Delaware
EASTMAN KODAK COMPANY, Rochester, New York
FAIRCHILD AVIATION CORPORATION, Jamaica, New York
FISH-SCHURMAN CORPORATION, New York, New York
GAERTNER SCIENTIFIC CORPORATION, Chicago, Illinois
W. & L. E. GURLEY, Troy, New York
INTERCHEMICAL CORPORATION, New York, New York
KEUFFEL & ESSER COMPANY, Hoboken, New Jersey
NATIONAL CARBON COMPANY, Cleveland, Ohio
SIMPSON OPTICAL MANUFACTURING COMPANY, Chicago, Illinois
SPENCER LENS COMPANY, Buffalo, New York
ARTHUR H. THOMAS COMPANY, Philadelphia, Pennsylvania

THE OPTICAL SOCIETY OF AMERICA was organized in 1916 "*to increase and diffuse the knowledge of optics in all its branches, pure and applied, to promote the mutual interests of investigators of optical problems, of designers, manufacturers and users of optical instruments and apparatus of all kinds and to encourage cooperation among them.*" It aims to serve the interests of all who are engaged in any branch of optics from fundamental research to the manufacture of optical goods.

MEMBERSHIP

Regular Members: "Any person who has contributed materially to the advancement of optics is eligible for regular membership."

Associate Members: "Any person who is interested in optics is eligible for associate membership."

Corporate Members: "Any corporation desirous of encouraging the work of the Society is eligible for corporation membership."

Patrons: The payment, within any one year, of $1000 or more toward the expenses of the Society by any corporation or individual entitles such corporation or individual to the rank of patron.

The Society cordially invites to membership all who are interested in any branch of optics, either in research, in instruction, in optical or illuminating engineering, in the manufacture and distribution of optical goods of all kinds or in physiological and medical optics.

ANNUAL DUES

Regular members, $8.50; Associate members, $6.00; Corporate members, $50.00; Patrons, $1000.00. These dues include subscription to the Society's official journal, the *Journal of the Optical Society of America*.

CHANGES OF ADDRESS

All changes of address of members of the Optical Society of America should be communicated to the Secretary, Professor Arthur C. Hardy, Massachusetts Institute of Technology, Cambridge, Massachusetts.

Journal of the
OPTICAL SOCIETY
of AMERICA

VOLUME 33, NUMBER 2 FEBRUARY, 1943

Activating Light Sources for Luminescent Materials*

E. W. BEGGS
Westinghouse Electric & Manufacturing Company, Bloomfield, New Jersey

INTRODUCTION

WITH increasing general interest in fluorescence and phosphorescence and particularly with increased military applications, it seems desirable to present fundamental characteristics of the various types of activating light sources available. There being four general groups of light sources from which to choose, it is especially important to analyze the relative efficiency of the various types of lamps and to compare them one with another to determine their practicability and to establish the procedure to follow in determining which is the proper lamp to use for any particular application. Relative fluorescent and phosphorescent efficiencies were determined by the direct comparison method giving a quick approximate evaluation of the relative merits of each type of light source in actual use.

INCANDESCENT FILAMENT LAMPS

These are tungsten filament lamps with the filament operating in vacuum or inert gas enclosed in a relatively thin lime glass envelope. Regular types for general lighting and other services are often used. Special types designed for activation of luminescent materials are available.

Filament temperatures (color temperature scale) range from approximately 2500°K to the melting point of tungsten which is 3800°K. Ordinary incandescent lamp filaments for general lighting service operate at about 2800°K. At this temperature the average lamp life is 1000 hours. As the filament temperature is increased, the lamp life is shortened. The standard photoflood lamp filaments operate at approximately 3400°K and have an average life of 5 hours.

These incandescent filament lamps radiate a small but still appreciable amount of near ultraviolet energy. The amount of ultraviolet increases

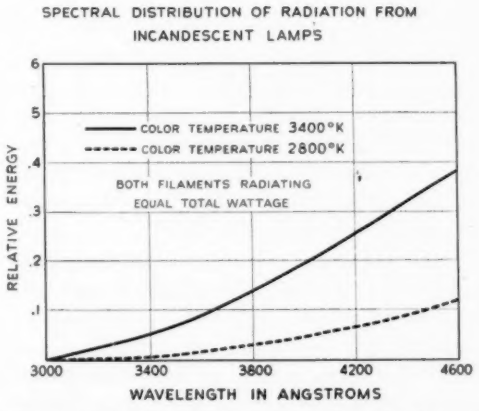

FIG. 1. Relative near ultraviolet (black light) energy radiated by incandescent lamp filaments of equal wattage operating at 2800°K and 3400°K. The higher temperature (photoflood filament) is about 5 times as effective as the lower which is that of standard 60-watt general lighting lamps.

* Paper presented at Symposium on Fluorescence and Phosphorescence of the Optical Society Meeting held at the Massachusetts Institute of Technology, Cambridge, Massachusetts, July 21, 1942.

BOSTON UNIVERSITY
COLLEGE OF LIBERAL ARTS
LIBRARY

FIG. 2. Relative fluorescence (pair 5) and phosphorescence (pair 6) of zinc sulfide under equal wattages with incandescent filaments at 3400°K (left) and 2800°K (right).

FIG. 3. Strontium sulfide is similar to zinc sulfide in its greater reaction to the higher filament temperatures.

FIG. 4. Fluorescent dyes show relatively higher reaction to 3400°K incandescent filament activation.

as the filament temperature increases. The relative amounts are shown in the diagram of radiant energy in Fig. 1. The filaments are compared on the basis of equal wattage. On this basis, the filament at a temperature of 3400°K radiates about 5 times as much energy between 3200 and 4200 angstroms as at 2800°K. Where ultraviolet output is more important than long lamp life, therefore, high filament temperatures should be used. Overvoltage operation of regular lamps, as operation of a 3-cell flashlight bulb on a 4-cell battery (lamp life will be less than 1 hour), or the use of photoflood or projection lamps at normal voltage provides this high and efficient filament temperature. The 250-watt Purple X lamp is of this type—see Table I.

Figure 2 shows a photographic record of fluorescence and phosphorescence of zinc sulfide under the two filament temperatures. The upper pair (5) shows relative fluorescence, the lower pair (6) relative phosphorescence. Figure 3 shows the same relationships for strontium sulfide. The upper pair (4) shows fluorescence and the lower pair (7) shows phosphorescence.

Figure 4 shows the relative reaction of typical fluorescent dyes under filament lamp activation. Pair 1 at the top is red, pair 2 is yellow and pair 3 is blue.

Both fluorescence and phosphorescence with representative available materials show that the higher filament temperature has a greater effect. The improvement is about in proportion to the relative amount of near ultraviolet energy available as shown in Fig. 1.

Photoflash lamps, while not generally considered in the same category with incandescent filament lamps, are nevertheless incandescent light sources and therefore fall under the same classification when incandescent activation is considered. Photoflash lamps are useful for charging phosphorescent materials.

Photoflash lamps operate with a mean temperature of approximately 3800°K. At this relatively high temperature the amount of near ultraviolet is relatively high when compared with that given off by incandescent tungsten filaments for general lighting. The spectral distribution of the energy radiated is almost identical to that shown in Fig. 1 for the 3400°K filament tem-

TABLE I.

Type	Purple X	Projection	Photoflood No. 1	Photoflood No. R-2
Watts	250	500	250	500
Bulb—				
Designation	A-21	T-20	A-21	R-40
Finish	Red Purple	Clear	I.F.	Reflector
Screw base	Med.	Med.	Med.	Med.
Rated av. life (hr.)	50*	50	3	6
Lumens	——	13,000	8650	†
Burning position	Any	Base Down	Any	Any

* Intermittent burning only.
† Approximately 6400 beam candlepower.

TABLE II.

Photo-flash number	Voltage range for operation	Maximum lumen-seconds	Approx. color temp. °K	Diam-eter bulb inches	Maximum over-all length inches	Base
5	3*	19,000	3800	1⅛	2⅛	SC Bay*
11	3*	32,000	3800	1⅛	4	Med. screw
16A	3*	45,000	3800	2⅛	4¼	Med. screw
21	3–125	60,000	3600	2⅛	5	Med. screw

* Flash with two or more dry cells only.

perature except, of course, the relative amount of ultraviolet will be higher.

A wide range of sizes and ratings of filament lamps is available making them useful for a wide range of applications. The smallest useful incandescent lamps are flashlight lamps. High powered projection lamps such as the 10-kw motion picture studio lamp are available where high power is needed.

Those lamps that appear to be most suitable for activation of fluorescent materials are given in Table I.

Phosphorescent materials are effectively "charged" by the lamps listed in Table I. In orinary practice, however, they will be activated by means of regular general lighting lamps which will produce less phosphorescent brilliance than the special higher efficiency types but will yet provide an effective afterglow as shown in the photographs in Figs. 2, 3 and 4.

Several sizes of photoflash lamps available are listed in Table II. Note, however, that photoflash lamps will be restricted during the war because of shortage of aluminum.

TABLE III.

Bulb	T-4½	S-14
Nominal watts	¼	2½
Rated volts	105–125 a.c.	105–125 a.c. or d.c.
Base	Cand. sc.	Med. sc.
Gas filling	Argon	Argon
Approx. starting volts		
a.c.	80	65
d.c.	**	90
Average hours useful life	1000	2000
Approx. ohms resist. in base	*15,000	*2500
Electrode shape	Hemisphere	Half round plates
Maximum over-all length	1½″	3 5/16″

* Additional resistance permits operation on higher line voltage.
** Not recommended for d.c. service.

TABLE IV.

Type	Outer bulb	Base	Rated av. life (hours)	Burning position
100-W A-H4	T-10 (772 Glass)	Admed. screw	1000	Any
100-W B-H4	T-16 Red purple (5040 Glass)	Admed. screw	1000	Any
100-W C-H4	PAR-38 (Spot.) (776 Glass)	Admed. sc. skt.	1000	Any
100-W E-H4	PAR-38 (Flood.) (776 Glass)	Admed. sc. skt.	1000	Any
100-W S-4 (Sun lamp)	A-21 (721 Glass)	Admed. screw	1000	Any
250-W A-H5	T-14 (774 Glass)	Mog. screw	1000	Any
900-W B-H6	*T-2 (Quartz)	Sleeve	75	Horizontal
1000-W A-H6	†T-2 (Quartz)	Sleeve	75	Horizontal
Sterilamp	½″ (974 Glass)	Special cap	4500	Any

* Requires air blast cooling.
† Requires water cooling. Pyrex (772) and quartz water jackets are available.

FIG. 5. Visible spectra of high, medium and low pressure mercury vapor arcs. The upper spectrum is that of the 1000-watt water-cooled quartz capillary lamp which operates at high pressure. The middle strip shows the medium pressure 400-watt A-H1 mercury vapor lamp and the bottom shows the low pressure Sterilamp. Note the widening of lines and bands as the pressure rises. This also occurs in the ultraviolet region.

ARGON GLOW LAMPS

At present, there are two important types of argon glow lamps available. These are the ¼-watt T-4½ bulb and 2½-watt S-14 bulb lamps. The essential technical data are listed in Table III.

In these lamps the radiant energy is generated in the negative glow which develops close to the surface of the electrode proper. The visible spectrum consists essentially of lines as also does the ultraviolet spectrum. The output of visible light is low and so these lamps are sometimes used without filters. The lines at the blue end of the spectrum dominate.

A small but appreciable portion of the total radiant energy emitted by these lamps lies in the near ultraviolet and is of value for activating luminescent materials. The most effective rays are those in the neighborhood of 3300 angstroms.

These lamps are of especial use where long lamp life and low total wattage are required. They are also self-starting. Their use is chiefly limited by their low power.

MERCURY VAPOR LAMPS

The most widely used light source for non-military activation of luminescent materials is the mercury vapor type of lamp. These vary in size and power and also somewhat in spectral distribution as well as in intrinsic brilliance of the source. They are particularly useful because of their high power, high efficiency and, in all but the 3-kw A-H9 and the Sterilamp, because of the small size and high intrinsic brightness of the radiating arc. The essential technical data on the most impor-

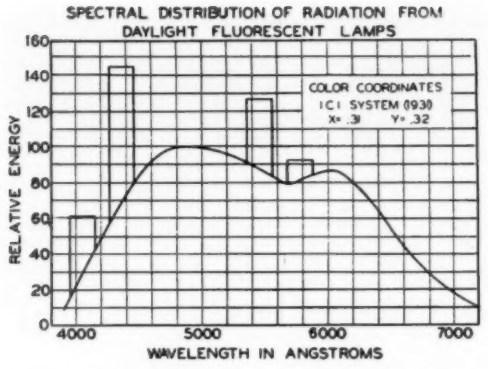

FIG. 6. The radiant energy of the standard daylight Mazda F lamp is mostly a continuous band with a small amount of mercury line spectrum. Rich in blue light these lamps are efficient activators of chief value with phosphorescent materials.

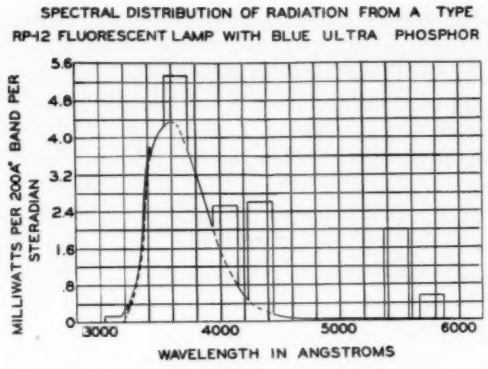

FIG. 7. The new "360 BL" phosphor radiates much energy in a band in the near-ultraviolet. The mercury vapor spectral lines shown as blocks in the diagram add to the efficiency of "black light" production.

tant types available for this application are given in Table IV. All of these have a quartz arc tube and operate at high pressure.

In the visible spectrum, the low pressure, medium pressure and high pressure lamps differ quite widely as is shown in Fig. 5. This is also true in the ultraviolet range.

A low pressure lamp such as the Sterilamp or the special Germicidal lamp operating at about 5 microns of mercury vapor pressure produces relatively little visible light, but about 50 percent of the radiant energy is in the 2537 resonance line of mercury. A very small amount of near ultraviolet, chiefly of 3650 angstroms, is also emitted. These lamps are designed to operate with the bulb at a relatively low temperature of approximately 100°F. Special glass is used in order to permit the 2537-angstrom energy to pass.

Medium pressure lamps such as the standard 400-watt type A-H1 and the 3-kw A-H9 operating at about 800-mm pressure, radiate a large amount of visible light primarily of the wave-lengths 4358, 5461 and 5770–90 (see middle spectrum Fig. 5). These lamps also radiate an appreciable amount of energy at 3650 angstroms and smaller amounts of 3341-, 3126- and 3025-angstrom wave-lengths of ultraviolet. The standard lamps, however, are equipped with arc tubes of Corning No. 172 glass that absorb practically all rays of wave-lengths shorter than 3650 so that they are not of great interest in connection with activation of fluorescent materials. They are, however, quite effective when used for general lighting and to activate phosphorescent substances.

TABLE V.

Watts	Bulb	Designation
3*	RP-12	360 BL
4†	RP-12	360 BL
6	9″—T-5	360 BL
15	18″—T-8	360 BL
30	36″—T-8	360 BL
40	48″—T-12	360 BL

* Designed for operation in series with tungsten filament ballast on 12–16-volt d.c. circuits.
† Designed for operation on 24–28-volt d.c. circuits with either tungsten filament or nichrome ballast.

High pressure mercury vapor lamps operate at from 10 to 100 atmospheres of mercury vapor pressure and are made with quartz inner bulbs. They are characterized by the existence of continuous as well as line type of visible spectrum (see the top spectrum of Fig. 5). The ultraviolet spectrum is similar in character.

The quartz inner bulb, of course, transmits most of the ultraviolet rays generated which makes this type of lamp especially valuable for activating luminescent materials. The type of outer bulb used determines the amount of energy in the various bands of the ultraviolet region that is transmitted and thereby available for use. Where bulbs of Corning Nos. 721, 772, 774, 776 and 5040 are used, the practical cut-off is at about 3000 angstroms although with No. 721 and 774 glass some energy is passed down through the 2967 line.

For experimental use it is sometimes found practicable to cut off the outer bulb and operate the quartz inner bulb in open air. This results in gradual oxidation of the sealed in lead wires, however, which generally causes an early failure due to cracked seals.

With the 1000-watt water-cooled type of lamp it is possible to increase the pressure of the mercury vapor during the operation of the arc to approximately 100 atmospheres. This develops a continuous visible spectrum plus the visible line spectrum consisting chiefly of the 4047, 4358, 5461 and 5770–90 lines. In the ultraviolet, the energy radiated by the quartz arc tube itself consists of spectral lines, chiefly 3650, 3341, 3126, 3022–26, 2967, 2925, 2894, 2804, 2652 and 2537 angstroms, plus spectral bands. The range of ultraviolet transmitted is determined by the type of outer jacket used.

The Pyrex water jacket is generally used with the 1000-watt water-cooled lamp. With it a strong band of radiant energy exists between 3000 and 4000 angstroms. The quartz outer jacket transmits the shorter wave-lengths of ultraviolet which are strong down to the 2537-angstrom line. An appreciable amount of energy is also radiated from 2500 down to about 2000 angstroms.

An almost identical lamp, known as the 900-watt type B-H6 lamp, is available for air-cooled operation using a powerful air blast impinging upon the quartz capillary arc tube instead of the stream of cooling water. This type of operation is of especial interest primarily where the short wave ultraviolet is required because, having no outer bulb at all, the ultraviolet emission from the quartz inner bulb is completely usable.

FLUORESCENT LAMPS

A new fluorescent phosphor has been developed which converts the 2537-angstrom ultraviolet energy generated in the low pressure mercury arc of the ordinary tubular Mazda F fluorescent type lamp to a band of radiant energy ranging from 3000 angstroms to 4200 angstroms with a slight amount of visible light (less than 10 percent as much as emitted by a comparable white lamp). Superimposed upon this band of radiant energy are the 3650, 3341 and 3126–32 near ultraviolet lines which are transmitted by the thin walled tubes of lime glass used to manufacture these lamps. Energy of shorter wave-lengths—that is, primarily the 2537 line—is not transmitted at all and the other lines of wave-lengths shorter than 3000 angstroms are likewise absorbed by the glass and are, consequently, not present in the radiations of the lamp. The diagrams above in Figs. 6 and 7 show the spectral distribution of energy emitted by fluorescent lamps with the

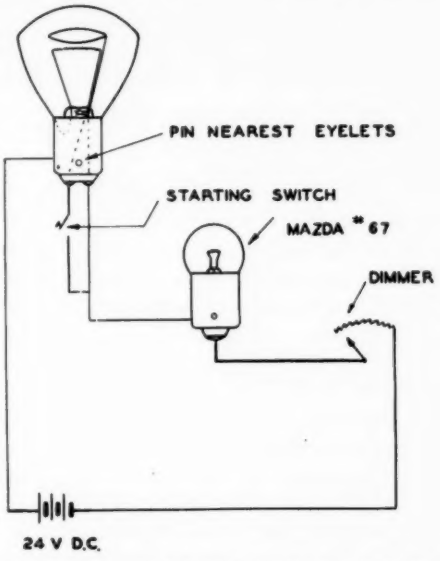

FIG. 8. The recommended circuit for the 4-watt 24–28 volt RP-12 bulb lamp for aircraft instrument lighting.

standard daylight phosphor and the new phosphor which is now known as 360 BL. By the use of this phosphor the desirable characteristics of the fluorescent lamp, which are primarily its high efficiency, coolness, quick starting and low local intensity, are made available for the activation of luminescent materials.

The 4-watt RP-12 bulb lamp now used by our air forces for illumination of airplane instrument dials is designed to operate on 24–28-volt d.c. circuits. This lamp utilizes the 360 BL phosphor. It is made possible by the fact that with impregnated "hot" cathodes a discharge through low pressure mercury vapor can be maintained at relatively low voltage.

Actually today the 4-watt RP-12 lamp is the most widely used of all activators for luminescent

FIG. 9. Phosphorescence developed by activation with equal wattages of (left to right) mercury vapor, 360 BL and daylight tubular fluorescent, 360 BL RP-12 fluorescent, sterilamp, argon glow and general lighting incandescent lamps. Upper series—zinc sulfide; lower series—strontium sulfide.

materials and for this reason it and its new companion lamp, the 3-watt 12–16 volt lamp, deserve special attention. The electrical circuit required for the operation of the 4-watt lamp is indicated in the diagram in Fig. 8.

The Mazda F fluorescent lamps now available with the 360 BL phosphor are given in Table V. Where phosphorescent materials are used they may be activated efficiently by standard white and daylight fluorescent lamps used for general lighting service.

RELATIVE EFFICIENCY OF ACTIVATORS

The intensity of the fluorescent or phosphorescent effect produced by a given wattage of power consumed in the light source is generally of chief interest when a decision must be made as to which type of activating lamp to apply. Efficiencies vary with the material and also with the filter used, if any, and with other conditions. These efficiencies can be computed from spectral energy and sensitivity data but a practical method is the simple comparison test which was used in this analysis.

Test compartments were built to contain each of seven different types of light sources which were compared for phosphorescent effects. Six different types of lamps were compared for fluorescent effects in conjunction with No. 5840 filter glass about 6 mm thick. These test lamps were mounted at a height above the test specimen in proportion to the square root of the total wattage of the lamp plus the wattage of its auxiliary—see Table VI.

The brightness of the test specimen in each compartment could be used to determine the practical over-all efficiency of the light source used. Where phosphorescent effectiveness was to be determined the brightness of the specimens was estimated by eye and was also recorded by photographic prints. The brightnesses were judged by several different observers and represent a practical estimate of relative effectiveness. The fluorescent brightness was measured by means of a photometer and was also recorded photographically.

The phosphorescent materials tested were zinc sulfide and strontium sulfide. These two materials represent the more common of the commercial phosphorescent pigments available and in general use. Table VII shows the visual estimates of brightness obtained with the various lamps tested.

Uniform illumination of the entire test panel was obtained in all cases but the 4-watt RP-12 and the 2½-watt argon glow lamp. These low output small lamps were mounted quite close and directly above the front half of the test panel so only that portion should be considered in the comparison. The luminescent material was irradiated for 30 minutes before the comparison was made. Each of several observers was partially dark adapted (5 minutes) before viewing the test panels.

The photographic reproduction of these initial phosphorescent brightnesses checks the visual

TABLE VI.

Compartment number	Type of lamp	Total wattage	Mounting height
(From left to right)			
1	Mercury vapor, A-H4	120	41.6″
2	6-watt fluorescent, 360 BL	8½	11.1″
3	6-watt fluorescent, daylight	8½	11.1″
4	4-watt fluorescent, 360 BL RP-12	8	10.7″
5	WL-782-10, Sterilamp	20	17″
*6	2½-watt argon glow	2½	6″
*7	60-watt filament, general lighting	60	29.4″

* The argon glow lamp and the filament lamp were installed in compartments No. 5 and No. 6 in later tests of fluorescence where the Sterilamp was omitted.

TABLE VII. Visual estimates of phosphorescent brightness, in percent.

	Activator						
Material	100-w A-H4 mercury vapor	6-w T-5 360 BL	6-w T-5 daylight	4-w RP-12 360 BL	WL-782 sterilamp	2½-w argon glow	60-w A-19 filament
Zinc sulfide							
Initial brightness	100	100	80	80	75	50	20
After 10-minutes decay	100	100	85	90	80	60	40
Strontium sulfide							
Initial brightness	100	100	90	90	70	60	30
After 10-minutes decay	100	100	95	90	85	70	60

fairly well as will be noted from the photographs shown in Fig. 9. A two-minute photographic exposure was used which gave an integrated value between that obtained immediately after the activation ceased—that is, "initial" values—and the "10-minute" visual estimates of Table VII. However, photographs can only show a limited range of brightness and there is always danger of over-exposure of bright areas when the timing is set to obtain a record of the dim ones.

Fluorescent materials were exposed to the light of each of the six types of light sources used with Corning No. 5840 filter glass of about 6-mm thickness used throughout. For certain applications other of the available filter materials would be preferable with some of these lamps. For example, unless a small amount of visible light is objectionable, Corning No. 5874 would ordinarily be used with mercury vapor lamps and filament lamps because of its high resistance to thermal breakage. Similarly No. 5860 would be required where very low levels of fluorescence are to be examined such as the fluorescence of fungus or other organic substances of low fluorescent brightness. The No. 5840 glass, however, is quite generally applicable where it can be used and so was chosen for the comparison work here reported. It is entirely practical of course with the new 360 BL lamps with which it is recommended.

TABLE VIII. Relative fluorescent brightness (percent footlamberts) measurements. Two samples of zinc sulfide.

Compartment number	Activator	Zinc sulfide sample No. 1*	Zinc sulfide sample No. 2†
1	100-w A-H4 mercury vapor	100	100
2	6-w T-5 360 BL	85	96
3	6-w T-5 daylight	2.95	4.05
4	4-w RP-12 (360 BL)	26	37
5	2½-w argon glow	6.73	7.85
6	60-w filament (2800°K)	1.4	1.47

* Luminescent coating on canvas roller screen (approximately one year old).
† Luminescent coating on metal as for airplane meter dials (new).

TABLE IX. Photometric brightness (footlamberts) measurements of fluorescence of organic dyes.

Material	Activator: 100-w A-H4 mercury vapor	6-w T-5 360 BL	6-w T-5 daylight	4-w RP-12 360 BL	2½-w argon glow	60-w A-19 filament
Red Rhodamine B Stearate (basic dye) Color index 749	0.215	0.26	0.005	0.13	0.02	0.0038
Yellow Fluorescent yellow AA (experimental semi-acid)	1.95	1.90	0.092	0.75	0.12	0.027
Blue Fluorescent violet G Ultramarine blue (acid dye) Color index 654	0.18	0.16	0.01	0.06	0.015	0.004

FIG. 10. Fluorescence of zinc sulfide activated by equal wattages of (left to right) mercury vapor, 360 BL and daylight tubular fluorescent, 360 BL RP-12 fluorescent, argon glow and general lighting incandescent lamps.

FIG. 11. Fluorescence of blue (top row), yellow (middle row) and red (bottom row) dyes activated by equal wattages of the six different types of lamps. Mercury vapor lamps and fluorescent lamps with 360 BL phosphor are about equally efficient.

The approximate fluorescent brightnesses were measured by means of a Macbeth photometer and the Taylor brightness meter as recorded in Tables VIII and IX. Photographs were taken using panchromatic film and a "noviol" filter over the camera lens to eliminate fogging of the film by reflected ultraviolet. The results are shown in Figs. 10 and 11.

The photographs in Fig. 11 check fairly well with the photometric measurements made except in the case of the yellow. With that color the overexposure of the high brightness destroys the contrast.

AUXILIARY EQUIPMENT

Incandescent Lamps

Where filament lamps are used for activation of phosphorescent materials no auxiliaries are required. In general, this activation will be obtained by exposure of the phosphorescent materials to the rays of light from the lamps used in the general lighting system of the room.

Where incandescent filaments are used for the activation of fluorescent materials, however, some means is required to eliminate most, if not all, of the visible light. Ordinarily, a reflector or housing will be required to prevent spilled visible

light and to concentrate as much as possible of the ultraviolet light on the fluorescent material to be activated. The only exception to this requirement is the 250-watt Purple X lamp which is made with its own filter bulb.

All other incandescent lamps require filter glass or other filter type of material. The type and thickness of glass to be used depend upon the application. Thicker and denser filters reduce the amount of visible light and thereby improve the contrast between the fluorescent appearance and its appearance in visible light. In order to obtain high contrast, however, some sacrifice is made in the brightness of the fluorescence.

Because of the large amount of infra-red radiations emitted by incandescent light sources it is imperative that precautions be taken to prevent cracking of the filter glass. Except where the power of the light source is low such as with flashlight lamps, it is generally required that heat resisting glass such as Corning 5874 be used. Even with this glass, however, care should be taken to avoid overheating with the resultant breakage of the filter plate.

Argon Glow Lamps

Argon glow lamps require no auxiliaries although when they are used with fluorescent materials best results are generally obtained if filters are used to eliminate visible rays. The most effective power of the argon glow lamp lies in the neighborhood of 3300 angstroms. With such lamps, therefore, glasses such as Corning No. 5840 are recommended. There is no need in the case of the argon glow lamp of the heat resisting glass.

Mercury Vapor Lamps

Mercury vapor lamps require electrical as well as optical auxiliaries. Special transformers are needed to initiate the arc and control the flow of current to the proper value. For fluorescence, filter plates or similar materials are generally needed to eliminate visible light.

Each one of the different sizes of mercury vapor lamps requires a transformer designed for it. All lamps designated as type H-4 will operate from the H-4 transformer, all various types of lamps designated as H-5 operate from H-5 transformers, etc. Practically all of these transformers are available for standard 110–120-volt, 60-cycle, a.c. lighting circuits.

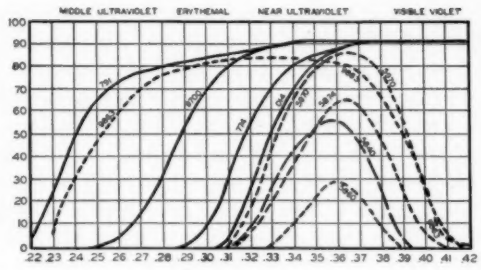

FIG. 12. Transmission data on Corning ultraviolet filter glasses.

Most commercial luminescent materials are activated efficiently and effectively by near-ultraviolet at or near 3650 angstroms. Mercury vapor lamps are highly efficient in the production of 3650-angstrom energy, and where the proper glass is used the light rays are rich in ultraviolet light of this wave-length. Therefore, the filter plates that should be used are those which have a high transmission at the 3650 line such as Corning No. 5874, No. 5840 and No. 5860—see Fig. 12.

The filter plates are apt to crack due to thermal strain where mercury vapor lamps are used and particularly where the projector type such as the C-H4 and E-H4 lamps are applied. In such cases, heat resisting glass such as Corning No. 5874 is recommended and even with that glass care should be taken to avoid overheating.

Fluorescent Lamps

Each fluorescent type lamp requires a starting device to preheat the electrodes before the arc strikes and a ballast to control the flow of current through the arc. Normally the starter is an automatic device containing a glow switch and the ballast is a wire wound iron core choke, as is regularly used with Mazda F lamps for general lighting service.

In some cases, however, as in airplane cockpit lights, it is preferable to use a manual starting switch. Also, for d.c. operation of the larger sized lamps a thermal switch starter is recommended.

Similarly it is occasionally desirable to use

resistance ballast instead of the copper-iron inductive ballast. This may be tungsten filament provided in special resistance ballast lamps made for the purpose or in some cases it consists of a regular tungsten filament lamp. Tungsten is especially desirable because of its peculiar steep temperature-resistance curve. This provides the relatively high preheat current required for the electrode, it holds the operating current down to the proper value and maintains a steady arc condition over a wide range of circuit voltage. Nichrome resistors are nevertheless frequently used and are particularly valuable where dimming is required. Nichrome may be used exclusively or to provide extra dimming resistance in combination with tungsten ballast lamps.

Filter glass is not subject to thermal breakage where the fluorescent lamp is used. Corning No. 5840 is generally recommended. Due to the cool operation of the lamps other filter material such as lacquer and gelatine is applicable, but so far the dyes available tend to fade seriously as they age in use.

The various sizes of lamps require different values of circuit voltages for proper operation. Where the lamp required for the application requires voltages other than normally available an additional electrical element such as a transformer or converter may be required.

CHOICE OF ACTIVATING LAMP

In order to determine which of the several different types of activators to use, the primary consideration is efficiency. Other factors, such as convenience, speed of operation, power requirements, shock resistance, etc., may nevertheless be still more important particularly in military applications.

Filament Lamps

Filament lamps are used primarily where the lamp must operate direct from the power line without auxiliaries. They are especially appropriate for use where the lamp must come to full brilliance instantly, for charging phosphorescent materials when the total amount of ultraviolet rays required is relatively small and where the large amount of heat present and the high wattages required are not objectionable.

For intermittent use to activate fluorescent materials, the 250-watt Purple X lamp is quite good. It is convenient, being operable direct from ordinary 120-volt range lighting circuits of either direct or alternating current. If power is available no accessories need be carried except perhaps a cord and socket and, if necessary, the lamp may be inserted in any ordinary lamp socket.

The Purple X lamp is not applicable to general fluorescent uses because when burned continuously for more than 10 minutes, the bulb is likely to overheat and soften. Also, the total output of black light is limited and being of the filament type with strong radiations at the red end of the spectrum, it is rather difficult to eliminate entirely the visible red light.

Other filament lamps, however, are entirely practical for general use within their range of power and efficiency if proper provisions are made for filtering, cooling, etc.

Where only a portable hand flashlight is practical, those with suitable filter lenses may be used. They provide the maximum of convenience but the low output is only of use for close work in absolute darkness and for short periods where battery drain will not be too severe.

Argon Glow Lamps

These lamps are small in size and if a small amount of visible light is acceptable, they may be used with no auxiliaries at all. Where visible light must be eliminated, the only auxiliaries required consist of a deep red purple filter such as Corning No. 5840 installed across the mouth of a simple metal reflector around the lamp.

Argon glow lamps are limited because of their low output. They light up automatically with no delay, the life is very long and the current drain is small. They are recommended for remote applications where ordinary 110-volt a.c. lighting service is available.

Mercury Vapor Lamps

Where high power is needed and particularly where the light source must also be small in physical size, as in projectors to project the energy to a distant point the mercury vapor lamp with the quartz inner bulb is recommended.

Mercury vapor lamps require alternating

current and each lamp must have an individual transformer in order to provide the proper starting and operating volts and amperes.

Mercury vapor lamps are especially suitable for general lighting where charging of phosphorescent tape, etc., is involved.

The water cooled A-H6, the air blast cooled B-H6 and the Sterilamp start and restart instantly. Other mercury vapor lamps require a few minutes warmup time to bring the light output up to normal and if the lamp is turned off, they must cool for a few minutes before they will restart. Also, a momentary drop in voltage exceeding 10 percent may cause these lamps to go out.

They are indicated where short ray ultraviolet is needed and where it is desired to minimize the size of filter glass required.

Fluorescent Lamps

The standard general lighting fluorescent lamps with the daylight or white phosphor are very efficient and effective activators when used with phosphorescent materials. These lamps in regular standard equipment for general lighting service will be found effective and extremely practical in rooms or corridors, etc., where phosphorescent tape, signs or other materials are used.

For fluorescent materials, fluorescent types of lamps with the 360 BL phosphor are highly efficient and are strongly recommended. In small sizes these are available for operation on a.c. or d.c. as low as 12 volts. The 3-watt RP-12 may be operated on 12–16 volt d.c. circuits. The 4-watt RP-12 will operate down to 24 volts d.c. These lamps may be dimmed to about one-tenth of normal output by introduction of resistance to the circuit.

The 6-watt tubular type lamp is suitable for operation with regular auxiliaries on regular 110-volt 60-cycle a.c. circuits. With special equipment it is also operable on other circuits of higher or lower voltage and on d.c. Larger sizes of fluorescent types with 360 BL phosphor are designed for operation on 110-volt a.c. circuits. With fairly simple auxiliaries they are also applicable to 110-volts d.c. and higher voltages of a.c. or d.c.

These fluorescent type lamps are recommended where medium or low local intensities of cool, diffuse near-ultraviolet energy are required. They are especially recommended for direct substitution for regular fluorescent general lighting lamps in regular fluorescent equipment such as in show windows. Because of their long tubular shape, they are suited for use in strip lighting of extended areas such as meter power plant panels, maps, charts and wall areas. In RLM type reflectors they are recommended where a flood of black light is needed.

They start and restart in a few seconds and should be applied where that characteristic is needed, for example, in military instrument lighting.

Because of the extended size of these lamps, a considerable area of filter material is required. This is somewhat of a handicap but where the small amount of visible light radiated will not be harmful and no filters are needed these lamps are especially suitable. Also, since these lamps are cool, suitable gelatine or similar filtering material may be developed.

Flux Calculations in Optical Systems[1]

ARTHUR C. HARDY
Massachusetts Institute of Technology, Cambridge, Massachusetts

THE important attributes of an optical image are its size, position, quality, and flux content. This paper is concerned with the fourth attribute. No claim can be made that the results reported herein are new; indeed, they are very old. Nevertheless, the subject is still misunderstood or ignored to an extent that belies its importance.

In one sense, the calculation of the flux content of an image may be likened to a calculation based on Ohm's law for a simple series circuit. The brightness of the source plays the role of electromotive force, the limiting aperture is analogous to a resistance, and the flux content of the image is determined almost as simply as the flow of electric current. The validity of this analogy is unfortunately discredited by the attention devoted to Ohm's law in even the most elementary texts on general physics and the omission of the corresponding material pertaining to optics. Because this omission is largely due to complexities arising from unfamiliarity with photometric concepts, the present treatment is carried through to its final stages in energy units.

IRRADIANCE DUE TO A CIRCULAR SOURCE

Assume in Fig. 1 that the plane surface AB is infinite in extent and that it radiates W watts per unit of area. If this radiant flux falls on an adjacent surface CD, it is evident that the number of watts received by a unit area of CD is numerically equal to W. In other words, the *irradiance* of CD is equal to the *radiant emittance* of AB.

If the surface AB does not extend to infinity, the irradiance at some point on CD depends upon the geometry of the particular arrangement and upon the law of emission. The special case of greatest practical interest is shown in Fig. 2, where AB is the surface of a circular disk of radius r that radiates uniformly in accordance with Lambert's law. The radiant intensity (watts per unit solid angle) from an elemental area of AB is then proportional to $\cos\alpha$; and the determination of the irradiance of an element of area $d\sigma$ at a distance d is a simple problem in integration familiar to any illuminating engineer. The result of the integration is given by Eq. (1),

$$H = W[r^2/(d^2+r^2)], \tag{1}$$

where H is the irradiance of $d\sigma$ in watts per unit area, W is the radiant emittance of AB in watts per unit area, r is the radius of the circular disk, and d is the distance of $d\sigma$ from the plane of AB. It is worthy of note that H becomes equal to W when the disk is so large that d is negligible compared to r. When r is small compared to d, H is directly proportional to the area of the source and inversely proportional to d^2. The latter case is familiar because of the emphasis that is customarily placed on the law of inverse squares.

Because the usefulness of an equation often depends on the ease with which it can be remembered, it should be noted that the quantity in the parentheses is a fraction whose value is always less than unity. Furthermore, the denominator is the square of the distance of $d\sigma$ from the rim of the circular disk. For many purposes it is more convenient to write Eq. (1) in the form of Eq. (2),

$$H = W\sin^2\theta, \tag{2}$$

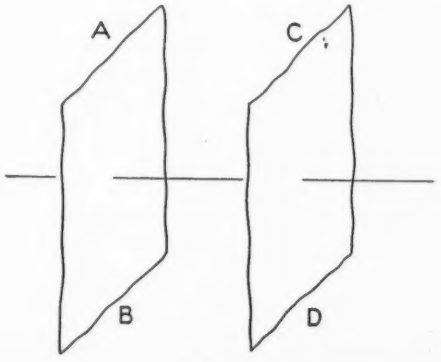

FIG. 1.

[1] Presented by invitation at the twenty-seventh annual meeting of the Optical Society of America, New York City, October 30–31, 1942.

where θ is the half-angle of the circular cone converging on $d\sigma$ from the entire source.

FLUX CALCULATIONS IN OPTICAL SYSTEMS

Suppose that the irradiated area $d\sigma$ of Fig. 2 is imaged by an optical system at $d\sigma'$, as shown in Fig. 3. Assume first that the angle θ is less than the angular opening of the optical system so that all the radiant flux incident on $d\sigma$ arrives at $d\sigma'$, neglecting losses in the optical system due to absorption and reflection. The irradiance of $d\sigma'$ is then related to the irradiance of $d\sigma$ inversely as the ratio of their respective areas.

Let the linear magnification between the conjugate planes containing $d\sigma$ and $d\sigma'$ be represented by m. The ratio of the areas $d\sigma$ and $d\sigma'$ is then indicated by Eq. (3),

$$d\sigma'/d\sigma = m^2. \tag{3}$$

Hence, the irradiance H' on $d\sigma'$ is expressed by

$$H' = W(\sin^2\theta/m^2). \tag{4}$$

It should be noted that the ratio $\sin^2\theta/m^2$ does not ordinarily exceed unity. The truth of this statement and some important generalizations can be seen from the relationship between θ and θ'. If the optical system is aplanatic, the magnification is independent of θ; and the second law of thermodynamics requires[2] that

$$m = n \sin\theta/n' \sin\theta', \tag{5}$$

where n and n' are the refractive indices of the initial and final media respectively. By substitution of this value of m, Eq. (4) becomes

$$H' = W\left(\frac{n' \sin\theta'}{n}\right)^2. \tag{6}$$

If the initial and final media are air,

$$H' = W \sin^2\theta'. \tag{7}$$

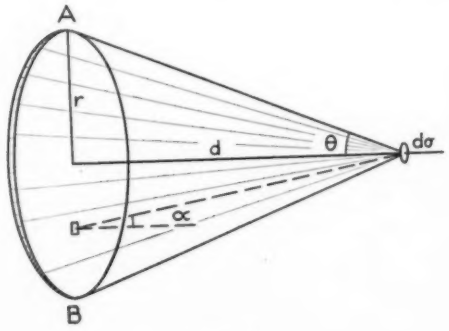

FIG. 2.

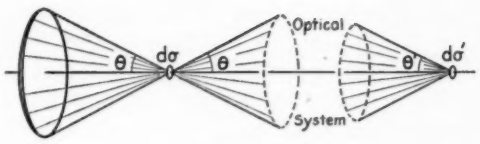

FIG. 3.

It is clear from the above equation that, in the image space, the irradiance *at any point* on the axis of an optical system depends only on the radiant emittance of the source and the angle θ' of the cone converging at the point in question. In general, θ' may be limited by the optical system rather than by the size of the source. This does not impair the usefulness of the preceding argument; since, if the source is larger than is required to fill the angular aperture of the optical system, the source could be reduced in size until the optical system is just filled. This would meet the condition assumed in the deviation of Eq. (6), and a larger source could evidently not increase the size of the convergent cone in the image space.

VISUAL INSTRUMENTS

The irradiance of the retina of the unaided eye is controlled by the size of the cone having its base at the exit pupil and its apex on the retina. The half-angle θ' of this cone varies with the size of the pupil, causing the quantity within the parentheses of Eq. (6) to vary from a minimum of about 0.005 to a maximum at about 0.08. At average levels of adaptation and neglecting absorption in the media of the eye, the irradiance of the retina is about one percent of the value that it would have if the retina were placed in immediate contact with the source.

It will be seen that no optical instrument placed before the eye can increase the value of θ'. Hence, the irradiance (watts per unit area) of the retina can not be increased by the use of an optical instrument. The irradiance may be

[2] In this connection, see Clausius, *The Mechanical Theory of Heat* (Macmillan & Company, New York, 1879), Chapter 12.

decreased, however, if the limiting aperture of the entire system (including the eye) is within the instrument. This occurs when the magnifying power of the instrument is higher than its normal value for the objective used.

When the eye is the ultimate receptor, the *luminous emittance* (lumens per unit area) of the source is of more significance than its *radiant emittance* (watts per unit area). Correspondingly, *illuminance* (lumens per unit area) is of more significance than *irradiance* (watts per unit area). The conversion of units is a simple matter when the luminous efficiency or *luminosity* of the radiant energy is known. As a rough guide, luminosity is at its maximum of 650 lumens per watt in the case of monochromatic green light, the luminosity of sunlight is in the neighborhood of 100 lumens per watt, and that of tungsten light rarely exceeds 20. Equation (7) may be rewritten in terms of luminous emittance L and illuminance E' as follows:

$$E' = L \sin^2 \theta'. \tag{8}$$

As an illustration in the use of these photometric terms and the applicability of the preceding results to the photometry of optical systems, consider the problem of illuminating the screen in the projection of motion pictures. Given a source having a certain luminous emittance and a projection lens of known diameter at a fixed distance from the screen, it is clear that Eq. (8) enables an upper limit to be found for the illuminance of the screen. Failure to realize that there is such a limit may not have retarded the development of this art, but it did lead to many disappointing experiments whose failure might easily have been predicted.

It may not be inappropriate to remark that the behavior of optical systems is often contrary to intuition. For the ordinary purposes of the illuminating engineer, the total luminous flux (lumens) emitted by a source of light is a concept that is grasped as easily as the concept of radiant flux (watts) emitted by the antenna of a radio broadcasting station. In projection systems, on the other hand, the luminous emittance (lumens per unit area) is the important characteristic of the source; and, because of the difficulty of estimating the area of an intense source, there is an understandable tendency to confuse the intrinsic property and the total luminous output. Thus, the illuminance at some point on the axis of a searchlight beam depends only on the distance of the point from the searchlight, the diameter of the mirror, and the luminous emittance of the source. A larger source of the same luminous emittance would not increase the illuminance at a point on the axis, but would merely cause the beam to become more divergent and hence to illuminate a larger area.

TABLE I.

f/-number	1	1.4	2	2.8	4	5.6	8	11	16
$\sin^2 \theta'$	1/4	1/8	1/16	1/32	1/64	1/128	1/256	1/512	1/1024

NON-VISUAL INSTRUMENTS

It is apparent from Eq. (7) that the light-gathering power of an optical instrument used in air is measured by $\sin^2 \theta'$. This factor is related to the f/-number (conventionally employed in marking photographic objectives) by the relationship

$$f\text{/-number} = 1/2 \sin \theta'. \tag{9}$$

Hence the factor $\sin^2 \theta'$ for an $f/1$ objective is 0.25; and the factors for other f/-numbers are as shown in Table I.

The values of $\sin^2 \theta'$ in this table apply only when the optical system is focused on an object at infinity, and a correction is necessary when the magnification in the image plane is not substantially zero. This correction can be made by dividing the factors in the table by $(1+m)^2$. The correction is of little consequence when m is less than unity, but becomes equal to m^2 for large values of m. Thus, a photograph made at unit magnification requires four times as much exposure as a photograph of a distant object having the same luminous emittance; and a photograph enlarged tenfold would require 101 times as much exposure.

With these principles in mind, the performance of an optical system can usually be estimated in advance of its construction or use, assuming the necessary data are available. At the worst, a few experiments with a simple optical system of known light-gathering power are worth conducting. Consider, for example, the problem of estimating the exposure when photographing

panels painted with luminous paint. Let one of the panels be placed in immediate contact with the film to be used until the film has the desired density after development. The factor indicating the light-gathering power of such an optical system is unity; and the time of exposure for any other system can be readily computed on the basis of the reciprocity law and the factors listed in the table above. If it happens that a photomicrograph is being attempted, the form of Eq. (4) may be more convenient. In this equation, $\sin\theta$ is known from the numerical aperture (N. A.) of the objective, m is the linear magnification, and no correction factor is necessary. Although this example has been chosen primarily because of its simplicity as an illustration,[3] corresponding procedures can usually be evolved and are frequently very useful.

PRECAUTIONS

For the sake of clarity of presentation, discussion of the limitations imposed by the assumptions made in the foregoing treatment has been reserved for this section. It should now be emphasized that the source has been assumed to be of such size that it can be resolved by the optical system. Also, the source has been assumed to be uniform in luminous emittance over its area. This assumption is usually unwarranted, especially in the case of coiled tungsten filaments. Fortunately, a correction based on the geometry of the filament usually yields results of the correct order of magnitude.

It should not be overlooked that the optical system was assumed to be aplanatic. If it is afflicted with aberrations, the computed values will be less than are indicated by the theory. The reduction from this cause is small in most cases, and the purpose of the theory is usually achieved if it indicates how a perfect optical system, free from aberrations and from losses due to reflection and absorption, would perform.

The assumption that the source obeys Lambert's law of emission is valid for most light sources. However, in view of the present interest in electron optics, it should be emphasized that electron sources do not usually obey Lambert's law, and the results obtained herein therefore do not apply.

[3] Unlike most sources or diffusely reflecting surfaces, luminous paints satisfy the conditions embodied in Lambert's law only approximately.

JOURNAL OF THE OPTICAL SOCIETY OF AMERICA VOLUME 33, NUMBER 2 FEBRUARY, 1943

Analysis of Errors in a Reflecting Prism*

PAUL W. STEVENS
Eastman Kodak Company, Rochester, New York

IN the large scale manufacture of reflecting prisms, it is necessary to determine requisite tolerances to insure satisfactory performance of the completed optical system. These tolerances are correlated with deviation errors in the prism which are in turn a function of errors in the dihedral angles. It is desirable to speed up inspection of the finished prism by gleaning as much information as possible from a single measurement in a test instrument.

Theoretically, a faulty prism may be considered as a perfect prism and a wedge of small angle in sequence (Fig. 1). This is true regardless of the complexity of the errors, provided they are of small magnitude, but it does not take into account departures of the surfaces from optical flats. While in general the wedge representing these errors will have its principal section inclined to that of the ideal prism, it may be resolved into two component wedges whose principal sections are parallel and perpendicular to the latter. The perpendicular component indicates pyramid error, while the one parallel to the principal section is a measure of the errors in the magnitudes of the angles.

* Presented at the Twenty-Seventh Annual Meeting of the Optical Society of America, New York, New York, October 30–31, 1942.

Since prisms of this sort are usually used in conjunction with lens systems having a circular field, one is interested in studying the behavior of a cone of light centered about the optical axis. We shall confine our attention to the study of changes in the deviation of the rays, which is the only property of primary importance in a collimated bundle or in light from a distant object. In actual practice, it is necessary to consider only the extreme rays in the principal section and in the plane of incidence normal to it. Accordingly, we shall first investigate the directional properties of a cone of light whose axis is incident normally at the first surface of the wedge.

Figure 2 shows the elevation view of a wedge of small angle. The axis of the cone will be deviated by the amount

$$a(n-1), \tag{1}$$

where n is the index of refraction of the glass and a is the angle of the wedge. Since this is the condition for minimum deviation, other rays in the cone will be deviated by a greater amount depending upon the angle of incidence and the inclination to the principal section.

In order to visualize these other rays, it is convenient to draw the spherical diagram corresponding to the plan view of the wedge (Fig. 3). The entrance face is parallel to the plane of the paper, and the normal to it is at the center A. The horizontal line MN is the projection of the principal section, while the vertical line PT is parallel to the refracting edge. At point B lies the normal to the second face, such that the angular distance AB is equal to a, the angle of the wedge.

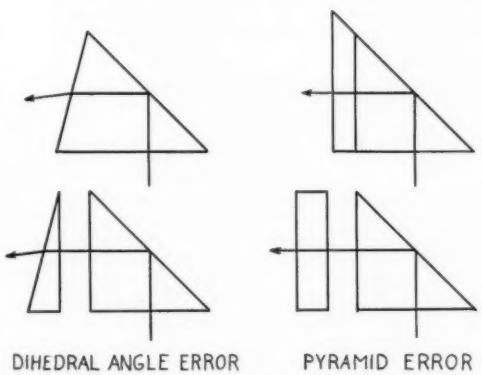

FIG. 1. Faulty prism and equivalent wedge.

A cone of rays incident at angle I will be uniformly refracted at the first surface so as to form a second cone of angle I'. These two cones are represented by the two small circles of the sphere drawn about A as a pole. Now let us

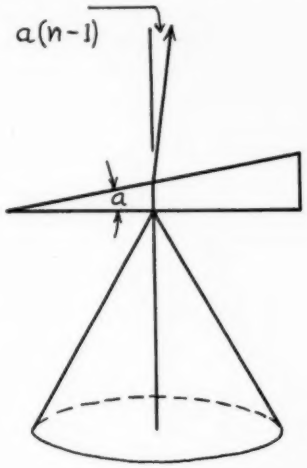

FIG. 2. Incident cone of rays.

consider an arbitrary ray Q in this cone, such that its plane of incidence at the first surface makes an angle ϕ with the principal section. The plane of incidence at the second surface will be the great circle through B and D, and the emergent ray will be in this plane at some point Q'. Solution of the spherical triangles PAQ and PBQ' establishes the interesting fact that Q and Q' lie on a small circle centered about the pole P under all conditions. In other words, the inclinations of the incident and emergent rays to the principal section are always equal.

To a first-order approximation, the angle QPQ' is independent of the inclination ϕ and depends upon the angle of incidence I according to the following equation:

$$\text{Angle } QPQ' = a(n \cdot \cos I' - \cos I)/\cos I. \tag{2}$$

This means that all the emerging rays will lie along the surface of a cone equal in angle to the incident cone but which is rotated about the axis P, with respect to the latter, by an amount equal to angle QPQ'.

The deviation QQ' will not be independent of

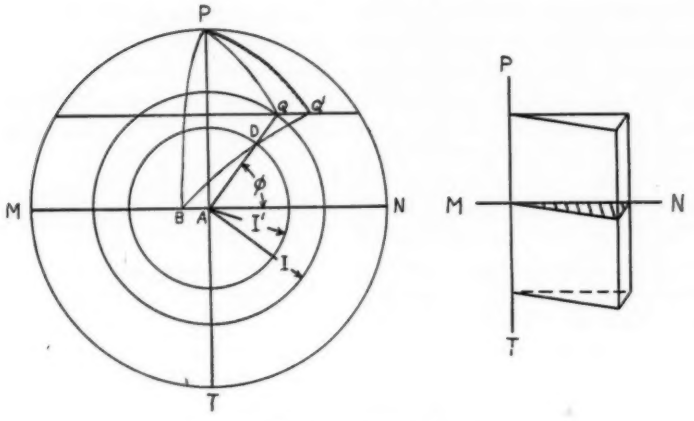

FIG. 3. Spherical diagram of wedge.

ϕ but will be proportional to the sine of the arc PQ.

Deviation error QQ'
$$= \text{Angle } QPQ'(1-\sin^2 I \cdot \sin^2 \phi)^{\frac{1}{2}}. \quad (3)$$

This quantity will reach a maximum in the principal section and will be at a minimum when the initial plane of incidence is perpendicular thereto.

Maximum deviation error
$$= a(n \cdot \cos I' - \cos I)/\cos I. \quad (4a)$$
Minimum deviation error
$$= a(n \cdot \cos I' - \cos I). \quad (4b)$$

In practice, one is usually interested in the residual error of deviation, because it is easy to correct for the error inherent in the ray normal to the entrance face of the wedge. Suppose then that we compare the positions of the emergent ray with the corresponding points on a small circle centered about C, the direction of emergence of this normal ray, where $AC = a(n-1)$ as in Fig. 4. The equations for maximum and minimum values of the residual error are

$$a \cdot n(\cos I' - \cos I)/\cos I, \quad (5a)$$

and

$$a \cdot n(\cos I' - \cos I). \quad (5b)$$

If in the general case this residual error be resolved into components parallel and perpendicular to the plane of incidence at the first surface, they are found to be as follows:

parallel component
$$= [a \cdot n(\cos I' - \cos I)/\cos I] \cos \phi, \quad (6a)$$
perpendicular component
$$= [a \cdot n(\cos I' - \cos I)] \sin \phi. \quad (6b)$$

A graph showing one of these quantities as a

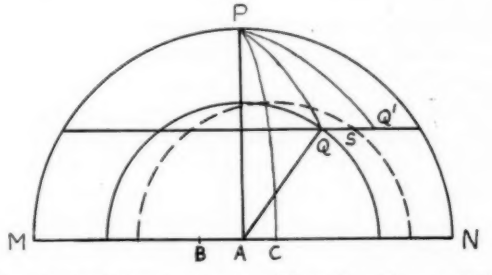

FIG. 4. Deviation error and residual. Actual error QQ'. Residual error SQ'.

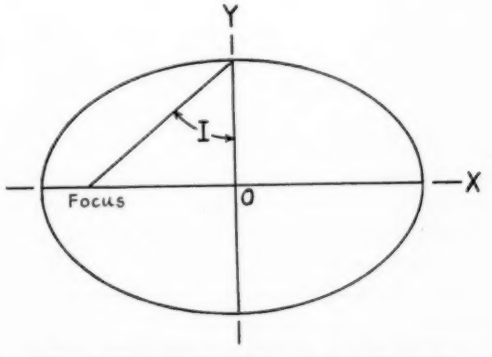

FIG. 5. Ellipse of deviation error. $X = D_1 \cdot \cos \phi$; $Y = D_1 \cdot \cos I \cdot \sin \phi$.

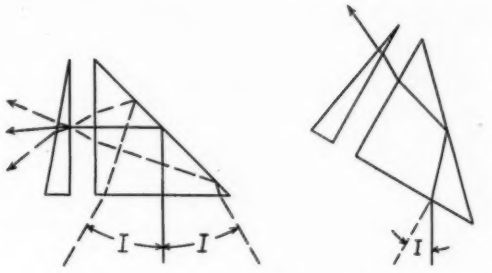

FIG. 6. Diagram for rays in principal section of prism afflicted with dihedral angle error.

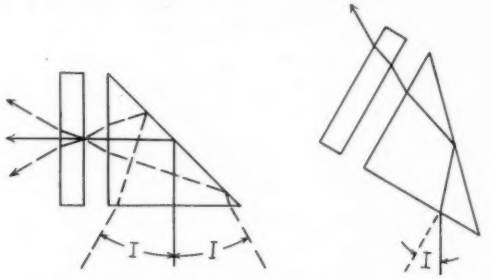

FIG. 7. Diagram for rays in principal section of prism afflicted with pyramid error.

function of the other, for a constant angle of incidence, will therefore be an ellipse of eccentricity (sin I) as shown in Fig. 5, where D_1 is the maximum error according to Eq. (5a). A similar ellipse can be plotted from actual deviation errors, in which case the value of D_1 is indicated by Eq. (4a).

Let us apply these principles to an analysis of rays lying in the principal section of the common right-angled reflecting prism. If the magnitudes of the prism angles are incorrect, the equivalent wedge will have its principal section parallel to that of the prism (Fig. 6), and the residual deviation error will be according to Eq. (5a). On the other hand, suppose there is pure pyramid error. Then the equivalent wedge will have its principal section perpendicular to that of the prism (Fig. 7). The residual deviation error will now be perpendicular to the principal section of the prism by the amount indicated in Eq. (5b). Rotation of the prism will produce similar errors in the ray which was originally at normal incidence.

It will now be interesting to see how these two quantities vary with the angle of incidence (Fig. 8). The residual error in deviation due to pyramid is very nearly a linear function of the square of the angle of incidence and is, therefore, approximately a parabolic function of the angle itself (curve *b*). The error resulting from discrepancies in the magnitudes of the angles is nearly linear and parabolic for small angles of incidence because the two quantities are in the ratio of the

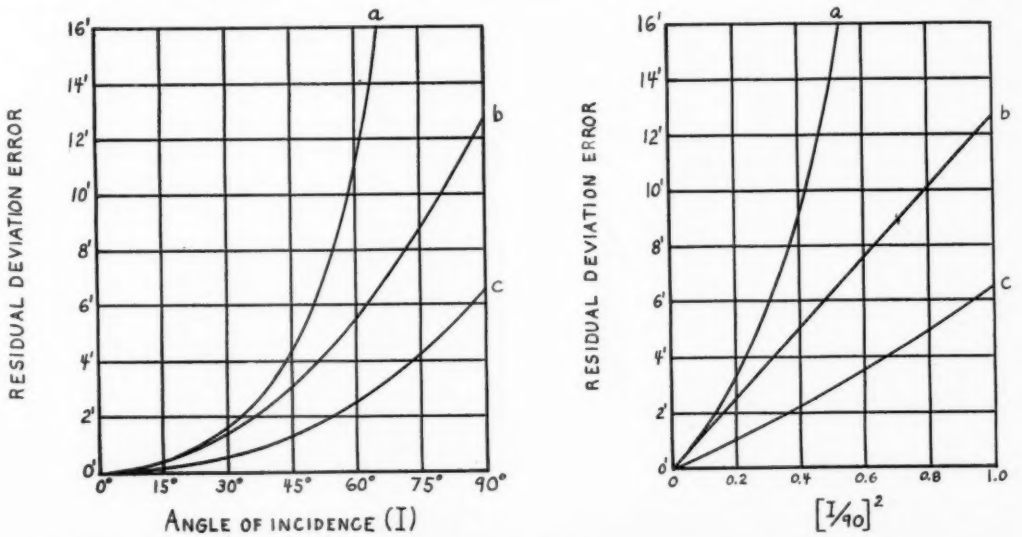

FIG. 8. Variation of residual errors with angle of incidence for a ten-minute wedge of index of refraction 1.617.

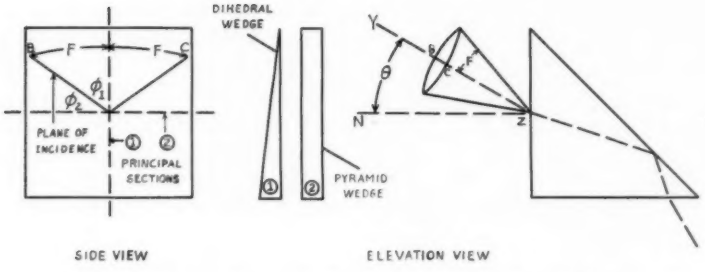

FIG. 9. Diagram for rays inclined to principal section of prism.

cosine of this angle (curve *a*). In computing the residual error in deviation due to pyramid, it is sometimes of interest to compare the deviation directly with that for the ray incident normally at the first surface. This gives a resultant which is smaller than that according to (5b), namely:

$$a[(1-\cos I)-n(1-\cos I')]. \qquad (5c)$$

It is plotted in Fig. 8 as curve *c*.

Suppose we wish to analyze the rays of the cone which lie in a plane perpendicular to the principal section of the prism. Such a plane is shown projected as the line *YZ* in Fig. 9. If the axis of the cone is not parallel to the normal to the prism face, the plane of incidence of the rays at the wedge will be neither parallel nor perpendicular to the principal section of the wedge, i.e., the angle ϕ will be somewhere between zero and ninety degrees. Accordingly, the special Eqs. (4) and (5) will not apply. Rather it is necessary to compute the deviation error by means of the general Eqs. (2) and (3) after solving for the angles I and ϕ as follows:

$$\cos I=\cos F\cdot\cos\theta, \qquad (7)$$

where F is the inclination of the ray to the principal section of the prism, and θ is the angle of incidence of the axis of the cone; and

$$\cos\phi_1=\cos F\cdot\sin\theta(1-\cos^2 F\cdot\cos^2\theta)^{-\frac{1}{2}}, \qquad (8a)$$

for the component wedge indicating error in the magnitudes of the prism angles; or

$$\sin\phi_2=\cos F\cdot\sin\theta(1-\cos^2 F\cdot\cos^2\theta)^{-\frac{1}{2}}, \qquad (8b)$$

for the component wedge indicating pyramid error.

In conclusion, it may be stated that a mathematical analysis such as this enables one to judge the performance of a prism simply by measuring in a test instrument the beam of light incident normally upon the surface of the prism. Provided the errors are small, the pyramid and principal section components may be considered independently and then the resultant found by vectorial addition of the two components. Furthermore, these methods may be applied to many other types of reflecting prisms, and also to windows and filters having plane parallel faces.

An Absorption Tube for the Investigation of Gases at Low Pressures

PHILIP A. LEIGHTON AND DAVID H. VOLMAN*
Department of Chemistry, Stanford University, Stanford University, California
(Received November 20, 1942)

IN connection with photochemical studies of aldehydes and ketones under investigation in this laboratory, it was found desirable to study the predissociation spectra of several of these compounds in the ultraviolet. It is known that predissociation may be induced by the fields of neighboring molecules. To distinguish between induced and true predissociation, it is desirable to observe the molecule in a relatively force-free field such as is the case at low pressures.

To study absorption spectra at low pressures, it is necessary to provide a long enough light path so that absorption is experimentally detectable. Although there is no unique solution to such a problem, where sufficient space is available, the simplest method is by use of a single long tube.

Prior to the completion of the apparatus, the longest absorption tube which had come to our attention was the 70-foot tube at the California Institute of Technology.[1] Since the completion of the tube in this laboratory, investigations utilizing two other tubes of considerable length have been described. The first of these is 328 feet in length and is located at the observatory in Lyon, France;[2] the second is 105 feet long and is located at Duke University.[3] All three of these tubes are similar in construction. Each consists of sections of steel pipes with vacuum and pressure proof gaskets between the several sections and quartz windows at the ends.

Since a metal tube would be unsuitable for studying the absorption spectra of many chemical substances, and since it was desired to make the tube of wide applicability, it was decided to use glass as the construction material. Consequently, we constructed a tube 155 feet in length from Pyrex glass pipe supplied by the Corning Glass Works. The inside diameter of the pipe was 3 inches, and the individual section lengths were 10 feet. The sections ended in conical flanges which were shallow grooved. Joints were made with De Khotinsky cement and strengthened by the use of cast iron flanges. Access to the tube was gained through a side arm supplied with one of the tubes. The windows were of crystal quartz and were held in place by sealing wax.

In practice a vacuum of 10^{-4}–10^{-5} mm could be readily obtained using an oil diffusion pump backed by a Cenco Megavac. When the tube was closed off from the pumps, a pressure of 10^{-3} mm could be maintained indefinitely.

THE OPTICAL SYSTEM

The optical system is shown in Fig. 1. The angle of light rays entering the slit with the optic axis is such that the grating is just filled.

THE LIGHT SOURCE

For a number of reasons, the fraction of light emitted from any source ultimately reaching the plate is low. First, since long focus lenses must be used, the light source must be placed at such a distance from the lens that a considerable portion of the emitted light does not strike the lens. Second, only rays originating in a narrow

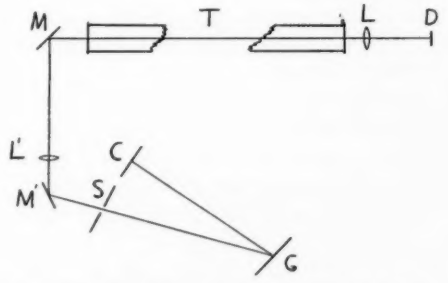

FIG. 1. The optical system. *D*—light source; *LL*'—lenses of 60-in. focal length for visible light; *T*—absorption tube, 155 ft. in length; *S*—spectrograph slit; *G*—grating; *C*—plateholder.

* Standard Oil Company of California Fellow, Stanford University, 1939–40. On leave of absence from University of California. Present address: The Technological Institute, Northwestern University, Evanston, Illinois.

[1] R. M. Badger, L. G. Bonner, and P. C. Cross, J. Opt. Soc. Am. **25**, 355 (1935).

[2] L. Herman, Ann. de physique **11**, 549 (1939).

[3] H. Sponer and L. G. Bonner, J. Chem. Phys. **8**, 33 (1940).

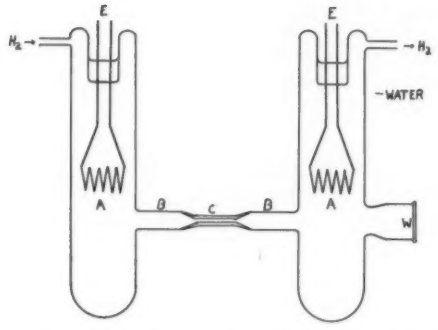

FIG. 2. Low voltage high amperage discharge tube, U type, with capillary arc tube; *AA*—"oxide-coated" nickel electrode; *BB*—Pyrex-fused silica seals; *C*—fused silica capillary; *EE*—tungsten leads; *W*—quartz window. In operation, the entire tube is immersed in water to the level shown, with water jets directed on *B* and *C*. Will operate continuously on 4 to 5 amperes at about 500 volts.

element of volume within a discharge tube can be focused. Third, the reflectivity of the two aluminum surface mirrors is relatively small. Finally, the speculum surface of the grating reflects poorly in the ultraviolet.

The foregoing considerations make it desirable to have a lamp of high intensity if inordinately long exposure times are to be avoided. In addition the lamp must give a continuous emission spectrum down to 2500A.

To meet these requirements, the lamp shown in Fig. 2 was constructed. The electrodes were made of nickel strips, $0.005 \times 1 \times 20$ in. These were folded as shown and coated with a commercial oxide coating material supplied by the Callite Products Company, Union City, New Jersey. Prior to coating, the electrodes were spot welded to large diameter tungsten leads sealed through glass. The entire assembly was then sealed into Pyrex glass tubing, 3 inches in diameter. The discharge took place through a 4-cm section of 2-mm quartz capillary sealed to the Pyrex jacket with quartz-glass graded seals. The window was of crystal quartz, 40 mm in diameter, and was sealed to the tube with Glyptal lacquer. The lamp was operated in a water bath.

Figure 3 shows the electrical circuit employed. The variable voltage transformer T_1 is regulated

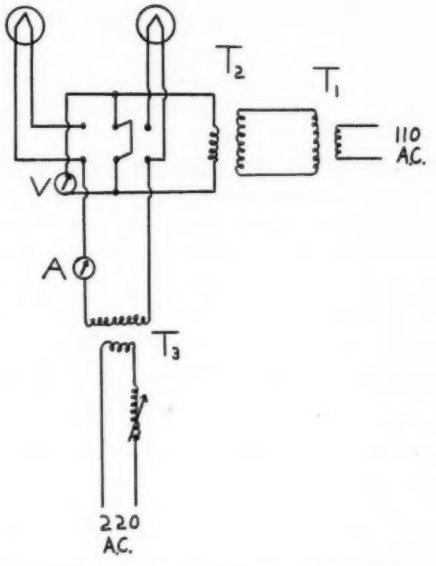

FIG. 3. Electrical circuit for starting and operating hydrogen discharge tube. T_1—variable voltage transformer; T_2—fixed voltage step down transformer; T_3—fixed voltage step up transformer; *V*—voltmeter; *A*—ammeter.

so that the voltage drop through the filament nearest the window is slowly increased to about 4 volts. This corresponds to a current of approximately 75 amperes, and the filament is heated to a dull red. Hydrogen is passed through the tube at a pressure of 1–2 mm. The arc is then struck by closing the arc circuit through the transformer T_3. The voltage across the secondary of T_3 is regulated by a variable iron cored inductance.

THE SPECTROGRAPH

The spectrograph used was a 21-foot focus concave grating in an Eagle mounting. The grating was speculum metal 5×2 in. with 15,000 lines per inch.

Using various light sources and plates, spectrograms have been taken from 2300 to 11,000A, and, although the exposure times vary widely, several hours exposure is usually sufficient for the least favorable conditions.

Solarization with X-Rays and Visible Light

ALBERT MAY
The Catholic University of America, Washington, D. C.
(Received November 30, 1942)

INTRODUCTION

IT is well known that when a photographic emulsion is exposed to visible light or to x-rays, the blackening that it will acquire on development first increases with the exposure until a maximum value of the density is reached and then decreases with further exposure. This decrease of density is called solarization or photographic reversal. Experiments show[1] that the first reversal due to solarization is followed by alternate increases and decreases of density as shown in the H and D curve (or characteristic curve) of Fig. 1.

It has been found[2] that about one hundred visible light quanta absorbed by a silver bromide grain of the emulsion will render it developable, but this number undoubtedly varies greatly from grain to grain. On the other hand one x-ray quantum may cause a grain to be developable[3] and it is probable that usually a single such quantum absorbed by a grain will be sufficient.

The various theories of solarization[4] will not be discussed here. It is necessary only to assume that a grain is solarized as a result of the absorption by the grain of many more quanta than are required to render it developable. The number needed may depend greatly on the conditions of irradiation.

On the rise of the curve in Fig. 1, there is, of course, a point at which the tangent has a maximum inclination to the abscissa. The slope of this tangent is called the gamma of the developed image. The inertia value I, that is, the exposure indicated by the point A at which this tangent intersects the abscissa, has been used as a measure of the speed of the emulsion. Trivelli and Jensen[5] have suggested that the exposure I_s corresponding to the point B at which the tangent of maximum negative slope in the region of the first reversal intersects the line of maximum density, furnishes a convenient measure of the beginning of solarization. The maximum slope (negative) in this solarization region will be indicated by γ_s. The quantity[6] $\log I_s/I$ is a convenient measure of the width of the first maximum of the blackening curve.

EXPERIMENTAL

A very important difference between the blackening curves produced by x-rays and by light is apparent when strips of the same film are exposed to each. This difference is shown in the H and D curves of Fig. 2. These curves are for Eastman Ultra-Speed x-ray film exposed in the following manner. Strips of film were irradiated by either tungsten light or the "white" x-rays from a tube operated at about 30 kv. Step wedges were formed by varying the exposure along the strip by covering the strip in successive steps by a screen opaque to the radiation used. The densities plotted have been reduced by a factor so that the maximum density $D_m=1$. This is convenient for intercomparison as will be seen later. In addition the curves have been bodily displaced laterally so that the normal exposure regions of the two curves are approximately superimposed.

As is seen from Fig. 2 the width of the first maximum is considerably greater for visible light than for x-rays. Apparently this result was obtained in 1908 by Walter who reported[7] that for x-rays "the decrease of blackening in the region of solarization with the same increase of irradiation time was even stronger than with light." On the other hand Mott predicted[8] that solarization would occur at a much later stage in the exposure for x-rays because of the difficulty of bromine release.

[1] A. J. Reardon and H. P. Griggs, J. Opt. Soc. Am. **24**, 331 (1934).
[2] J. Eggert and W. Noddack, Sitzungsber. preuss. Akad. wiss. p. 631 (1921).
[3] J. Eggert and W. Noddack, Naturwiss. **15**, 57 (1927).
[4] A. P. H. Trivelli, J. Frank. Inst. **209**, 373 (1930).
[5] A. P. H. Trivelli and E. C. Jensen, J. Frank. Inst. **209**, 37 (1930).
[6] In this paper all logarithms are to base 10.
[7] B. Walter, Ann. d. Physik [4], **27**, 83 (1908).
[8] N. F. Mott, Phot. J. **78**, 286 (1938).

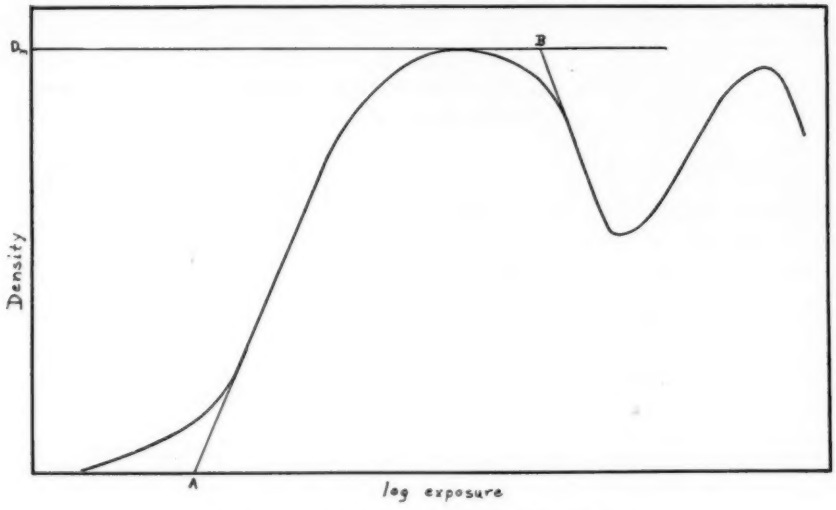

FIG. 1. Blackening curve of photographic emulsion.

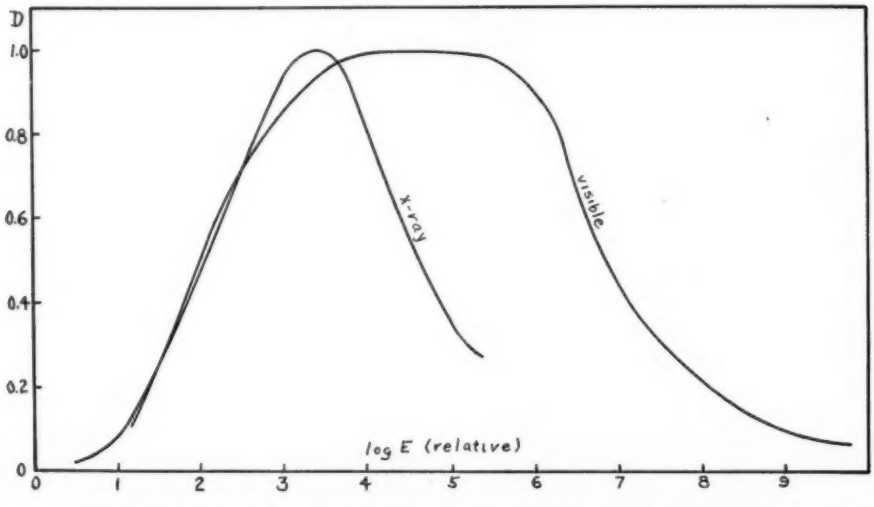

FIG. 2. Blackening curves of Ultra-Speed x-ray film with x-ray and optical exposures.

Webb and Evans[9] reported a similar difference between the curves for low and high intensity visible irradiation, the peak for a low intensity exposure being wider by a log value of 0.5 than that due to an irradiation 400 times as intense. They have given a very reasonable explanation of the effect in terms of the regression theory of solarization, suggesting that an increased intensity of illumination may increase the intensity of the bromine attack on the silver centers and thus be more effective in solarization. The cause

TABLE I.

Type of film	log I_s/I x-rays	log I_s/I visible
Ultra-Speed x-ray	2.6	5.2
commercial	3.6	4.6
process	3.1	5.3
Tri-X pan	3.6	5.6

[9] J. H. Webb and C. H. Evans, J. Opt. Soc. Am. **30**, 445 (1940).

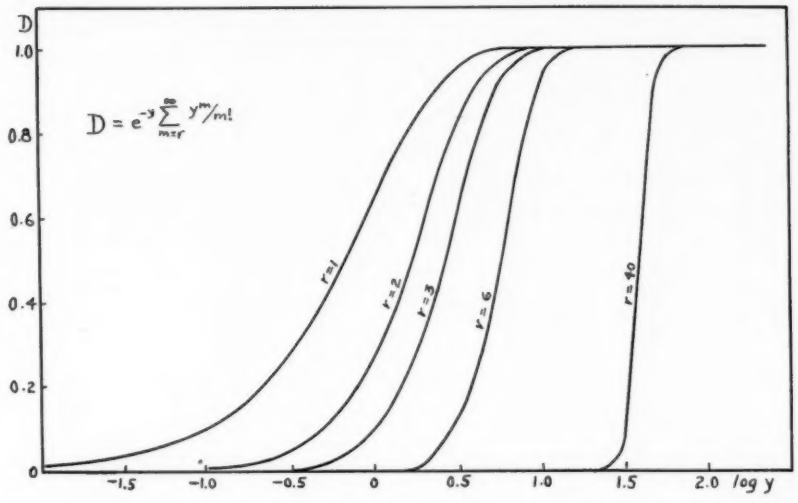

FIG. 3. Curves from formula based on simple probability.

of the difference in the x-ray and optical curves will be discussed later.

Ultra-Speed x-ray film solarizes almost completely, that is, the first minimum is only slightly above the fog level. The depth of this minimum varies greatly with different emulsions and may change considerably for a given emulsion with varying storage conditions. Apparently humidity causes a large decrease in the degree of solarization.

With prolonged development the first maximum increases in width and the solarization decreases, finally vanishing entirely. For this reason specimens of the same emulsion whose first maxima are to be compared must be given approximately the same development. Gamma increases steadily during the usual time of development and furnishes a suitable criterion of extent of development with a given emulsion.

For the curves of Fig. 2, $\log I_s/I$ is 4.93 for the optical exposure and 2.65 for x-rays. In addition to tests with Ultra-Speed x-ray film which is not color-sensitized, measurements were made on the following Eastman films: No-Screen x-ray, contrast process orthochromatic, commercial orthochromatic and Tri-X panchromatic. These were chosen for wide variety of emulsion types. Several tests were made with x-rays and with visible light on each emulsion. All films were developed in Eastman DK-60a for such times (varying from one to two and one-half minutes) as to give a value of gamma of about 1.8 for the process film and a value of 0.9 for all other films. When reduced to $D_m=1$ the gamma values were between 0.4 and 0.5 for the latter films, while the process film had a gamma of about 0.6.

Various intensities of visible light were used and the change of peak width noted by Webb and Evans was found. This variation was not large, however, and in every test the width for visible light was considerably greater than for any test with x-rays. Average values of the peak widths for the various films are given in Table I. The No-Screen x-ray film requires very large exposures for solarization and no quantitive data for this emulsion were obtained.

CALCULATED BLACKENING CURVES

An investigation of theoretical blackening curves was made in an attempt to estimate the number of x-ray quanta required to produce solarization. Many analytical expressions have been derived for the density as a function of exposure, but apparently none has been developed to show the solarization region.

Let us assume that quanta strike the emulsion in a random manner and that some of these are absorbed by the grains, that all grains are of the same size, that the probability of absorption of a quantum by a grain is the same for all grains

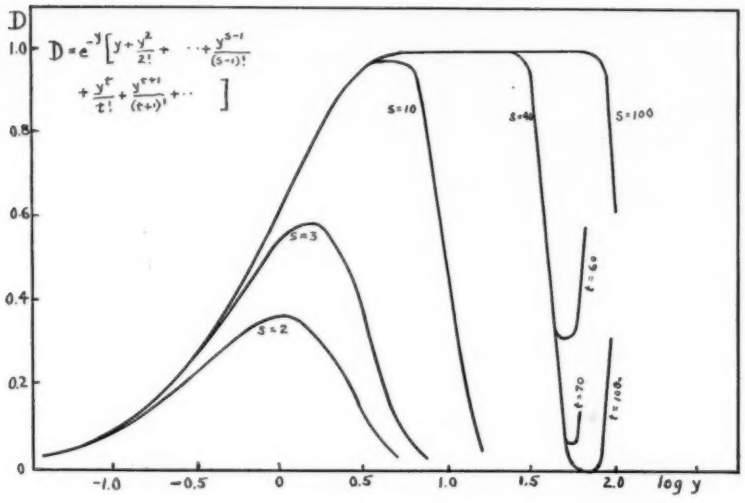

FIG. 4. Curves obtained when solarization is added to the simple probability formula.

and that r quanta must be absorbed by a grain to make it developable. These considerations lead to the equation

$$D=e^{-y}\sum_{m=r}^{\infty} y^m/m! \qquad (1)$$

Here y may be regarded as the exposure. Actually it is found to be the total number of (effective) quanta absorbed times the probability that any quantum absorbed will be absorbed by a particular grain. The formula is written so that the maximum density is unity. This may be regarded as an assumption of a certain blackened area per grain.

Equation (1) has been investigated frequently.[10] Curves computed from it are given in Fig. 3 for various values of r. It will be noted that with increasing r the curves move toward larger exposures and become steeper. Gamma is 0.85 for $r=1$ and nearly six for $r=40$. These values are considerably higher than the usual experimental values of gamma (for $D_m=1$).

Solarization can be added to these curves by assuming that all grains are developable if they have received at least r quanta but less than s quanta. This assumption merely limits the series of Eq. (1) to $s-r$ terms. The second rise of the curve will be obtained if it is further assumed that a larger number of quanta t absorbed by a grain again renders it developable. The formula and a few curves for $r=1$ are shown in Fig. 4.

It is seen that if $r=1$ and s is 2 or 3, the curves bend down rapidly, but for larger values of s, say 40, the maximum density ($D_m=1$) is reached and persists for some range of exposure. One might assume from Fig. 4 that the smaller values of s would give the lower values of gamma found experimentally, but this is not the case. While the gammas of the curves plotted for $s=2$ and $s=3$ are lower than 0.85, they will be larger than 0.85 if all ordinates are multiplied by a factor sufficient to make $D_m=1$. The negative slopes in the solarization region are very steep as are the positive ones following. These graphs then fail completely in representing the experimental curves, because the maximum slopes are invariably too great and because the shapes of the peaks are unsuitable. Even the narrow peak found experimentally for the Ultra-Speed film would require $s=60$ with $r=1$, giving a flat portion at maximum density which is not found in most experimental curves except with prolonged development.

While Eq. (1) does not give curves in agreement with experiment, it is possible by abandoning some of the simplifying assumptions, to

[10] L. Silberstein, J. Opt. Soc. Am. **31**, 343 (1941). J. H. Webb, J. Opt. Soc. Am. **29**, 309 (1939); **31**, 348, 559 (1941).

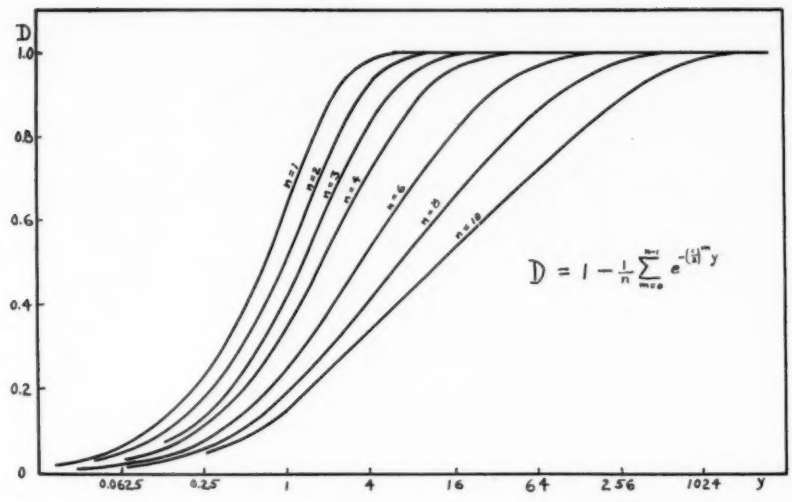

FIG. 5. Ross' curves based on various absorption probabilities.

improve it greatly, in particular, so that low values of gamma are obtained.

Webb has investigated[11] the curves obtained when it is assumed that a variety of values of r are present among the grains of an emulsion under various distributions of these sensitivities among the grains. He has shown that suitably low values of gamma can be obtained on the basis of suitable sensitivity distributions.

Ross has considered[12] the formula

$$D=D_m[1-(1/n)\sum_{m=0}^{n-1}\exp(-a^m y)]. \qquad (2)$$

n is a small integer and a is a constant to which Ross assigned the value one-half. Equation (2) may be regarded as the superposition of n formulas of the type of Eq. (1). Since y represents the number of quanta absorbed times the probability that any one of these quanta will be absorbed by a certain grain, the n quantities $a^m y$ with $a=\frac{1}{2}$, represent n grain classes of which the first ($m=0$) has a basic probability of absorption, the second ($m=1$) has a probability for absorption one-half of this, and so on. This varying probability might be due to various sizes of grains or to shielding of grains by others in a multi-layered emulsion. The latter cause would be unimportant with x-ray exposures.

The fact that the different items of the summation are equally weighted can be interpreted in various ways. If it is assumed that the areas of the grains are proportional to their absorption probabilities, then the numbers of grains of a class must be inversely proportional to their sizes. If on the other hand the grains are equally distributed among all sensitivity classes, all developed areas must be equal. This assumption of equal areas might appear to be inconsistent with the fact that the cause of the variation of absorption has been ascribed to different areas. It is well known that a reasonable prolongation of development time does not appreciably change the inertia value of the emulsion for suitable developing solutions, that is, the tangents of maximum slope for the blackening curves for film differing only in time of development, intersect the abscissa at a common point. Houston[13] suggested that this indicates that grains of various sizes develop at the same rate, that is, at a certain time all of the developable grains will be half reduced, and so forth. It appears more reasonable that grains that start to develop at the same time and have developable centers of the same size will develop together, so that they will have the same area blackened at any given time. A development of this type will give a constant inertia for varying

[11] J. H. Webb, J. Opt. Soc. Am. **31**, 348 (1941).
[12] F. E. Ross, *Physics of the Developed Photographic Image* (van Nostrand, New York, 1924) p. 55.
[13] R. A. Houston, Phil. Mag. [7], **21**, 1113 (1936).

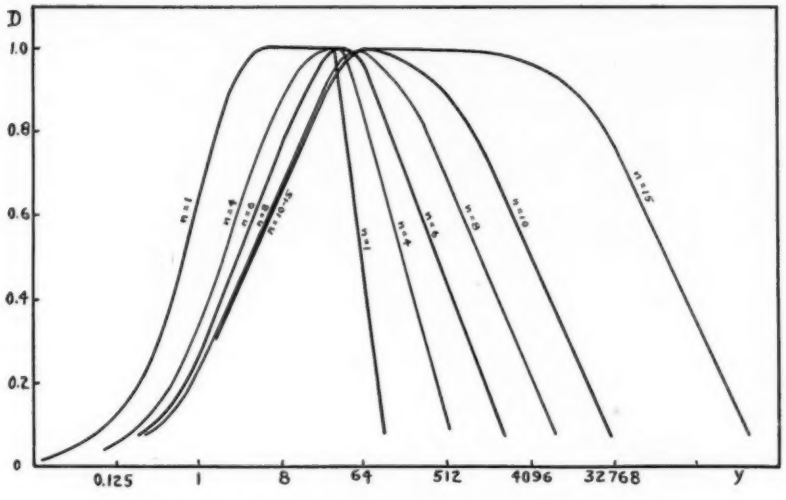

FIG. 6. Ross' curves with solarization added. $r=1$ and $s=64$.

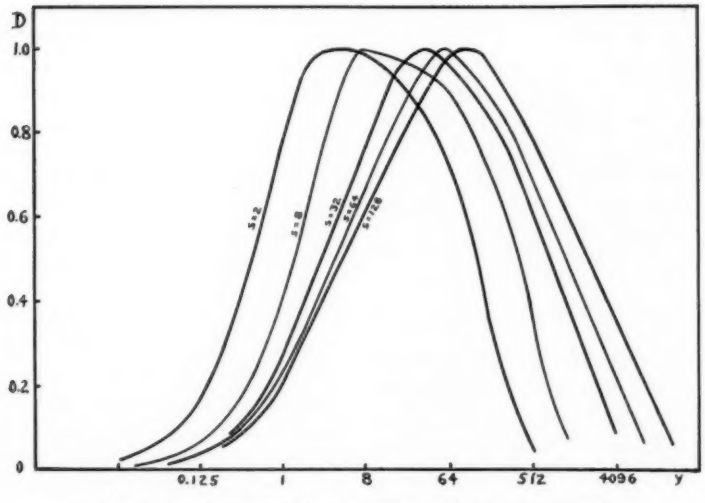

FIG. 7. Ross' curves with solarization added. $r=1$ and $n=8$.

development until an appreciable number of the smaller grains become totally developed, and makes an equality of grain size reasonable. Curves derived from Eq. (2) are given in Fig. 5.

The assumption of various values of r is surely correct for optical exposures since the original silver centers are certain to be varied in size. For x-rays, however, it is probable that most grains are rendered developable by a single quantum although the number requiring a few quanta may be appreciable. On the other hand, the size difference of the grains will cause a

TABLE II. Constants of the curves of Fig. 6. $r=1$, $s=64$.

n	γ	$-\gamma_s$	$\log I_s/I$
1	0.80	1.73	2.28
4	0.63	0.87	2.18
6	0.56	0.60	2.21
8	0.51	0.53	2.60
10	0.50	0.50	3.08
15	0.48	0.48	4.50

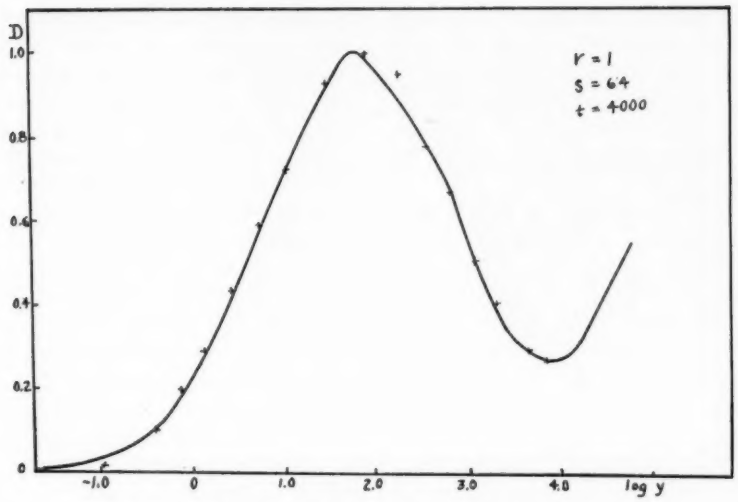

FIG. 8. Comparison of calculated curve with experimental densities.

variable probability of absorption and hence make Ross' modification reasonable. Assuming $r=1$, Ross' formula with solarization added, becomes

$$D=\frac{1}{n}\sum_{m=0}^{n-1}\left[a^m y+\frac{(a^m y)^2}{2!}+\cdots+\frac{(a^m y)^{s-1}}{(s-1)!}+\frac{(a^m y)^t}{t!}+\frac{(a^m y)^{t+1}}{(t+1)!}+\cdots\right] \quad (3)$$

with $a=\frac{1}{2}$. It will be seen that Eq. (3) does not give $D_m=1$ unless s is so large that with a given value of n, all of the n grain classes give their maximum blackening simultaneously for some value of exposure y. The ordinates of all curves calculated from Eq. (3) have been increased by a factor sufficient to make $D_m=1$.

In obtaining graphs from Eq. (3) the values of y used were various integral multiples (positive and negative) of two. This choice results in great simplification where $a=\frac{1}{2}$. Strictly a smooth curve drawn through these values of D does not represent Eq. (3) in the solarization region when s and t are large (say, 64 or greater). In this region the n component curves of Eq. (3) have steep negative slopes as shown for the larger values of s in Fig. 4, and these do not overlap. As a result the true curves drop and rise again in a series of rounded steps. This is the same effect as that discussed by Webb[11] for a similar calculation. It was felt that the inaccuracy in the shape of the curves was not sufficient to justify a smoothing-out method such as that given by Webb. Accordingly the curves to be discussed were drawn smoothly through the density values for the 2-power values of y, as described. Figure 6 gives these curves for $s=64$ and t infinite and various values of n, and Fig. 7 those for $n=8$ and several values of s.

TABLE III. Constants of the curves of Fig. 7. $r=1$, $n=8$.

s	γ	$-\gamma_s$	$\log I_s/I$
2	0.87	0.88	2.44
8	0.85	0.85	2.44
32	0.58	0.58	2.53
64	0.51	0.53	2.60
128	0.46	0.49	2.70

An attempt was made to calculate from Eq. (3) a curve whose shape would be that of the x-ray curve of Fig. 2. For this curve $\gamma=0.51$, $-\gamma=0.51$ and $\log I_s/I=2.65$. These quantities together with the general shape, are most useful in evaluating the parameters, n and s. Data obtained from the families of curves of Figs. 6 and 7 are given in Tables II and III.

From Table II it is seen that when $s=64$ the value of gamma decreases with increasing n. For early solarization (small values of s) this decrease is very small since large values of n

then drag down the peak of the curve. Making $D_m=1$ brings the slope almost up to (or even above) the value with $n=1$. For example if $s=8$, gamma remains 0.8 for n-values of one to ten. A relatively large value of s is required, therefore, in order that gamma may be reduced to the experimental value.

Further it is seen from Table II that n must be relatively large, the experimental value of 0.51 being reasonably satisfied for values of n from 7 to 15, when $s=64$. The width of the peak ($\log I_s/I=2.65$) requires $n=8$ for this same value of s. These choices are confirmed by Table III where we see that for $n=8$ a suitable value of gamma is obtained only when s is about 64.

In Fig. 8 the experimentally determined densities for the x-ray curve of Fig. 2 (reduced to $D_m=1$ and displaced laterally for superposition) are plotted on the curve for $r=1$, $s=64$, and $t=4000$. The same value of n ($n=8$) is assumed to apply throughout. The agreement is good except at the beginning of the solarization region.

It appears justifiable, as has been mentioned, to assume only one value of r ($r=1$) for x-rays, and the same value of n will be expected throughout if the various probabilities of the grains absorbing depend only on the sizes of the grains. The use of a single value of s (and, of course, t), however, appears unreasonable. A curve was calculated with $r=1$, $n=8$ and the grains divided into three equal groups having values of $s=32$, 64, and 128. The only appreciable change was to raise $\log I_s/I$ from 2.60 to 2.73, an equally acceptable value. Apparently the use of several values of s in this manner changes the required values of n and (average) s to smaller values of n and larger values of s.

The Ultra-Speed x-ray film was chosen for the preceding analysis primarily because of the almost complete solarization which it exhibited. In addition its curve was the most symmetrical and an attempt to match experimental and theoretical curves for the other emulsions met with little success. Those emulsions exhibit a longer shoulder than is found in the theoretical curves and their higher values of $\log I_s/I$ indicate the probability of a slightly higher value of s, perhaps a value of 128.

Obviously the much greater values of $\log I_s/I$ for the optical than for the x-ray curves indicate greater values of s/r. Webb and Evans' explanation of the dependence of the peak width upon the intensity for optical curves based on the more efficient production of solarization at higher intensities, may be applicable to the difference of x-ray and optical curves. While the instantaneous action of an x-ray quantum is similar to that of very intense visible light, the average time rate of energy absorption per grain was small. If equal areas are assumed for all grains, the density is easily found to be proportional to the number of developed grains. At $D=D_m/2$ we should expect that roughly half of the active grains would be blackened. For tests with the Ultra-Speed film the exposure differences for the two points with this value of density were from two to five hours for x-rays and less than one hour for the lowest intensity optical exposure used. For $s=64$ we obtain, very roughly, an interval of two to five minutes between successive absorptions of x-ray quanta by an individual grain.

A probable cause of the $\log I_s/I$ difference may be found in the great number of atoms formed per x-ray quantum. If the atoms deposited on a center by a single quantum are more than enough to produce developability, the grain may already be carried on the way toward solarization and the value of s/r may obviously be expected to be less than for visible light where each quantum produces only one silver atom.

Analytical Representation of Standard Response Curves

PARRY MOON AND DOMINA EBERLE SPENCER
Massachusetts Institute of Technology, Cambridge, Massachusetts
(Received November 21, 1942)

1. INTRODUCTION

IT is increasingly evident that the most satisfactory foundation for any work dealing with radiant energy is the spectroradiometric curve. Given a curve representing a spectral distribution of radiant energy, $L(\lambda)$ vs. λ, the various effects of this radiant energy can be calculated from the equation,

$$L=\int_0^\infty w(\lambda)L(\lambda)d\lambda, \qquad (1)$$

where $w(\lambda)$ is a weighting function representing the response of the particular receptor of radiant energy. It may represent the spectral response of a photo-cell, the visibility curve for the eye, the erythemal curve for human skin, or other photochemical and photoelectric effects. Three equations of this kind give the trichromatic specification of color. In all cases, the same kind of equation is used, and the integrals can be evaluated by exactly the same methods.

Ordinarily these weighting functions have been expressed as tabulated sets of values,[1] and the most important ones have been standardized and made the basis for systems of units.[2] But the representation of these important functions by tables has many disadvantages. Interpolation, which is often necessary in practice, introduces ambiguity unless the precise method of interpolation has been specified. Differentiation and integration are difficult when the functions are not expressed in analytic form. These disadvantages might be largely academic were it not for the fact that Eq. (1) is being evaluated continually in hundreds of laboratories and there is every reason to believe that the use of such integrals will continue to increase. Anything that will make the evaluation more precise and less laborious will be advantageous.

Tabulated values of $w(\lambda)$ have little theoretical basis and are determined experimentally. Like any other experimental values, they are subject to error—in the case of visual response, to very large errors because of the variability of the human organism. The standardized data can be represented by empirical equations; and the use of sufficiently complicated expressions allows the given data to be represented to any desired precision. In view of the uncertainty of the experimental data, however, a more logical way would be to *standardize a simple equation that approximates the data*, rather than to standardize the data themselves. It is hoped that such a procedure will be used in future standardization by international organizations.

It is interesting to note that all the response curves have the same general shape. At sufficiently short wave-lengths or sufficiently long wave-lengths, radiant energy has no effect. At intermediate wave-lengths, the response curve rises to one or more maxima and then declines again as λ increases. Thus the subject of analytical representation of the weighting functions used in Eq. (1) can be considered in its generality, and the type of equation found most convenient in one case will probably be satisfactory in others. The use of a single type of equation for all weighting functions has obvious practical advantages.

The purpose of the present paper is to investigate the analytic representation of weighting functions used with spectroradiometric curves. The methods apply to any of the weighting functions encountered in illuminating engineering, but attention is directed particularly to the analytic representation of the *standard lamprosity function*.[3] A number of expressions are considered

[1] "Illuminating engineering nomenclature and photometric standards," Illum. Eng. **36**, 820 (1941).

[2] Parry Moon, "A system of photometric concepts," J. Opt. Soc. Am. **32**, 348 (1942).

[3] Usually called "visibility" or "luminosity." See Parry Moon, "Basic principles in illumination calculations," J. Opt. Soc. Am. **29**, 108 (1939). It has been customary to use two distinct symbols to represent the same set of values, $v(\lambda)$ being employed in photometry and $\bar{y}(\lambda)$ in colorimetry. The two symbols represent identical relative values, on the basis of a maximum ordinate of approximately unity. There seems to be no merit in having two symbols for the same function, so in this paper $\bar{y}(\lambda)$ will indicate relative values while $v(\lambda)$ will be in lumens per watt.

and the errors are compared. Integrations are also studied and recommendations are formulated.

2. HISTORY

Of the various weighting functions, the lamprosity function $\bar{y}(\lambda)$ is the most important. A number of empirical equations have been developed to express the experimental data on $\bar{y}(\lambda)$. Goldhammer[4] in 1905 used the equation,

$$\bar{y}(\lambda)=\frac{A}{\lambda^p}e^{p(1-a/\lambda)}. \tag{2}$$

This form of equation (which, incidentally, is a special form of the Pearson Type V equation used by statisticians) has been employed by a number of investigators. Nutting[5] determined $\bar{y}(\lambda)$ experimentally and found that his data could be approximated in the range 0.48 to 0.65μ if $a=0.555\mu$ and $p=181$.

In 1916, Kingsbury[6] obtained a better fit by employing three terms of the form of Eq. (2). His equation was

$$\bar{y}(\lambda)=\frac{A_1}{\lambda^{200}}e^{-111.20/\lambda}+\frac{A_2}{\lambda^{400}}e^{-186.00/\lambda}+\frac{A_3}{\lambda^{1000}}e^{-610.00/\lambda}, \tag{3}$$

where

$$\log A_1=\ 35.87343,$$
$$\log A_2=\ 39.30106,$$
$$\log A_3=218.6020.$$

The formula approximates the data of Ives and Kingsbury over the range 0.40 to 0.76μ.

In 1924, the values of $\bar{y}(\lambda)$ recommended by Gibson and Tyndall[7] were standardized by international agreement,[8] and the question of analytic representation of the new data arose. Tyndall and Gibson[9] found a four-term expression which represented the standard data to within approximately one percent of the maximum ordinate of the curve over the range 0.43 to 0.72μ. The equation, similar to that of Kingsbury, is

$$\bar{y}(\lambda)=\frac{A_1}{\lambda^{200}}e^{-111.00/\lambda}+\frac{A_2}{\lambda^{550}}e^{-333.85/\lambda}+\frac{A_3}{\lambda^{2000}}e^{-1046.0/\lambda}+\frac{A_4}{\lambda^{630}}e^{-294.21/\lambda}, \tag{4}$$

where

$$\log A_1=\ 35.71296,$$
$$\log A_2=118.5296,$$
$$\log A_3=304.4053,$$
$$\log A_4=\ 63.84921.$$

Walsh[10] modified the numerical values in Eq. (4) and obtained a better fit to the standard data. His equation is

$$\bar{y}(\lambda)=\frac{A_1}{\lambda^{220}}e^{-122.32/\lambda}+\frac{A_2}{\lambda^{700}}e^{-427.00/\lambda}+\frac{A_3}{\lambda^{2000}}e^{-1046.0/\lambda}+\frac{A_4}{\lambda^{350}}e^{-166.25/\lambda}, \tag{5}$$

where

$$\log A_1=\ 39.45907,$$
$$\log A_2=152.7582,$$
$$\log A_3=304.5747,$$
$$\log A_4=\ 37.58620.$$

A different type of equation was developed by Houstoun.[11] The curve of $\bar{y}(\lambda)$ vs. λ resembles a Gaussian probability curve, though it is slightly skewed, while the probability curve is symmetric about its mean. Houstoun found that this skewness could be introduced into the calculations by making a transformation of the independent variable. He used the equation,

$$\bar{y}(\lambda)=A\exp\left[\frac{(\log\lambda-\log\lambda_0)^2}{2\sigma^2}\right]. \tag{6}$$

[4] D. A. Goldhammer, "Die Farbenempfindlichkeit des Auges und die photometrische Helligkeit der leuchtenden Körper," Ann. d. Physik **16**, 621 (1905).
[5] P. G. Nutting, "The luminous equivalent of radiation," Bull. Bur. Stand. **5**, 261 (1908–9).
[6] E. F. Kingsbury, "A spectral luminosity curve equation and its use," Phys. Rev. **7**, 161 (1916).
[7] K. S. Gibson and E. P. T. Tyndall, "Visibility of radiant energy," Sci. Pap. Bur. Stand. **19**, 131 (1924); Trans. I. E. S. **19**, 176 (1924).
[8] Commission Internationale de l'Eclairage, Geneva, Switzerland, 1924. See report by E. C. Crittenden, Trans. I. E. S. **19**, 607 (1924).
[9] E. P. T. Tyndall and K. S. Gibson, "Visibility of radiant energy equation," J. Opt. Soc. Am. **9**, 403 (1924).
[10] J. W. T. Walsh, "Visibility of radiant energy equation," J. Opt. Soc. Am. **11**, 111 (1925).
[11] R. A. Houstoun, "The visibility of radiation and dark adaptation," Phil. Mag. **10**, 416 (1930). "Color vision," Phil. Mag. **11**, 565 (1931). *Vision and Color Vision* (Longmans, Green and Company, London, 1932), p. 81.

TABLE I. The standard lamprosity function.

λ	Standard	Tyndall and Gibson (1)	Tyndall and Gibson (2)	Tyndall and Gibson (3)	Tyndall and Gibson (4)	Walsh (4)	Houstoun (1)	Probability (1)	Pearson (1)
0.38μ	4400	7789	7789	7789	7789	5456	5365	4961	6409
0.39	3120	6778	6778	6778	6778	4383	4189	3261	5327
0.40	3400	5601	5601	5601	5601	3231	4854	3671	4209
0.41	2120	4379	4379	4379	4379	2104	3331	2163	3110
0.42	2400	3193	3193	3193	3193	2355	2112	2373	3477
0.43	1116	3815	3815	3815	3815	2952	2336	2807	2176
0.44	1230	2289	2289	2289	1149	1207	2893	1165	2552
0.45	1380	2550	2550	2550	1330	1370	1212	1318	1151
0.46	1600	1232	1232	1232	1580	1610	1456	1580	1360
0.47	1910	1531	1531	1531	1900	1920	1888	1999	1763
0.48	0139	0108	0108	0108	0138	0136	0158	0163	0144
0.49	0208	0196	0196	0197	0215	0207	0257	0250	0247
0.50	0323	0320	0320	0329	0337	0322	0386	0362	0383
0.51	0503	0474	0474	0509	0509	0501	0537	0496	0543
0.52	0710	0641	0641	0704	0704	0707	0695	0643	0710
0.53	0862	0797	0797	0851	0851	0855	0840	0785	0861
0.54	0954	0917	0919	0943	0943	0943	0951	0907	0972
0.55	0995	0982	0987	0992	0992	0994	1.014	0989	1.027
0.56	0995	0982	0985	0985	0985	0997	1.020	1.018	1.021
0.57	0952	0922	0949	0949	0949	0950	0971	0991	0960
0.58	0870	0817	0863	0863	0863	0863	0877	0910	0855
0.59	0757	0686	0752	0752	0752	0752	0755	0790	0725
0.60	0631	0547	0626	0626	0626	0629	0620	0647	0587
0.61	0503	0417	0498	0498	0498	0503	0487	0501	0456
0.62	0381	0303	0376	0376	0376	0378	0366	0366	0340
0.63	0265	0212	0268	0268	0268	0265	0265	0253	0244
0.64	0175	0143	0181	0181	0181	0168	0184	0165	0169
0.65	0107	1925	0116	0116	0116	0103	0124	0102	0114
0.66	1610	1581	1707	1707	1707	1580	1803	1592	1740
0.67	1320	1353	1414	1414	1414	1320	1504	1325	1469
0.68	1170	1209	1236	1236	1236	1160	1306	1169	1289
0.69	2820	1120	1120	1120	1120	2840	1181	2827	1174
0.70	2410	2671	2671	2671	2671	2450	1104	2383	1102
0.71	2210	2367	2367	2367	2367	2240	2578	2167	2587
0.72	2105	2196	2196	2196	2196	2116	2318	3692	2331
0.73	3520	2103	2103	2103	2103	3576	2167	3270	2183
0.74	3250	3526	3526	3526	3526	3272	3865	4994	3993
0.75	3120	3265	3265	3265	3265	3130	3438	4344	3531
0.76	4600	3133	3133	3133	3133	4604	3217	4114	3279

Houstoun fitted the equation to various sets of data. For the C.I.E. standard data, he found

$$\bar{y}(\lambda) = 1.024 \exp\left[-\frac{(\log \lambda - \bar{1}.7451)^2}{2(0.0330)^2}\right]$$

$$= 1.024 \exp\left[-\frac{(\ln \lambda + 0.586929)^2}{2(0.075986)^2}\right]. \quad (7)$$

The differences between experimental and calculated values were as much as 3 percent of the maximum ordinate with the Ives data and somewhat more for the C.I.E. data. Thus the Houstoun expression, though simpler than Eqs. (4) and (5), does not give as good a fit.

These various empirical expressions for $\bar{y}(\lambda)$ were apparently worked out to satisfy the intellectual curiosity of the originators, with little idea of possible applications. In fact, the assumption seems to be made universally that the only way that Eq. (1) can be evaluated is by the crude and time-consuming methods of mechanical quadrature. The present paper will show that analytic representation of the weighting functions can be of practical value.

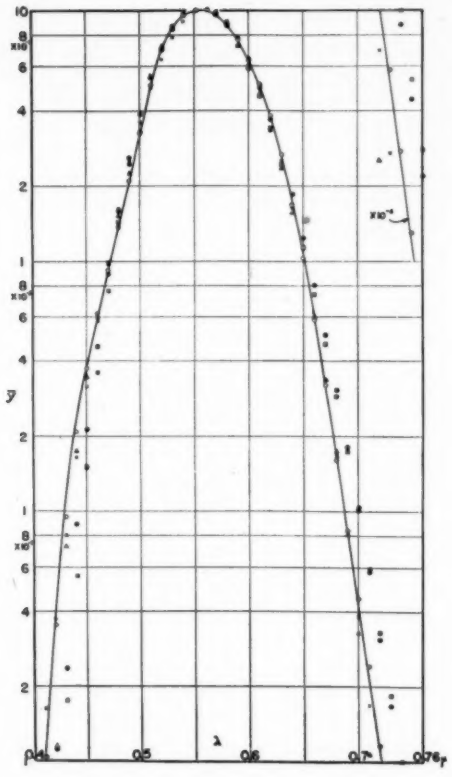

FIG. 1. Standard lamprosity curve and various analytic approximations. — standard C. I. E. curve; ○ computed by Walsh equation; ● Houstoun; × probability; □ Pearson; △ composite.

3. COMPARISON OF ANALYTICAL EXPRESSIONS

Previous equations that have been used in expressing weighting functions were discussed in Section 2. The shapes of the experimental response curves are similar to the "frequency distributions" of statistical theory. Thus it seems reasonable to apply the standardized methods of the statisticians to the present problem. There are two well-known methods of this kind: the Gram-Charlier method,[12] in which the function is expressed as a sum of Hermite functions, and the Pearson method,[13] in which any one of a number of single-term expressions may be used. A comparison will now be given between the standard data for $\bar{y}(\lambda)$ and the values calculated by means of various equations.

Table I gives the results. A superscript indicates the number of zeros after the decimal point. For instance, $^{2}120 = 0.00120$. The numbers in parentheses at the top of the columns show the number of terms in the analytical expression. The second column gives the standard C.I.E. data. The third column indicates the calculated values obtained from the first term only of Eq. (4). Similarly, the Tyndall and Gibson columns marked (2), (3), and (4) give results obtained from Eq. (4) by using 2, 3, and 4 terms, respectively. The improved representation of Walsh, Eq. (5), four terms, is tabulated in the seventh column. Houstoun's expression, Eq. (7), is employed in calculating the eighth column.

The Gram-Charlier method expresses an arbitrary function $f(z)$ in the series:

$$f(z) = c_0\varphi_0(z) + c_1\varphi_1(z) + c_2\varphi_2(z)\cdots, \qquad (8)$$

where c_0, c_1, $\cdots$ are constants and $\varphi_0(z)$, $\varphi_1(z)$, $\cdots$ are

$$\varphi_0(z) = H_0(z)\exp[-z^2/2],$$
$$\varphi_1(z) = -H_1(z)\exp[-z^2/2],$$
$$\varphi_2(z) = H_2(z)\exp[-z^2/2],$$
$$\cdots\cdots\cdots$$

with $H_n(z)$ the nth Hermite polynomial. It is customary to evaluate the constants by use of first, second, third, and fourth moments,[12] and to eliminate c_1 and c_2 by suitable transformation of variable. Then Eq. (8) becomes, for the lamprosity curve,

$$\bar{y}(\lambda) = c_0\varphi_0(\lambda) + c_3\varphi_3(\lambda) + c_4\varphi_4(\lambda) \qquad (9)$$

and

$$\varphi_0(\lambda) = (1/2\pi\sigma)\exp[-\tfrac{1}{2}(\lambda-\lambda_0/\sigma)^2], \qquad (10)$$

where λ_0 = mean wave-length, σ = standard deviation.

Use of the standard lamprosity data from 0.41

[12] C. V. L. Charlier, *Die Grundzüge der mathematischen Statistik* (Hamburg, 1920). A. Fisher, *Mathematical Theory of Probabilities* (Macmillan, New York, 1930). N. R. Jørgensen, *Undersøgelser over Frequensflader og Korrelation* (København, 1916).

[13] K. Pearson, "Supplement to a memoir on skew variation," Roy. Soc., Phil. Trans. **197A**, 446 (1901). W. P. Elderton, *Frequency Curves and Correlation* (Cambridge University Press, 1938).

to 0.71μ, inclusive, taken at 0.01μ intervals, gave the following values:

$$\lambda_0 = 0.560168\mu,$$

$$\sigma = 0.0418466,$$

$$\varphi(\lambda) = \frac{1}{0.0418466(2\pi)^{\frac{1}{2}}} \exp\left[-\frac{1}{2}\left(\frac{\lambda - 0.560168}{0.0418466}\right)^2\right],$$

$$c_0 = 0.106832,$$

$$c_3 = -5.14385 \times 10^{-4},$$

$$c_4 = 6.21915 \times 10^{-5}.$$

The first term is the ordinary Gaussian probability function, and it can be shown that the method used evaluates λ_0 and σ to give the best possible fit to the data on the basis of least squares. The next term of Eq. (9) skews the curve, while the final term broadens the curve symmetrically or makes it more peaked, depending on the sign of c_4. Unfortunately for the present purpose, $\varphi_3(\lambda)$ and $\varphi_4(\lambda)$ are negative over part of the range of λ, and the calculated values of $\bar{y}(\lambda)$ are found to be negative at some places near the ends of the visible spectrum. Though the use of all terms of Eq. (9) may be beneficial on the least-squares basis, the photometrist will object to negative values. Thus the elegant mathematical method of Gram and Charlier will be abandoned in this paper.

There remains, however, the use of the Gaussian probability function alone, which according to Eq. (9) gives

$$\bar{y}(\lambda) = 1.0185 \exp\left[-\frac{1}{2}\left(\frac{\lambda - 0.560168}{0.0418466}\right)^2\right]. \quad (11)$$

True, this function is symmetric about the mean while the standard curve is slightly skew. Nevertheless, Eq. (11) gives a reasonably good representation of the data and is particularly valuable at the long wave-lengths. The values calculated by means of Eq. (11) are tabulated under the heading, "Probability."

Of the twelve types of Pearson curves,[13] the one that seems best fitted for the representation of radiometric weighting functions is Type V:

$$\bar{y}(\lambda) = \frac{A_1}{\lambda^p} e^{-q/\lambda}. \quad (12)$$

Moments were used in the ordinary way, giving the values,

$$p = 182.19050,$$
$$q = 100.93700,$$
$$\log A_1 = 32.41070.$$

For computation, Eq. (12) is most conveniently employed in the form,

$$\log \bar{y} = 32.41070 - 182.19050 \log \lambda - 43.83638/\lambda. \quad (12a)$$

Wave-length is expressed in microns, as in other parts of this paper. Values calculated according to Eq. (12a) are given in the "Pearson" column on Table I.

The results of Table I are plotted in Fig. 1. The curve is a plot of the standard lamprosity

TABLE II. The composite curve.

λ	$\bar{y}(\lambda)$ Standard	Composite
0.40	$^{3}400$	000
0.41	$^{2}120$	$^{3}268$
0.42	$^{3}400$	$^{2}215$
0.43	$^{1}116$	$^{2}728$
0.44	$^{1}230$	$^{1}174$
0.45	$^{1}380$	$^{1}344$
0.46	$^{1}600$	$^{1}605$
0.47	$^{1}910$	$^{1}986$
0.48	$^{0}139$	$^{0}152$
0.49	$^{0}208$	$^{0}226$
0.50	$^{0}323$	$^{0}325$
0.51	$^{0}503$	$^{0}544$
0.52	$^{0}710$	$^{0}721$
0.53	$^{0}862$	$^{0}854$
0.54	$^{0}954$	$^{0}945$
0.55	$^{0}995$	$^{0}992$
0.56	$^{0}995$	$^{0}997$
0.57	$^{0}952$	$^{0}958$
0.58	$^{0}870$	$^{0}876$
0.59	$^{0}757$	$^{0}751$
0.60	$^{0}631$	$^{0}602$
0.61	$^{0}503$	$^{0}460$
0.62	$^{0}381$	$^{0}336$
0.63	$^{0}265$	$^{0}235$
0.64	$^{0}175$	$^{0}157$
0.65	$^{1}925$	$^{1}999$
0.66	$^{1}581$	$^{1}600$
0.67	$^{1}353$	$^{1}337$
0.68	$^{1}209$	$^{1}174$
0.69	$^{1}120$	$^{2}811$
0.70	$^{2}671$	$^{2}327$
0.71	$^{2}367$	$^{2}107$
0.72	$^{2}196$	$^{3}254$
0.73	$^{2}103$	$^{4}333$
0.74	$^{3}526$	$^{4}104$
0.75	$^{3}265$	000

values, while the points calculated by the various formulas are represented by circles, crosses, and squares. By far the most accurate representation of the data is Walsh's equation, but this equation has four terms of complicated form. The three single-term expressions—Houstoun, probability, and Pearson—are on a par. Of the three, the probability function gives worst representation near the peak of the curve, but extraordinarily good representation for $0.65 \leqq \lambda \leqq 0.72\mu$. The logarithmic transformation advocated by Houstoun does not seem to be appreciably better than the unmodified probability curve.

4. A COMPOSITE CURVE

All previous methods have attempted to obtain a single expression for the complete lamprosity curve from $\lambda=0$ to $\lambda=\infty$. But, unfortunately, none of the elementary functions is represented by curves of the desired shape; and thus investigators have been forced to use probability functions and other complicated expressions.

An entirely different attack on the problem is obtained by breaking the curve into three parts and representing each by a simple analytic expression. This method has the obvious disadvantages that (a) there is no longer a single equation which can be used at all wave-lengths, and (b) the integrations involve finite limits. On the other hand, the expressions are easily calculated and the integrations are all very simple.

It was decided to express all curves by polynomials in λ. The visible region was broken into three wave-length bands: 0.400 to 0.500μ, 0.500 to 0.590μ, and 0.590 to 0.750μ. The three expressions were found to be

$$0.400 \leqq \lambda \leqq 0.500\mu,$$

$$\bar{y}(\lambda) = 268(\lambda - 0.400)^3 + 5.7 \times 10^4 (\lambda - 0.400)^6, \quad (13)$$

$$0.500 \leqq \lambda \leqq 0.590\mu,$$

$$\bar{y}(\lambda) = 1.000 - 215.24(\lambda - 0.556)^2, \quad (14)$$

$$0.590 \leqq \lambda \leqq 0.750\mu,$$

$$\bar{y}(\lambda) = 1.05 \times 10^4 (0.750 - \lambda)^5 - 5.0906 \times 10^6 (0.750 - \lambda)^9. \quad (15)$$

Values calculated by means of these equations are listed in Table II, which indicates that the errors obtained with the composite representation are not markedly different from those of Table I. The calculated values are indicated by triangles in Fig. 1.

5. INTEGRATION

Sections 3 and 4 have treated various analytic representations of the standard lamprosity curve and have evaluated the errors introduced by these expressions. The evaluation of integrals containing the foregoing functions will now be considered. The integrals are of the form,

$$L_l = \int_a^b \bar{y}(\lambda) L(\lambda) d\lambda. \quad (16)$$

The lamprosity function $\bar{y}(\lambda)$ is expressed in the various forms considered previously, while $L(\lambda)$ may have almost any form. However, there are certain functions of common occurrence that can be used in many practical cases.

The two types of functions $L(\lambda)$ that will be employed are

$$L(\lambda) = \sum_{m=0}^{\infty} K_m \lambda^m \quad (17)$$

and

$$L(\lambda) = \sum_{n=1}^{\infty} K_n x^5 e^{-nx}, \quad (18)$$

where $x = C_2/\lambda T$. Equation (17) includes as special cases the equal-energy spectrum, the linear variation, and other simple expressions. Moreover, all experimental curves obtained in practice can be approximated by using a sufficiently large number of terms of this power series.

Equation (18) is employed in the treatment of radiation from incandescent radiators. For temperatures up to approximately 3000°K, the Wien radiation equation may be used:

$$L(\lambda) = \frac{C_1}{\lambda^5} \exp\left[-\frac{C_2}{\lambda T}\right], \quad (18a)$$

which is a special case of Eq. (18) with $n=1$, $K_1 = C_1(C_2/T)^{-5}$. For higher temperatures, the

more general equation of Planck must be employed:

$$L(\lambda)=\frac{C_1}{\lambda^5}\frac{1}{\exp[C_2/\lambda T]-1}. \quad (19)$$

But Eq. (19) can be expressed as a series of terms of the Wien form, or

$$L(\lambda)=C_1\left(\frac{C_2}{T}\right)^{-5}x^5[e^{-x}+e^{-2x}+e^{-3x}+\cdots], \quad (20)$$

which is again of the form of Eq. (18). This series converges for all values of x greater than zero. Thus unmodified radiation from incandescent radiators can be handled by use of Eq. (18), while other $L(\lambda)$ curves can be expressed by Eq. (17).

All lamprosity curves considered in the previous sections can be expressed by one or more terms of the following four types:

$$\text{(I)} \quad \bar{y}(\lambda)=A\exp[-(\lambda-a)^2/2\sigma^2], \quad (21)$$

$$\text{(II)} \quad \bar{y}(\lambda)=A\exp[-(\ln\lambda-c)^2/2\sigma^2], \quad (22)$$

$$\text{(III)} \quad \bar{y}(\lambda)=(A/\lambda^p)e^{-q/\lambda}, \quad (23)$$

$$\text{(IV)} \quad \bar{y}(\lambda)=B_n(\lambda-b)^n. \quad (24)$$

The first three always enter into integrals with infinite limits, which greatly simplifies the integration. The fourth type is used in the composite representation and thus requires finite limits for the integration.

(I) Consider first the integral of Eq. (16) with $\bar{y}(\lambda)$ and $L(\lambda)$ given by Eqs. (21) and (17). The terms will be of the form,

$$L_l=A_1K_m\int_0^\infty\lambda^m\exp[-(\lambda-a)^2/2\sigma^2]d\lambda. \quad (25)$$

Let $x=(\lambda-a)/\sigma$. Then

$$L_l=A_1K_m\sigma^{m+1}\int_{-\infty}^{\infty}(x+a/\sigma)^m\exp[-x^2/2]dx. \quad (25a)$$

The lower limit, corresponding to $\lambda=0$, becomes $x=-a/\sigma$. But this quantity is always so large that the corresponding integrand is practically zero. Thus the lower limit is essentially $-\infty$. Expansion by the binomial theorem gives

$$\begin{aligned}L_l=A_1K_m\sigma^{m+1}\Big[&\int_{-\infty}^{\infty}x^m\exp[-x^2/2]dx\\&+m(a/\sigma)\int_{-\infty}^{\infty}x^{m-1}\exp[-x^2/2]dx\\&+\frac{m(m-1)}{2!}(a/\sigma)^2\int_{-\infty}^{\infty}x^{m-2}\exp[-x^2/2]dx\\&+\cdots+(a/\sigma)^m\int_{-\infty}^{\infty}\exp[-x^2/2]dx\Big]. \quad (25b)\end{aligned}$$

Note that when m is odd, the integrals are zero. If m is even, the integrals become

$$\begin{aligned}&\int_{-\infty}^{\infty}\exp[-x^2/2]dx=(2\pi)^{\frac{1}{2}},\\&\int_{-\infty}^{\infty}x^r\exp[-x^2/2]dx=1\cdot3\cdot5\cdots(r-1)(2\pi)^{\frac{1}{2}},\end{aligned} \quad (26)$$

where $r=2, 4, 6, \cdots$. There seems to be no satisfactory way of using the Wien or Planck equation with the probability curve.

(II) The Houstoun representation of the lamprosity curve can be handled in a similar way. Equations (22) and (17) give

$$L_l=A_1K_m\int_0^\infty\lambda^m\exp[-(\ln\lambda-c)^2/2\sigma^2]d\lambda. \quad (27)$$

Let $\ln\lambda-c=\sigma x$. Then

$$\begin{aligned}L_l&=A_1K_m\sigma e^{c(m+1)}\int_{-\infty}^{\infty}e^{\sigma(m+1)x}\exp[-x^2/2]dx\\&=A_1K_m\sigma e^{c(m+1)}\exp\left[\frac{\sigma^2(m+1)^2}{2}\right]\\&\quad\times\int_{-\infty}^{\infty}\exp\{-\tfrac{1}{2}[x-\sigma(m+1)]^2\}dx\\&=(2\pi)^{\frac{1}{2}}A_1K_m\sigma\exp\left[c(m+1)+\frac{\sigma^2(m+1)^2}{2}\right]. \quad (27a)\end{aligned}$$

Again there is no simple way of using the Wien equation in the integration.

(III) With the Pearson representation, Eqs.

(23) and (17) give

$$L_l = A_1 K_m \int_0^\infty \lambda^{m-p} e^{-q/\lambda} d\lambda. \tag{28}$$

If $q/\lambda = z$,

$$L_l = A_1 K_m q^{m-p+1} \int_0^\infty z^{p-m-2} e^{-z} dz.$$

But

$$\int_0^\infty x^r e^{-ax} dx = \frac{\Gamma(r+1)}{a^{r+1}}, \tag{29}$$

TABLE III. The equal-energy spectrum. $L(\lambda) = 1.00000$.

Method	L_l	Percent error
Summation, 0.001μ steps	0.10687	0.00
Summation, 0.01μ steps	0.10686	0.01
Selected ordinates (30)	0.10686	0.01
Probability	0.10683	0.04
Houstoun	0.10621	0.62
Pearson	0.10683	0.04
Walsh	0.10636	0.48
Composite	0.10586	0.94

so Eq. (28) becomes

$$L_l = A_1 K_m \frac{\Gamma(p-m-1)}{q^{p-m-1}}. \tag{28a}$$

With the Wien equation and the Pearson representation, Eqs. (23) and (18a) lead to

$$L_l = A_1 C_1 \int_0^\infty \lambda^{-(p+5)} \exp\left[-(q+C_2/T)\frac{1}{\lambda}\right] d\lambda. \tag{30}$$

Let $(q+C_2/T)\dfrac{1}{\lambda} = z$. Then Eq. (30) becomes

$$L_l = \frac{A_1 C_1}{(q+C_2/T)^{p+4}} \int_0^\infty z^{p+3} e^{-z} dz$$

$$= A_1 C_1 \frac{\Gamma(p+4)}{(q+C_2/T)^{p+4}}. \tag{30a}$$

Similarly, if the more general expression of Eq. (18) is used instead of the Wien equation,

$$L_l = A_1 C_1 (C_2/T)^{-(p+4)} \int_0^\infty x^{p+3} \times \exp\left[-(n+qT/C_2)x\right] dx$$

$$= A_1 C_1 \frac{\Gamma(p+4)}{(q+C_2 n/T)^{p+4}}. \tag{30b}$$

Another interesting case occurs when Planckian radiation is reflected from a surface having the reflection factor,

$$\rho = \sum_{m=0}^{\infty} a_m \lambda^m. \tag{31}$$

Then

$$L_l = A_1 C_1 \left(\frac{C_2}{T}\right)^{-(p+4)} \sum_{m=0}^{\infty} \sum_{n=1}^{\infty} \int_{x=0}^{x=\infty} a_m \lambda^m x^{p+3} \times \exp\left[-(n+qT/C_2)x\right] dx$$

$$= A_1 C_1 \left(\frac{C_2}{T}\right)^{-(p+4-m)} \sum_{m=0}^{\infty} \sum_{n=1}^{\infty} \int_0^\infty a_m x^{p+3-m} \times \exp\left[-(n+qT/C_2)x\right] dx. \tag{32}$$

The terms are of the form,

$$L_l = A_1 C_1 a_m \left(\frac{C_2}{T}\right)^{-(p+4-m)} \int_0^\infty x^{p+3-m} \times \exp\left[-(n+qT/C_2)x\right] dx$$

$$= A_1 C_1 a_m \frac{\Gamma(p+4-m)}{(q+C_2 n/T)^{p+4-m}}. \tag{33}$$

(IV) With the composite curve and with $L(\lambda)$ given by Eq. (17), all integrals are of the form,

$$L_l = K_m B_n \int_a^b \lambda^{m+n} d\lambda = \frac{K_m B_n}{m+n+1} \times (b^{m+n+1} - a^{m+n+1}). \tag{34}$$

TABLE IV. Three-term energy distribution. $L(\lambda) = 8.1802 - 36.512\lambda + 41.285\lambda^2$.

Method	L_l
Summation, 0.01μ steps	0.080743
Selected ordinates (30)	0.080340
Probability	0.080587
Pearson	0.080407
Pearson, Planckian 1999°K	0.080600

When the Wien equation is used with the composite curve,

$$L_l = C_1 B_n \int_a^b \lambda^{n-5} e^{-C_2/\lambda T} d\lambda$$

$$= C_1 B_n \left(\frac{C_2}{T}\right)^{n-4} \int_{C_2/Tb}^{C_2/Ta} \frac{e^{-z} dx}{x^{n-3}}. \tag{35}$$

But

$$\int x^m e^{-x}dx = -x^m e^{-x} + m\int x^{m-1}e^{-x}dx,$$

so

$$L_l = -C_1 B_n \left(\frac{C_2}{T}\right)^{n-4} Ei(-x), \quad n=4,$$

$$L_l = C_1 B_n \left(\frac{C_2}{T}\right)^{n-4}\left[-x^{3-n}e^{-x} + (3-n)\int x^{2-n}e^{-x}dx\right], \quad n\leqq 3, \quad (36)$$

$$L_l = -C_1 B_n \left(\frac{C_2}{T}\right)^{n-4}\left[\frac{e^{-x}}{x^{n-4}} + \int \frac{e^{-x}dx}{x^{n-4}}\right], \quad n\geqq 5.$$

The calculations are carried out without difficulty by use of tables that are now available. Among these tables may be mentioned the new W.P.A. tables of the exponential function[14] and the probability function.[15] Gamma functions for arguments up to 1200 are obtained from Peters' table[16] or from Fry's book on probability,[17] making use of the relation,

$$\Gamma(m) = (m-1)!$$

Gamma functions for arguments over 1200 (or for lower values if tables are not available) are calculated by Stirling's formula:

$$\Gamma(x) = (2\pi)^{\frac{1}{2}}(x-1)^{x-\frac{1}{2}}e^{-(x-1)} \times\left[1+\frac{1}{12(x-1)}+\frac{1}{288(x-1)^2}+\cdots\right],$$

which may be written

$$\log\Gamma(x) = 0.39908993 + (x-\tfrac{1}{2})\log(x-1) - 0.4342945(x-1) + \log\left[1+\frac{1}{12(x-1)}+\cdots\right]. \quad (37)$$

The exponential integral $Ei(-x)$, which is needed in the composite representation is also obtainable in tabulated form.[18]

[14] *Tables of the Exponential Function* e^x (Nat. Bur. Stand., Washington, 1939).
[15] *Tables of Probability Functions* (Nat. Bur. Stand., Washington, 1941), Vol. I.
[16] J. Peters, *Zehnstellige Logarithmen* (Berlin, 1922), Vol. I, Table 6.
[17] T. C. Fry, *Probability and Its Engineering Uses* (Van Nostrand Company, New York, 1928), p. 429.
[18] *Tables of Sine, Cosine, and Exponential Integrals* (Nat. Bur. Stand., Washington, 1940), Vol. I.

6. COMPARISON OF INTEGRATIONS

In practice, integrals as given by Eq. (16) are evaluated with the greatest variety of $L(\lambda)$ functions. Because of this variety, the question of what analytic representation of $\bar{y}(\lambda)$ gives the best results has no exact meaning. The only way of comparing the various expressions for $\bar{y}(\lambda)$, as regards their accuracy in integrations, is to choose arbitrarily a number of representative functions $L(\lambda)$ and to carry through the necessary numerical work. The following functions were taken:

(1) $L(\lambda)=1$ (equal-energy spectrum),
(2) $L(\lambda)=8.1802-36.512\lambda+41.285\lambda^2$,
(3) Planckian distributions for 3500, 5500, and 7000°K,
(4) Planckian radiation (3500°K) reflected from a brown surface:
$$\rho = 1.630\lambda - 0.620.$$

TABLE V. Planckian distribution. ($C_2=14320$).

T	Method	L_l
3500°K	Simpson's rule	47.704
	Summation, 0.01μ steps	47.686
	Pearson	47.674
5500	Summation, 0.01μ steps	684.8540
	Pearson	685.2781
7000	Summation, 0.01μ steps	1903.428
	Pearson	1904.543
Linear reflection factor and Planckian distribution		
3500	Summation, 0.01μ steps	14.5311
	Pearson	14.5147

The results for the equal-energy spectrum are given in Table III. The common method of summation of ordinates at 0.01μ wave-length intervals makes use of the standard C.I.E. lamprosity values. The same procedure was then used at 0.001μ steps by employing Judd's interpolated values.[19] Thirty selected ordinates[20] gave essentially the same result. The other values were

[19] D. B. Judd, "Extension of the standard visibility function to intervals of 1 millimicron by third-difference osculatory interpolation," J. Opt. Soc. Am. **21**, 267 (1931). Z. Yamauti, "Interpolation of the standard visibility function with one millimicron steps," Res. Elec. Lab. Tokyo, No. 388 (1935).
[20] Bowditch and Null, "Selected ordinates for computing trichromatic coefficients and candlepower of a light source," J. Opt. Soc. Am. **28**, 500 (1938).

calculated by use of the equations developed in Section 5. The greatest error is seen to be less than one percent.

The three-term distribution (2) is a typical example of a more complicated energy distribution. The coefficients were evaluated to give an approximation to a Planckian distribution with $T=1999°\text{K}$ and with unit ordinate at $\lambda=0.590\mu$. Table IV presents the calculated results. The first four values were obtained from Eq. (17), while the last was obtained by assuming a Planckian distribution and the Pearson representation of $\bar{y}(\lambda)$. The maximum spread of the values is only about one-half of one per cent.

Results for Planckian distributions[21] are given in Table V. A brown reflecting surface is also used, in conjunction with 3500° Planckian radiation. The analytic expression for the reflection factor approximates the experimental curves for light reflected from stained oak flooring. In all cases, good agreement is obtained between the direct summation and the Pearson representation.

TABLE VI. Calculated values of lamprosity.

λ	$v(\lambda)$	λ	$v(\lambda)$
0.360μ	^{5}1877 2959 lumens/watt	0.580μ	530.8 7780 lumens/watt
0.365	^{5}7082 6548	0.585	491.8 0649
0.370	^{4}2492 4529	0.590	450.2 2067
0.375	^{4}8207 8409	0.595	407.4 4272
0.380	^{3}2537 0436	0.600	364.6 6103
0.385	^{3}7382 0296	0.605	322.8 9332
0.390	^{2}2027 4751	0.610	282.9 6635
0.395	^{2}5269 6998	0.615	245.5 1029
0.400	^{1}1299 3479	0.620	210.9 6546
0.405	^{1}3046 3279	0.625	179.5 9817
0.410	^{1}6805 9567	0.630	151.5 2291
0.415	^{0}1451 9893	0.635	126.7 2800
0.420	^{0}2963 8306	0.640	105.1 0224
0.425	^{0}5799 2218	0.645	86.46 0806
0.430	1.089 6380	0.650	70.56 8814
0.435	1.969 3477	0.655	57.16 1920
0.440	3.429 1427	0.660	45.96 3324
0.445	5.761 4680	0.665	36.69 7208
0.450	9.353 9409	0.670	29.09 8745
0.455	14.69 4989	0.675	22.92 1036
0.460	22.36 8043	0.680	17.93 9433
0.465	33.03 0480	0.685	13.95 3723
0.470	47.37 4941	0.690	10.78 8666
0.475	66.07 3036	0.695	8.293 3110
0.480	89.70 4423	0.700	6.339 4870
0.485	118.6 7749	0.705	4.819 7761
0.490	153.1 5048	0.710	3.645 2234
0.495	192.9 6360	0.715	2.742 9718
0.500	237.5 9253	0.720	2.053 9570
0.505	286.1 3218	0.725	1.530 7514
0.510	337.3 1605	0.730	1.135 6108
0.515	389.5 7229	0.735	^{0}8387 4884
0.520	441.1 1271	0.740	^{0}6168 4458
0.525	490.0 4654	0.745	^{0}4517 7565
0.530	534.5 0754	0.750	^{0}3295 5887
0.535	572.7 8157	0.755	^{0}2394 7724
0.540	603.4 2166	0.760	^{0}1733 6948
0.545	625.3 3969	0.765	^{0}1250 5833
0.550	637.8 6691	0.770	^{1}8989 5250
0.555	640.7 7944	0.775	^{1}6440 1513
0.560	634.2 8885	0.780	^{1}4598 7520
0.565	619.0 0170	0.785	^{1}3273 5306
0.570	595.8 5443	0.790	^{1}2323 1205
0.575	566.0 3182	0.795	^{1}1643 8075
		0.800	^{1}1159 8389

[21] Parry Moon, "A table of Planck's function from 3500 to 8000°K," J. Math. Phys. **16**, 133 (1937); M. I. T., E. E. Contr. No. 131 (1938).

7. THE RECOMMENDED LAMPROSITY FUNCTION

Comparison of the foregoing data shows that an expression of Pearson Type V fits the standard lamprosity data reasonably well and allows integration to be performed analytically with errors that are generally a small fraction of one percent. The probability function and the Houstoun expression are discarded because of difficulty with some of the integrations, while the composite curve and the Walsh formula are rejected because of their complexity.

We suggest, therefore, that a new standard lamprosity function be defined by the equation,

$$v(\lambda)=\frac{A}{\lambda^{p}}\epsilon^{-q/\lambda}\ \text{(lumens/watt)}, \qquad (12b)$$

where

$$\log A = 35.2037916,$$
$$p=182.19050,$$
$$q=100.93700.$$

The wave-length λ is expressed in microns and the relative values $\bar{y}(\lambda)$ used previously have been multiplied by 621 to give $v(\lambda)$ in lumens per watt. It seems more logical to define $v(\lambda)$ completely in one equation than to use the old method of a relative $\bar{y}(\lambda)$ in conjunction with a physical standard of candlepower. The analytic definition of $v(\lambda)$ also has advantages over the old definition in terms of a table of values, since the new method eliminates all ambiguity about interpolation, is more compact, and allows analytic integration and differentiation. New values, calculated from Eq. (12b), are given in Table VI. It should be realized that these values *do not constitute the proposed standard* but only illustrate the use of Eq. (12b). The employment of eight significant figures may seem strange to those who still think of $v(\lambda)$ as an experimentally determined curve. The essence of the new proposal, however, is that $v(\lambda)$ is the *mathematical function*

TABLE VII. Examples of calculations for Planckian radiators. $C_1=36970$, $C_2=14320$, $p=182.19050$, $q=100.9370$, $\log[621C_1A\cdot\Gamma(p+4)]=380.81916$.

n	$\frac{14320n}{7000}$	$\left[q+\frac{14320n}{7000}\right]$	log [ ]	186.1905 log [ ]	log L_l	L_l
$T=7000°K$						
1	2.04571	102.98270	2.012 7643	374.75759	6.06157	1.1523×10^6
2	4.09143	105.02842	2.021 3069	376.34814	4.47102	29581
3	6.13714	107.07413	2.029 6846	377.90799	2.91117	815.06
4	8.18286	109.11985	2.037 9038	379.43833	1.38083	24.035
5	10.22857	111.16557	2.045 9703	380.94023	1.87893	0.75669
					Total=	1.1827×10^6 lumens/cm²
$T=3500°K$						
1	4.09143	105.02842	2.021 3069	376.34814	4.47102	29581
2	8.18286	109.11985	2.037 9038	379.43833	1.38083	24.035
					Total = 29605 lumens/cm²	

that relates the photometric and radiometric units. As such it can be calculated to any number of decimal places and is *correct by definition*, irrespective of how many of these figures are significant in present practice.

The standard lamprosity function $v(\lambda)$ provides the connecting link between the photometric and radiometric units. As soon as a standard lamprosity function, expressed in lumens per watt, is defined, all photometric quantities are automatically placed on a physical basis and no separate standard of candlepower is needed or allowed. Thus, if $L(\lambda)$ represents the ordinate of a spectroradiometric curve, expressed in watt micron^{-1}, watt m^{-2} micron^{-1}, watt m^{-2} steradian^{-1} micron^{-1}, or other physical units, the corresponding photometric quantity is defined as

$$L_l=\int_0^\infty v(\lambda)L(\lambda)d\lambda. \tag{16a}$$

If $L(\lambda)$ is represented by a power series,

$$L(\lambda)=\sum_{m=0}^{\infty}K_m\lambda^m, \tag{17}$$

then each term of the resulting series is of the form,

$$L_l=AK_m\frac{\Gamma(p-m-1)}{q^{p-m-1}}. \tag{28b}$$

Equation (28b) may be calculated by using logarithms:

$$\log L_l=35.203\ 7916-2.004\ 0505(181.19050-m)+\log\Gamma(181.19050-m)+\log K_m. \tag{28c}$$

If the radiation is Planckian,

$$L(\lambda)=\frac{C_1}{\lambda^5}\frac{1}{\exp[C_2/\lambda T]-1}, \tag{19}$$

then Eq. (16a) becomes

$$L_l=AC_1\sum_{n=1}^{\infty}\frac{\Gamma(p+4)}{(q+C_2n/T)^{p+4}}. \tag{30c}$$

The terms have the form,

$$\log L_l=380.819\ 158-186.19050\times\log(100.9370+14320n/T). \tag{30d}$$

The Wien equation results in the special case of Eq. (30c) with $n=1$.

If Planckian radiation is reflected from a surface having the reflection factor,

$$\rho=\sum_{m=0}^{\infty}a_m\lambda^m, \tag{31}$$

the terms have the form,

$$L_l=AC_1a_m\frac{\Gamma(p+4-m)}{(q+C_2n/T)^{p+4-m}}. \tag{33a}$$

Equation (33a) may be written

$$\log L_l=39.771\ 654+\log\Gamma(186.19050-m)+\log a_m-(186.19050-m)\times\log(100.93700+14320n/T). \tag{33b}$$

Table VII gives two examples of calculations made with the aid of the foregoing equations, showing the simplicity of integrations by the new method. Table VIII indicates the lumens per unit area of blackbody and the lumens per watt

for Planckian radiation, the calculations being made by Eq. (30d).

Equation (12b) is also easily differentiated. The slope of the curve of $v(\lambda)L(\lambda)$ for

$$L(\lambda)=K_m\lambda^m$$

is

$$\frac{d(vL)}{d\lambda}=\left[-\frac{(p-m)}{\lambda^{p-m+1}}+\frac{q}{\lambda^{p-m+2}}\right]AK_me^{-q/\lambda}$$

$$=\frac{AK_m}{\lambda^{p-m+2}}[-\lambda(p-m)+q]e^{-q/\lambda}. \quad (38)$$

TABLE VIII. Planckian radiation calculated by means of Eq. (16a).

T	Lt (lumen cm^{-2})	Lumens per watt
1000°K	9.0436×10^{-4}	1.584×10^{-4}
1500	2.3794×10^{0}	0.08233
2000	138.80	1.520
2500	1662.4	7.454
3000	8868.5	19.18
3500	29605	34.56
4000	73551	50.33
4500	1.4985×10^{5}	64.01
5000	2.6565×10^{5}	74.45
6000	6.3584×10^{5}	85.94
7000	1.1827×10^{6}	86.28
8000	1.9071×10^{6}	81.56
9000	2.7848×10^{6}	74.35
10000	3.7931×10^{6}	66.44
20000	1.7810×10^{7}	19.50

The wave-length λ_m at which the curve has its maximum is obtained by equating to zero, or

$$\lambda_m=\frac{q}{p-m}=\frac{100.9370}{182.1905-m}. \quad (38a)$$

For $m=0$, $\lambda_m=0.554\,0190$, which gives the wave-length corresponding to the lamprosity function itself, Eq. (12b).

For the Wien equation,

$$L(\lambda)=(C_1/\lambda^5)\exp[-C_2/\lambda T],$$

$$v(\lambda)L(\lambda)=\frac{AC_1}{\lambda^{p+5}}\exp\left[-\frac{1}{\lambda}\left(\frac{C_2}{T}+q\right)\right],$$

and the slope of the curve is

$$\frac{d}{d\lambda}(vL)=\frac{AC_1}{\lambda^{p+7}}\left[\left(\frac{C_2}{T}+q\right)-\lambda(p+5)\right]$$

$$\times\exp\left[-\frac{1}{\lambda}\left(\frac{C_2}{T}+q\right)\right]. \quad (39)$$

The wave-length λ_m for the maximum of the curve is therefore

$$\lambda_m=\frac{C_2/T+q}{p+5}=\frac{100.9370+14320/T}{187.1905}$$

$$=0.5392207+76.49961/T. \quad (39a)$$

For Planck's equation,

$$v(\lambda)L(\lambda)=\frac{AC_1}{\lambda^{p+5}}\frac{e^{-q/\lambda}}{\exp[C_2/\lambda T]-1}$$

and the slope of the curve is

$$\frac{d}{d\lambda}(vL)=\frac{AC_1e^{-q/\lambda}}{\lambda^{p+7}(\exp[C_2/\lambda T]-1)^2}$$

$$\times\left\{[q-\lambda(p+5)]\left(\exp\left[\frac{C_2}{\lambda T}\right]-1\right)\right.$$

$$\left.+\frac{C_2}{T}\exp\left[\frac{C_2}{\lambda T}\right]\right\}. \quad (40)$$

The wave-length λ_m corresponding to the peak of the vL curve is obtained from the equation,

$$q-\lambda_m(p+5)=[q-\lambda_m(p+5)+C_2/T]$$

$$\times\exp[C_2/\lambda_m T]$$

or

$$\exp[14320/\lambda_m]$$

$$=\frac{100.9370-187.1905\lambda_m}{100.9370-187.1905\lambda_m+14320/T}. \quad (41)$$

For $T<5000$°K, Eq. (39a) is accurate enough for most purposes. For higher temperatures, Eq. (39a) is an approximation, which is substituted into Eq. (41) and a cut-and-try process is used to obtain the correct λ_m. Values calculated in this way are given in Table IX. The foregoing treatment shows that the recommended lamprosity function results in simple formulas for integration and differentiation.

8. POSSIBLE OBJECTIONS

There are two ways in which the proposed lamprosity function can be introduced:

(1) The old tabulated data for $v(\lambda)$ can be scrapped and *the new lamprosity function of Eq.* (12b) *can be established by international agree-*

ment.[22] This will give for the first time an absolutely unambiguous specification of all photometric magnitudes. The function $v(\lambda)$ can be calculated to as many decimal places as desired and will be correct by definition. Analytic differentiation and integration are easily performed.

(2) The present C.I.E. data for $v(\lambda)$ can be kept as standard, and Eq. (12b) can be employed as a *convenient approximation.*

The advantages of the first proposal over the second have already been pointed out. The idea is sufficiently radical, however, to shock many who have grown accustomed to the present photometric methods and who feel that the proposal would replace experimental data by pure empiricism. Against such a criticism, one may consider the following facts:

(*a*) Any experimental data for $v(\lambda)$ are dependent on size of field, illumination of field, size and condition of surround, experimental method used,[7] the observer and his physiological condition at the time of the test.[23] Thus *any standardized set of* $v(\lambda)$ *data must necessarily be arbitrary* to a great extent. It makes comparatively little difference what $v(\lambda)$ function is used, provided it is convenient and is agreed upon by all photometrists.

(*b*) Even under the specialized conditions used in obtaining the C.I.E. data, there is a question as to their accuracy. Ratios of v for the mercury lines, for example, do not agree with the C.I.E. data,[24] according to a number of investigators. The careful research of Jainski[25] indicates marked departures from the standard curve. Preston's recent work[26] shows discrepancies of as much as 11 percent. Guild[27] also mentions difficulties with the standard data.

(*c*) Data obtained by averaging readings obtained with many observers differ from average data presented by other qualified investigators by as much as 15 percent of the maximum ordinate of the $v(\lambda)$ curve.[6] The proposed lamprosity function differs from the C.I.E. values by less than six percent.

(*d*) Lamprosity values obtained by *individuals* who appear to have "normal" color vision differ by even larger amounts.[7] The only reason that visual photometry has been at all feasible is that the lights being compared have been usually associated with continuous spectra having approximately the same spectral distribution.

Pending the approval of the proposed lamprosity function, there still remains the possibility of using Eq. (12b) as a convenient approximation. The principal objection to this idea will be on the grounds of inaccuracy. If the requirement be set up that the proposed function shall represent the standard data at every wave-length with negligible error, so that homogeneous radiation can be evaluated in accordance with the present C.I.E. standard, then even Walsh's complicated expression fails. But this restriction is so stringent that even the established method is of little value. For example what is $\bar{y}$ at

TABLE IX. λ_m for radiation from incandescent sources.

T	Wien distribution, Eq. (39a)	Planck distribution, Eq. (41)
1000°K	0.6157μ	0.6157μ
1500	0.5902	0.5902
2000	0.5775	0.5775
2500	0.5698	0.5698
3000	0.5647	0.5647
3500	0.5611	0.5611
4000	0.5583	0.5583
4500	0.5562	0.5562
5000	0.5545	0.5546
6000	0.5520	0.5522
7000	0.5501	0.5504
8000	0.5488	0.5492
9000	0.5477	0.5482
10000	0.5469	0.5475
20000	0.5430	0.5445

[22] These suggestions have no official sanction and are merely the personal opinions of the authors. It may seem visionary in 1943 to mention international agreement; but a little thought will indicate that the present is an excellent time to initiate a program, for it will allow time to assess the merits of the proposal in the U. S. and to determine if it should be submitted to the C. I. E.

[23] A. Dresler, "Über eine jahreszeitliche Schwankung der Spektralen Hellempfindlichkeit," Das Licht, 10 (1940).

[24] K. S. Gibson, "Spectral luminosity factors," J. Opt. Soc. Am. **30**, 51 (1940). W. Arndt, "Über neue Beobachtungen beim subjektiven Photometrieren," Das Licht **6**, 75 (1936). M. Jaggi, "Beitrag zur Kenntnis der spektralen Hellempfindlichkeit des menschlichen Auges," Helv. Phys. Acta **12**, 77 (1939).

[25] P. Jainski, "Die spektrale Hellempfindlichkeit des menschlichen Auges und ihre Bedeutung für die Lichtmesstechnik," Diss. Tech. Hochschule, Berlin (1938).

[26] J. S. Preston, "The relative luminosity of radiation for the average observer," Proc. Phys. Soc. London **51**, 757 (1939).

[27] J. Guild, "The colorimetric properties of the spectrum," Phil. Trans. Roy. Soc. London **230A**, 149 (1932).

$\lambda=0.406$? Linear interpolation between the nearest C.I.E. values (0.00040 at 0.40μ and 0.0012 at 0.41μ) gives 0.00088, which differs from Judd's interpolated value by 24 percent. The value of Judd,[19] obtained by third-order osculatory interpolation, is 0.00071; while Yamauti's value[19] (obtained by third-order osculatory interpolation of the logarithms, which is at least as legitimate a method) is 0.00077. Thus two highly refined methods of interpolation give values that differ by 8 percent. If the reader still feels that experimental results must be the guide, he need only examine some of these results, such as those of Gibson and Tyndall.[7] At 0.430μ, $\bar{y}$ for individual observers ranged from 0.014 to 0.064, or over 50 percent variation on each side of the mean. At $\lambda=0.700\mu$, a similar range was obtained, with values from 0.0028 to 0.0069, experimental conditions being identical in all cases.

If, on the other hand, one is interested in continuous spectra instead of homogeneous radiation, the proposed function is amply accurate for practical purposes, as indicated in Tables III to V. Moreover, the ordinary methods of mechanical integration are not above reproach. The summation of equally spaced ordinates does not give the exact value of the integral, nor does the selected-ordinate method. In some cases, appreciable errors are introduced by neglecting values at wave-lengths beyond 0.76μ, and these values are neglected because the C.I.E. specifies no way of obtaining $v(\lambda)$ at such wave-lengths. The errors of the summation method were calculated for a typical example and it was found that the discrepancy caused by summation at 0.01μ intervals was approximately the same as that caused by use of the proposed analytic function. The error caused by neglect of the spectrum beyond 0.76μ was about half as great as that caused by the summation method.

Thus for homogeneous radiation near the ends of the spectrum, even the present established methods are inadequate; while for continuous spectra, the proposed analytic representation leads to discrepancies that are no more serious than those caused by the usual methods of mechanical integration. This fact answers the objection that the standardization of Eq. (12b) would render obsolete a great mass of previous data which was based on the C.I.E. tabulated values. In most practical cases, results obtained by the two methods differ by less than the experimental error and the two methods can be employed interchangeably.

It is true that very complicated spectral distributions obtained experimentally will still be integrated mechanically because of the complexity of the empirical equations required to express the data. But even in such cases the analytic treatment may be useful in obtaining the wave-lengths used in the selected-ordinate method. In theoretical work dealing with light and color, analytical representation will allow powerful methods of analysis to be applied where previously only numerical investigations were possible.

9. SUMMARY

Various analytic representations of radiometric weighting functions are considered in the paper. In particular, a simple equation is found to approximate the standard lamprosity (visibility) data for the human eye. It is suggested that the present tabulated values of $v(\lambda)$ and $\bar{y}(\lambda)$ be replaced[22] by the *proposed standard equation*,

$$v(\lambda)=\frac{A}{\lambda^p}\epsilon^{-q/\lambda},$$

where the constants are as stated in Section 7 of this paper.

Such a procedure would have the following advantages: (1) It would increase precision. The whole system of photometric units rests on the standard $v(\lambda)$ function. But at present this function is specified by the C.I.E. only at intervals of 0.01μ. No standard method of interpolation is specified, and no method of extrapolation for wave-lengths beyond the tabulated ones.[23] The specification of a standard equation would eliminate all doubts as to the value of $v(\lambda)$ at any wave-length. (2) It would eliminate the need for standardization of a method of inter-

[23] The Illuminating Engineering Society (ref. 1) recommends the Judd interpolated values but still leaves the question of extrapolation undecided. The C. I. E. has not changed its original specification of $v(\lambda)$ at intervals of 0.01μ.

polation and extrapolation. The labor entailed in using one of these complicated methods of interpolation may be greater than that required for the direct computation by means of the proposed equation. (3) It would simplify integrations in which the spectroradiometric curve can be expressed analytically.

Pending standardization, the equation for $v(\lambda)$ can be used as a *convenient approximation* to the C.I.E. data. With continuous spectra, the analytic integrations generally agree with numerical integrations (using the C.I.E. data) to within a small fraction of one percent. Analytic differentiation is also possible, and both integration and differentiation will be of value in theoretical investigations of light and color, which have been handicapped by lack of analytic representation of the functions. That the same form of equation is useful for other standard weighting functions will be shown in another paper which considers the analytic representation of the standard trichromatic data. Other interesting applications would be to the scotopic curve of vision and to the erythemal curve.

Mercury Arc Lamps: Effect of Electrode on Energy Distribution

WILLIAM THEODORE ANDERSON, JR.[1]
Hanovia Chemical and Manufacturing Company, Chestnut Street and New Jersey Railroad Avenue, Newark, New Jersey
(Received October 24, 1942)

THE spectral energy distribution of radiation from quartz lamps with high pressure mercury vapor arcs is known to be influenced by the vapor pressure, physical structure, and electrical characteristics of the lamps. It was generally considered that if two lamps had approximately the same physical structure, the same vapor pressure, the same electrical input, and equal total radiant energy emission, and if the quartz glass of the envelope was of equal quality, then the spectral energy distribution of the radiations from the two lamps would be very similar. It was therefore somewhat surprising to discover that in some instances variations in the chemical nature of the electrodes and alterations in the electrode temperature, other variables being approximately equal, resulted in very dissimilar distribution of energy in the spectrum.

In order to establish this observation, two lamps were constructed with great care that all physical and electrical characteristics were nearly identical. The quartz bodies were made of selected fused quartz, worked to very close tolerances, and of equal radiation transmission. The electrodes were made of stranded tungsten wire. Each electrode weighed about 0.2 gram. Each lamp had two electrodes, one in each end of a straight arc tube. One lamp was designated Type A. Its electrodes were coated with a very thin layer of barium metal. Such electrodes are known as "activated electrodes" because the coating which is only a very small fraction of the total mass of the electrode reduces the work function of the electrode, e.g., in the particular instance from 4.53 to 1.1 volts. As a result the barium-coated electrode emits the required number of electrons at a much lower temperature than the pure tungsten electrode. The other lamp was designated Type B. Its electrodes were pure tungsten. Both lamps were filled with equal quantities of mercury vapor and argon gas. They were operated in turn upon the same electrical control circuit. A dimensional design of the lamps is shown in Fig. 1.

Careful examination of the test lamps disclosed that physically with respect to volume, surface area, mass, quartz wall thickness, and electrode mass they were similar. (See Table I.)

The average electrode temperatures were evaluated by optical pyrometry at the instant when the lamps were extinguished and are probably somewhat in error because of complicating factors such as uneven temperatures on electrode, rapidity of cooling, and dissimilarity in cooling rate. The quartz temperature was determined by thermopile immediately after the lamp was extinguished, a correction based upon a cooling curve of the lamp being applied.

MEASUREMENT OF RADIATION

The total radiation from the lamps and the radiation in spectral regions were determined by methods which had been painstakingly developed by the Laboratory during many years of experimentation. The spectral response curves of photo-cells, the transmission of glass filters, the spectral energy distribution of the light sources, and the calibration of thermopiles in absolute

TABLE I. Operating characteristics of test lamps.

	Lamp A	Lamp B
Electrical supply—no load volts	330	330
Terminal volts when normal operation	141	142
Current through lamp—amperes	2.75	2.80
Watts in lamp (by wattmeter)	350	357(Note)
Note: At these wattages, the lamps emitted *equal total* radiant energy.		
Work function of electrodes—volts	1.1	4.53
Average electrode temperature—Centigrade	900	2600
Electrode operates as incandescent type	Activated	*Non*-activated
Quartz tube temperature—Centigrade	342	344
Electrode and convection losses (by difference)—watts	120	127
Total radiant energy—watts	230	230

[1] Contribution from Laboratory, Hanovia Chemical and Manufacturing Company, Newark, New Jersey.

units had all been carefully measured and had been rechecked many times during the past 15 years.[2,3]

A detailed description of these methods would be voluminous and would detract from the object of this paper. However, a brief description of each method will be given so that one familiar with the art can follow the procedure.

Corrections for filter transmissions, photo-cell responses, reflection losses, and reflection gains were applied equally for both Lamps A and B. Every effort was made to minimize the errors which are always present in radiation measurement and to make the evaluation of the two lamps truly comparable.

1. Total Radiation

This comprises all wave-lengths of radiant energy from the lamp which produce response from a thermopile and should not be confused with the total radiant energy from the lamps referred to in Table I. The receivers were Adam Hilger bismuth-silver thermopiles with surface blackened by spermwhale oil soot. A sensitive microammeter was the indicating device. The piles were non-selective with respect to wave-length and were calibrated in absolute energy units by reference to Radiation Standard Bulbs Nos. 38 and 201 provided by the National Bureau of Standards and in accordance with the Bureau's specifications.[4] One-microampere reading on the meter represented 180 microwatts per sq. cm of radiant energy. The piles were also calibrated with a galvanometer for applications requiring greater sensitivity, one-millimeter deflection on a scale at two meters distance representing 1.45 microwatt per sq. cm of radiant energy when the temperature of the galvanometer was 26 degrees C.

When making measurements, the pile receiver was located 75 cm from the arc and on an axis through the center of the arc and perpendicular to it. The energy on the pile receiver included infra-red from the hot quartz and metal fittings.

[2] Wm. T. Anderson, Jr. and L. F. Bird, Phys. Rev. **32**, 293 (1928).

[3] Anderson, Fraser, and Bird, J. Opt. Soc. Am. **17**, 454 (1928).

[4] Thermopiles calibrated in Newark with the guidance of Mr. R. Stair, the National Bureau of Standards, through the courtesy of the Director of the Bureau and Dr. W. W. Coblentz, Radiometric Physicist.

2. Short Ultraviolet (1850–3200 Angstroms)

The measuring device was Hanovia Ultraviolet Meter No. 1073[2,5,6] which is non-selective for the spectral range 2300 to 3200 angstroms and nearly so for 1850 to 2300 angstroms. It is in structure a fluorescence photometer with a seasoned photronic cell to register the energy of green fluorescence and a glass filter and balancing cell to produce on the accompanying micro-

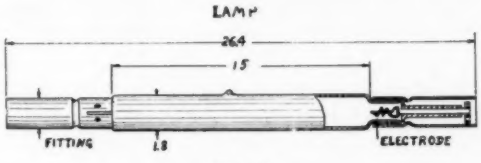

FIG. 1.

ammeter a zero reading for any radiations in the visible green not resulting from the fluorescence produced by ultraviolet 3200 angstroms and shorter wave-length. Before use, the constancy of the photronic cell was checked by readings made with the meter of the radiation from a standard quartz mercury arc.[7]

As an additional check upon the radiant energy in the spectral region 2500 to 2700 angstroms, a tantalum photo-cell with peak response at 2600A was employed.[8,9]

3. Long Ultraviolet (3200–4100 Angstroms)

The "long ultraviolet" from the mercury arc has most of its energy in the three bands at about 3340, 3660, and 4045 angstroms. The energy in this region was determined by the difference between two measurements:

(a) The measuring device was a RÇA No. 929 vacuum caesium cell with a response of 61 percent at 3340, 93 percent at 3660, 100 percent at 3800, 74 percent at 4045, and in the visible 58 percent at 4360, 12 percent 5460–5790, 0 at 6100A. All the radiation through a glass filter,

[5] Lester F. Bird, U. S. Patent No. 2,114,163 (April 12, 1938).

[6] National Bureau Standards Test No. 90,337 (October 10, 1940).

[7] National Bureau Standards Test No. 84,682 (January 20, 1939).

[8] H. C. Rentschler, Trans. Electrochem. Soc. **71**, 1 (1937).

[9] Rentschler, Henry, and Smith, Rev. Sci. Inst. **3**, 794 (1932).

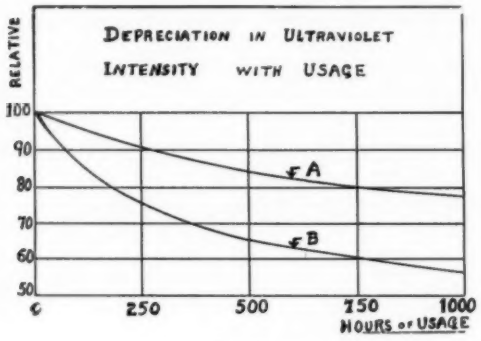

FIG. 2.

5-mm thickness, of Corning No. 774 (Chemical Pyrex) was measured on the cell, employing in the evaluation the calibration of the filter and cell, and the relative spectral energy distribution of the lamps as determined by monochromator and thermopile. The filter transmitted 90 percent of each wave-length 3660A to 6100A, inclusive, 77 percent at 3340A, and a trace of 3130A, which, however, did not register upon the photo-cell.

(b) The unwanted radiations, namely visible, were measured by interposing a filter of Corning 038 Noviol A glass, 3.2-mm thickness, which had zero transmission for the 4045 band and all ultraviolet, 58 percent transmission for 4360 band, and 78 percent for green, yellow, red, and infra-red to 14,000A. The necessary corrections were applied.

4. Visible and Short Infra-Red (4100–10,000A)

The energy in this region was determined by difference between two measurements:

(a) The thermopile was the measuring device. The Noviol A filter described in 3(a) provided the short wave-length cut-off. A quartz cell with plane polished surfaces 1 cm apart and filled with freshly distilled water provided a cut-off at 14,000A. Necessary corrections for reflection and transmission losses were made. The transmission of the watercell was 78 percent except near the cut-off at 14,000A.

(b) A black glass filter, Corning 254, 3.5-mm thickness, with short wave-length cut-off at 10,000A, and transmitting 61 percent of the radiations between 10,000 and 14,000A was interposed, and the unwanted radiations between 10,000 and 14,000A were determined. Necessary corrections were applied.

5. Long Infra-Red (10,000A and Greater)

This includes radiations from the arc, the hot mercury vapor, the hot quartz envelope, and the fittings. The radiation from the arc is principally in the bands at 10,140, 11,287, 13,570, 13,673, and 36,492 angstroms. The energy in this region was determined by three readings, the difference between (a) and (b) being added to (c).

(a) The thermopile was the measuring device. The black filter described in 4(b) was employed. The arc was operating.

(b) Conditions were as in 5(a). The reading was noted, the lamp extinguished, and a reading made on the galvanometer each 5 seconds as the lamp cooled. The 5-second interval readings were plotted and the curve was extrapolated to zero seconds, which represents the energy from hot quartz, fittings, etc.

(c) The measurement described in 5(b) was repeated with the filter glass removed. This result includes long wave-length infra-red which would not pass through the black filter.

All the foregoing measurements were made at a distance of 75 cm from the arcs and the results were expressed in microwatts per sq. cm.*

With measurements which involved so many calibrations and corrections, it is not to be supposed that results in the four regions would

TABLE II. Relative energy in mercury emission bands (4045A = 100).

Wave-length in angstroms	Lamp A	Lamp B
11,287	80	85
10,140	152	168
5790	310	327
5460	195	205
4360	155	162
4045	100	100
3660	286	274
3130	195	162
2652	82	56
2537	102	54

* The author was assisted in the calibrations of the filters and in the determination of the relative spectral energy distribution of the Lamps A and B by Mr. Lester F. Bird, physicist of this laboratory.

total to exactly the measured total radiation. In order to minimize the error, five absolutely independent measurements were made for each region, the equipment being newly assembled and aligned each time, and the average was taken. The averages were altered by ±1 percent in order to make the totals exactly equal the measured total radiation.

In order to determine the radiation in watts of electrical input, it was necessary to map by means of a photo-cell, the radiation field of equal radiant energy per unit area about the lamp. The field was found to resemble in form a pumpkin, the lamp being on the stem line through the center. By graphical means it was found that the pumpkin could be replaced by a sphere of radius 67.5 cm and that the lamp could be considered to be a point source located at the center of the sphere. The arrangement was such that the radiant energy measured in watts per sq. cm on a line 75 cm from the center of the arc could be considered the energy per sq. cm on the surface of the sphere. The total radiant energy from the lamp and the total energy in each spectral region were then the unit energy values multiplied by the area of the sphere.

In Table II are given the corrected relative distributions, for the Lamps A and B as measured by monochromator and thermopile, of some of the principal bands of the mercury spectrum. The band at 4045A is indicated "100" for both lamps, which was an arbitrary arrangement for means of comparison. It so happened that under the operating conditions, the energy in this band was equal for the two lamps.

TABLE III. Spectral energy distribution of radiant energy in watts from new lamps.

Type A activated	Watts input	Watts radiated	Angstroms 1850 to 3200	3200 to 4100	4100 to 10,000	10,000 and higher
A	350	230	39.0	25.5	45.5	120
2	350	229	39.7	25.8	45.0	119
3	362	241	41.2	26.7	47.0	126
4	355	233	40.1	25.7	45.9	122
Percent distribution	100		17.1	11.2	19.6	52.0
Type B non-activated						
B	357	230	27.8	24.8	46.4	131
6	360	231	28.0	24.9	46.5	132
7	352	227	27.4	24.2	46.3	129
8	350	226	27.1	24.0	45.9	129
Percent distribution	100		12.1	10.7	20.1	57.1

The difference between the two lamps' output at wave-length 2537A was nearly 100 percent, Lamp A with activated electrodes emitting nearly twice as much energy at this wave-length as Lamp B with non-activated electrodes.

Energy measurements made in the long wave-length infra-red suggest that Lamp B was radiating the energy lost from the ultraviolet as infra-red. In order to establish this and to

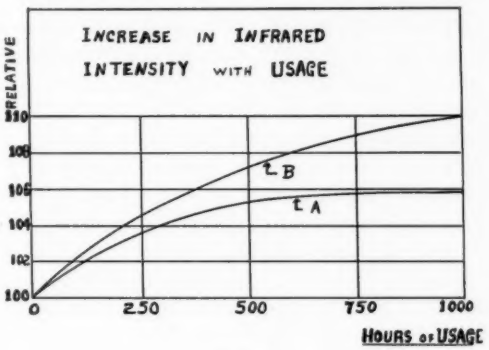

FIG. 3.

eliminate the possibility that the additional infra-red resulted from the higher temperature and greater losses of the electrodes of Lamp B, the long infra-red from both Lamps A and B was determined (1) with the entire lamp and fittings exposed to the thermopile; (2) with only the central 3 centimeters of the 15-cm length of arc tube exposed to the pile. The two ratios of the infra-red of Lamp B to Lamp A should indicate the probable origin of the additional infra-red from Lamp B. When these measurements were made, these ratios were found to be:

for the entire lamps, 1.091,
for 3 cm arc tube, 1.080.

Allowing for errors of measurement, this indicates that between 85 and 90 percent of the additional infra-red from Lamp B originates in the arc and from the arc tube and not at the electrodes.

It would be interesting to know the mechanism whereby the states of ionization and energy levels of the mercury atoms are altered by the mere substitution of one type of electrode for another. Or is an explanation to be sought in alterations in convection currents which occur

in all gaseous media and which are affected by temperature gradients? No attempt was made in this investigation to establish the causes for the effects observed.

In order to substantiate further the results indicated by the study of Lamps A and B, three additional lamps of each type, but of commercial tolerances, were obtained and measured for radiation output. The results for these six lamps and Lamps A and B have been grouped together in Table III. The measurements are in excellent agreement and suggest that when the short wave-length ultraviolet of the mercury spectrum is wanted, the lamp should have activated electrodes of low work function.

In order to study changes that may occur during operation, the six additional lamps were put on life test and the short ultraviolet and infra-red components were measured at approximately 250, 500, 750, and 1000 hours of operation periods. One of the Type B lamps failed at about 300 hours. The results of these tests are indicated in curves *A* and *B* of Figs. 2 and 3.

Both types of lamps show a decrease in ultraviolet output with usage, but the rate and extent of decrease for Type A with activated electrodes was just about one-half that for Type B. The infra-red output increased.

When after 1000 hours, the lamps were examined, the quartz tubes were yellowed and slightly opaque, and about the electrodes were blackened. The Type B lamps with non-activated electrodes were definitely more discolored than were those of Type A with activated electrodes. Much of the discoloration appeared to be due to evaporation of the electrodes. An inspection by microscope disclosed that the inner surface of the quartz walls was covered by untold number of small solid aggregates. Electrodes evaporate as a result of electrical phenomena known as sputtering and as a result of temperature. The first results from the reluctance of an electrode surface to emit the required number of electrons and the latter from the well-known rule that substances vaporize with increasing velocity as their temperatures increase. Both with respect to sputtering and evaporation the activated electrode has a very large advantage over the non-activated electrode. These phenomena probably account for the observation that Type A lamps with activated electrodes deteriorate much slower and to a lesser extent than the Type B lamps with non-activated electrodes.

CONCLUDING REMARKS

Experiments have indicated that the work function and temperature of the electrodes in high pressure mercury arc lamps in quartz may have a marked influence upon the spectral energy distribution of the radiations. It appears that for the attainment of maximum ultraviolet output, a lamp should be provided with activated electrodes of low work function and operating at low electrode temperatures.

The rate of depreciation of a lamp in ultraviolet output is influenced by the operating temperatures of its electrodes and their ability to provide the necessary electron emission at low temperatures. Activated electrodes with low work function decrease the rate of lamp depreciation.

Some Observations on the Use of Powders in Spectrochemical Analysis*

A. E. RUEHLE† AND E. K. JAYCOX
Bell Telephone Laboratories, Inc., New York, New York

IN applying spectrochemical methods to solutions or to samples which can be readily dissolved, it has become common practice to aliquot a portion of the solution directly to the supporting electrode and dry it there, thus ensuring a completely representative test portion. While this is probably the best procedure for many analyses, the authors have encountered cases where it has proved advantageous to take the solution to dryness apart from the electrode. This permits additional operations, such as the admixture of a buffer, which result in improved reproducibility in arcing. Such operations have been used by many workers in the analysis of minerals and other refractory materials, but only a few seem to have deliberately converted soluble materials to the form of dried salts for such treatment. Among the exceptions are Lewis[1] and Slavin[2] who used sulfates, Breckpot[3] and Hasler[4] who used oxides, Smith[5] who used chlorides, and the present authors[6] who used nitrates. Of these Smith worked on lead-tin solders, using dried chlorides in calibrating solid standards. He encountered difficulty with aluminum and suggested the use of sulfates or nitrates to overcome the trouble. The nitrate-oxide method described below has been employed for several years in the routine analysis of solders and the results amply verify Smith's deduction.

Among the advantages of using dried salts are the following:

1. A buffer may be intimately mixed with the sample. For example, purified carbon dust tends to reduce the oxides of many of the metals, and where these differ markedly from the metals themselves in volatility there is a tendency to reduce irregularities in vaporization rate, as shown by repeated moving plates on portions of the same specimen. Another useful material for admixture is an appropriate ammonium salt[1] whose rapid decomposition provides gases for carrying the powder into the arc stream.[7]
2. Soaking of solutions into supporting electrodes is eliminated. Halowax, collodion, kerosene, etc., provide only partial protection against this, especially with strongly acid solutions. Differences in distribution of dried salt on the electrodes are minimized.
3. More sample may be employed than with solution aliquots. This is useful in determining small amounts of very volatile elements, e.g., Zn in Pb down to 0.001 percent.[6] In these cases the sample is not burned to completion. The performance of the a.c. arc with the larger samples is also sometimes better than when solutions are dried on the electrode tips.
4. The complete sample does not have to be held in solution in preparing for transferring aliquot portions. This is an advantage in such cases as lead-tin solders as described below.
5. The sample arced is more representative and the state of combination of the metals is more constant during arcing than with filings, raspings, etc., or with self-electrodes.

THE ANALYSIS OF LEAD-TIN SOLDERS

In the control of the composition of lead-tin solders, it is ordinarily necessary to determine Al, As, Bi, Cu, Fe, Ni, Sb, and Zn in addition to the lead and tin. Since solder bars are frequently quite variable in composition from point to point, it is essential to employ an adequate sampling method. It has been found that sawings taken at definite intervals on alternate sides of a bar will be sufficiently

* Presented at the Tenth Summer Conference on Spectroscopy and its Application, Massachusetts Institute of Technology, July 20–22, 1942.
† Present Address: International Minerals and Chemical Corporation, Austin, Texas.
[1] S. J. Lewis, *Spectroscopy in Science and Industry* (Blackie, London, 1933), p. 42.
[2] M. Slavin, Eng. Min. J. **134**, 509 (1933).
[3] R. Breckpot, Ann. Soc. Sci. Brux. **53**, 219 (1935).
[4] M. F. Hasler, Proceedings of the Fifth Spectroscopy Conference (1938), p. 43.
[5] D. M. Smith, Pub. No. 105 Int. Tin. Res. Inst. (1941).
[6] A. E. Ruehle and E. K. Jaycox, Proceedings of the Seventh Spectroscopy Conference (1940), p. 10–15.
[7] M. F. Hasler, J. Opt. Soc. Am. **31**, 140 (1941).

representative of the whole bar for analytical purposes. However, it is wise to dissolve all of these sawings in making the analysis. Since the sulfate and chloride of lead are insoluble and since tin dissolved in nitric acid precipitates as metastannic acid, it is impracticable to hold both of these metals in the same concentrated solution.

It was soon found that by exercising reasonable precautions homogeneous powdered salts could be readily prepared from metallic specimens. When solder is dissolved in nitric acid the tin precipitates. Lead nitrate is soluble but precipitates out before the impurities when the solution is evaporated. The mother liquor containing the impurities dried out last and the dried impurities are not uniformly distributed in the powdered mass. However, thorough grinding makes a mixture sufficiently homogeneous so that tests on portions show no deviations not accountable for as being due to variable excitation.

EXPERIMENTAL CONDITIONS FOR SOLDER ANALYSIS

1. Standards

Treat weighed portions of spectrochemically pure tin in concentrated nitric acid until all action has ceased. To the cloudy solutions add a solution of pure lead nitrate so that the lead-tin ration is that expected in the samples. Add measured amounts of nitrate solutions of each impurity so that the weight percentage of each is 0.30 percent, 0.10 percent, 0.030 percent, 0.010 percent, 0.003 percent, and 0.001 percent in the appropriate standard. To a separate portion of the tin-lead mixture add a nitric-tartaric acid solution of antimony to make a weight percentage of 1.00 percent. (If any of the other impurities are likely to be higher than 0.3 percent they should also be included in this standard.) Evaporate the standard solutions to dryness without vigorous boiling, and bake until the excess nitric acid is expelled. Transfer the residues as quantitatively as possible to an agate mortar and grind to a fine powder. Mix the complete batch of each standard thoroughly with an equal weight of purified carbon dust containing 20 percent by weight of pure ammonium nitrate. Store in screw cap vials.

2. Preparation of Samples

Weigh out approximately three grams of the granulated sample to a 100 ml beaker, and add 10 ml of 15 percent nitric acid. When the sample is dissolved take to dryness, bake, grind, and mix it with carbon dust and ammonium nitrate as described under preparation of standards.

3. Excitation and Photography

Fill $\frac{1}{8}''$ deep cups, bored in $\frac{1}{4}''$ graphite electrodes with a number 15 drill, flush to the brim with portions of the samples and standards. Arc each electrode for 60 seconds at 250 volts and 9 amperes using a radial sector at the slit or a diaphragm at the collimator to cut the light reaching the plate so the final density of the impurity lines will be suitable for densitometry. Make one extra exposure of the highest standard through the stepped sector used for plate calibration.

4. Interpretation of Plates

Scan the plates visually using the lines listed in the second column of Table I. If it is evident that the sample is within the specification limits for all impurities, the analysis is complete. If there is any doubt, however, measure the densities of the appropriate impurity and reference lines listed in Table I. Convert densities to relative intensities by means of the calibration pattern taken through the stepped sector. Plot I_X/I_{Pb} *vs.* log percent X in the standards and read percent X in the samples from the curve. Where no reference line is given in Table I plot log g_x *vs.* log percent X.

RESULTS ON SOLDERS

Precision data for the analysis of lead tin solders are given in Table II.

The method has been in use for several years in the analysis of wiping solders and has been checked repeatedly by chemical methods. In a recent round robin test conducted by the A.S.T.M., our chemical and spectrochemical laboratories obtained the results given in Table III.

While this discussion has been concerned with lead-tin alloys, the method seems also to work

FIG. 1. Moving plate studies on aluminum oxide. The first two series of spectra are without carbon dust, the second two are with carbon dust.

TABLE I.

Impurity	Impurity line (A)	Lead line (A)
Aluminum	3082.2 or 3092.7	None
Antimony	2598.1	2657.1
Arsenic	2349.8	None
Bismuth	3067.7 or 2898.0	2657.1
Iron	3020.65 or 2719.0	2657.1
Lead	2833.1 (In alloys 2663.2 other than solders)	
Nickel	3101.6	2657.1
Zinc	3345.5	3220.5
Copper	3274.0	3220.5

TABLE II.

Impurity	No. of samples	Range covered	Percent deviation
Al*			
As	1	0.116	±6.0
Bi	10	0.003–0.054	±4.7
Cu	7	0.0075–0.088	±15.1
Fe	8	0.0011–0.012	±13.7
Ni			
Sb	10	0.0025–0.75	±6.8
Zn*			

* Estimated to be ±5–15 percent by deviation of standards from working curves.

TABLE III. Analysis of B.S. No. 127 solder for impurities.

	Chemical	Spectrochemical
Al	—	0.001%
As	0.12	0.12
Bi	0.041	0.041
Cu	0.014	0.013
Fe	0.001	0.0011
Ni	0.011	0.014
Sb	0.75	0.74
Zn	—	<0.003

TABLE IV. Calcium in zirconium oxide.

Sample	Excitation	No. of determinations	Average deviation	Average	Chemical
A	d.c.	8	30%	0.054	0.060
A	a.c.	8	14%	0.058	0.060
B	d.c.	4	27%	0.026	0.090
B	a.c.	4	15%	0.083	0.090

well on tin base die-casting alloys composed of tin, antimony, and copper, and on bronzes. We have had less experience with these, however, and have not worked out internal control methods for them, merely plotting log g_x against log percent X to obtain working curves from standards on each plate.

OTHER MATERIALS

In discussing powder methods, it might be well to record some experience with certain other materials, both with d.c. arc and a.c. arc excitation. In the analysis of aluminum oxide and other refractory materials it has been customary to employ the d.c. arc and high currents in order to drive the impurities into the arc column. We have found that more satisfactory results are obtained, at least when determining sodium, potassium, and silicon, by using the 2000-volt a.c. arc. The powdered sample is mixed with carbon dust (1 : 2), put into a shallow cup, and arced at 2.0 amperes using a small diameter carbon counter electrode. The greater precision of excitation is shown by comparative moving plate studies (Fig. 1). The same technique has also been applied to analyzing zirconium oxide for calcium, magnesium, aluminum, copper, and iron with even greater success, since this analysis in the d.c. arc works very poorly. Typical data obtained using a.c. and d.c. arc excitation on one of these materials are shown in Table IV.

ACKNOWLEDGMENT

The authors are indebted to C. L. Luke for the chemical determinations and to C. W. Tucker and W. Hartmann for taking some of the experimental data.

JOURNAL OF THE OPTICAL SOCIETY OF AMERICA VOLUME 33, NUMBER 2 FEBRUARY, 1943

A Light-and-Shadow Box as a Visual Aid in Measuring Spectra

JOHN J. HOPFIELD[1]
Naval Stores Research Division, Bureau of Agricultural Chemistry and Engineering, U. S. Department of Agriculture, Washington, D. C.

(Received December 7, 1942)

THE device described below is especially useful to spectroscopists. It was developed in connection with measurement of Raman spectra of terpenes where it was found useful in improving accuracy of setting the microscope cross-hairs on a line and in reducing eyestrain of the observer. This new illuminator does not replace the regular one but is a valuable adjunct.

The method of using the light-and-shadow box is shown in Fig. 1. The microscope (1) of the comparator is pointed into the shadow part of the box (5). The spectrum plate (2) placed on the table (3) of the comparator is illuminated by a bright surface (4) or the metal reflector (4′) adjacent to the shadow and placed so that its direct light cannot be seen through the microscope. The lines of the spectrum are then seen against the black opening (5) in the light scattered by the silver grains of the plate. A lamp (6), shielded by its reflector, serves as a light source. Any kind of lamp is satisfactory, but a 15-watt fluorescent lamp was used. The distance from (4) to (6) and from (2) to (4) was about 5 inches. The spectrum may be viewed in the normal way simply by moving the surface 4 or 4′ into the field of view of the microscope.

Figure 2 shows microphotographs of a portion of a Raman spectrum of one of the terpenes being studied with the iron comparison spectrum as viewed against the light (*A*) and shadow (*B*) portions of the light-and-shadow box. The photograph shows only poorly what is actually seen. Both *A* and *B* are positive prints. From *B* it is seen that with the shadow box illumination the individual silver grains of the photographic plate appear white. This results in the dimmer spectrum lines appearing white instead of black or gray, and stronger ones black or gray framed in white. In this way heavy lines are narrowed and light ones are more easily observed, since they do not tend to vanish into the cross-hairs. The dark core also helps to locate the densest portion of asymmetrical lines and is an aid in estimating line densities. Other things not

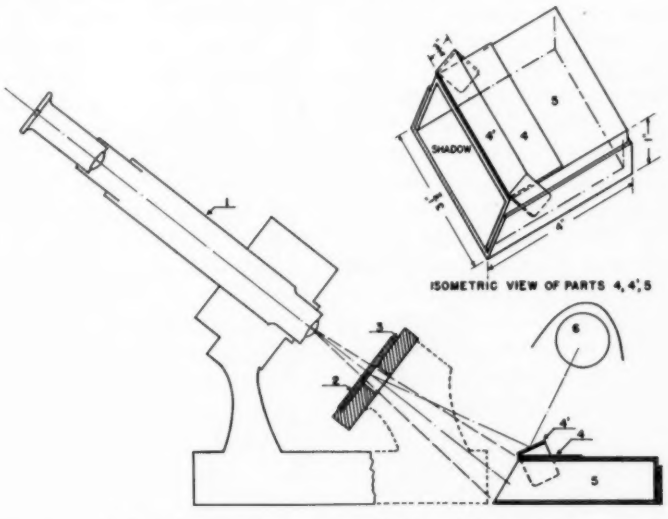

FIG. 1. Construction and use of light-and-shadow box.

[1] Now with National Bureau of Standards of the Department of Commerce, Washington, D. C.

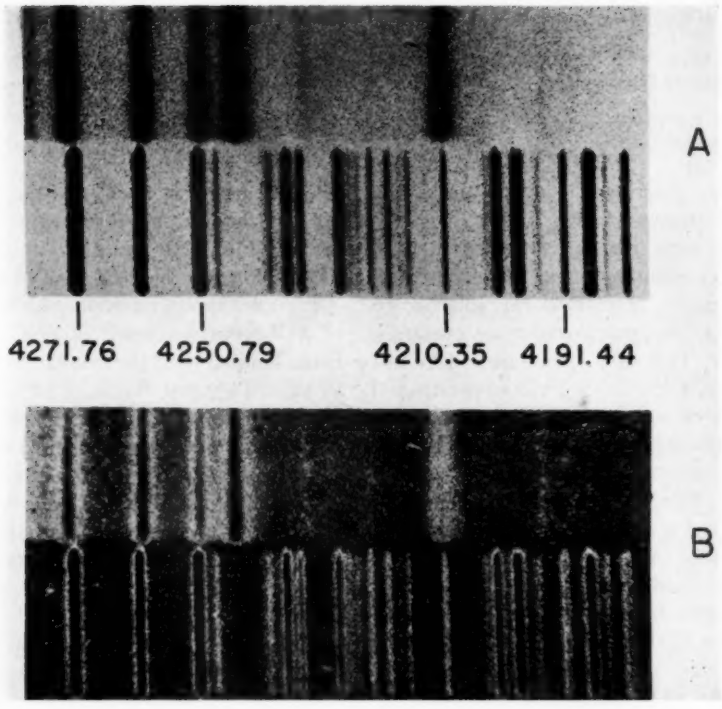

FIG. 2. Raman and iron comparison spectra viewed against the light (*A*) and shadow (*B*) portions of light-and-shadow box.

mentioned here also become apparent to the observer, e.g., one can more readily detect unresolved multiplicity of lines.

Figure 1 also shows an isometric drawing of the light-and-shadow box construction. To make it, take a box with its cover, cut off one end on the bias at an angle of about 45° and place a piece of white paper or cardboard (4) on top of it. (The cover of the box with attached white paper can be used alone if it is placed on a black surface.) It is best to have the box gray or black inside; a photographic plate box is admirable for this purpose. The open end is the shadow end. An adjustable metal reflector (4′) may be placed on top of (4) if desired. This helps to brighten the lines. A collimated light beam with an adjacent shadow can be used in a special form of the instrument. When this device is used with indirect lighting (Fig. 2) it functions best if the spectrum plates have little or no continuous background, and under conditions of room illumination which allow little or no light to fall on top of the spectrogram.

This device could, of course, be used in measuring star plates, Laüe photographs, and in viewing various microscope slides. Weak photographic negatives viewed in light from such a device appear somewhat like positives.

JOURNAL OF THE OPTICAL SOCIETY OF AMERICA VOLUME 33, NUMBER 2 FEBRUARY, 1943

New Methods of Calculating Illumination*

PARRY MOON
Massachusetts Institute of Technology, Cambridge, Massachusetts

I. INTRODUCTION

METHODS of illumination calculation are important in the design of lighting systems for rooms. At the present time, for instance, it is imperative that war plants be lighted to give adequate illumination so that work can be done with a minimum of eyestrain and visual fatigue. But this is not the extent of its practical usefulness. It is needed in meteorology, photography, and in the calculation of lens systems, projectors, and reflectors.

The subject of illumination calculation is rightly a branch of geometrical optics, but it is a branch that has never received a comprehensive treatment. Methods are fragmentary. Each investigator has worked out the procedures that were needed for his particular application, and very little work has been done to correlate and generalize these results.

Probably the outstanding attempt to present a unified treatment of illumination calculations was made by Lambert in his classical book[1] on photometry, published in 1760. Naturally, Lambert could not foresee the extraordinary developments in mathematics and in physics that have taken place in the last century. Nor could he foresee the technological advances in the lighting art which have given rise to so many new problems. Thus there is need for further work on this subject (which may be called *geometric photometrics*) to give a more exact and more unified treatment. Photometrics should be developed as a complete discipline, with methods of the greatest generality from which all special cases can be derived. There is nothing of the kind at present. Since the time of Lambert, hundreds of books have been published on the lighting art but not one has given a comprehensive treatment of photometrics.

Though the goal is still in the future, recent years have seen numerous improvements in the theory of illumination calculations. I shall attempt to evaluate these contributions and show where they fit into the general picture of photometrics. In some places it will be necessary to state some of the older results, but the emphasis will be on developments that have been made during the last five years.

2. BASIC METHODS

The subject of geometric photometrics treats of the geometric relations among various quantities. If radiant power is taken as a starting point, photometrics considers related quantities such as radiant power per unit area and radiant power per unit solid angle.[2] Or the radiant power may equally well be evaluated with respect to a receptor, such as a photo-cell, a photographic emulsion, or the eye. In the last case, one obtains everything in terms of lumens instead of watts. The point to be emphasized is that *the equations of photometrics are exactly the same, irrespective of what is taken as the basic quantity.*[3] It is customary to use photometric quantities throughout, but the subject applies equally well to radiometric quantities.

The fundamental concept will therefore be taken as luminous flux F, expressed in lumens and analogous to radiant power. It is also convenient to talk of luminous flux density D, expressed in lumens per square meter. There is a third concept[3] called *helios* H (a generalization of the ordinary idea of brightness). Helios is a scalar function of 5 independent variables, 3 specifying the position of a point P and the remaining 2 specifying a direction. It is defined by the equation,

$$H=\pi \lim_{\omega\to 0} \frac{D}{\omega}, \tag{1}$$

where D is the flux density on a surface that is normal to the given direction. The solid angle ω refers to the convergent light cone having its apex at P and its axis in the given direction.

From Eq. (1) is obtained directly the basic method of calculating illumination, for

$$dD=(H/\pi)d\omega.$$

* Paper presented at Twenty-Seventh Annual Meeting of the Optical Society of America, New York, New York, October 30–31, 1942.

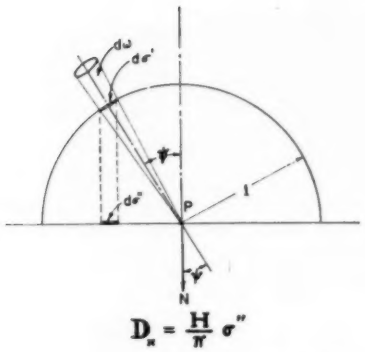

FIG. 1. The solid-angle method of calculating illumination.

Thus the flux density on any surface is (Fig. 1)

$$dD_N = (H/\pi)d\omega \cos\psi = (H/\pi)d\sigma''. \quad (2)$$

If the luminous source is an extended one,

$$D_N = \frac{1}{\pi}\int_S H d\sigma'' \quad (3)$$

and if H=const., the usual equation of the "unit-sphere method" is obtained:

$$D_N = \frac{H}{\pi}\int_S d\sigma'' = \frac{H}{\pi}\sigma''. \quad (4)$$

For two-dimensional problems, the analogous "unit-cylinder" method (Fig. 2) gives, for H=const.,

$$D_N = \frac{H}{2}s''. \quad (5)$$

It is often convenient to have general expressions which apply to any helios distribution and any tilted surface,[4] and it is found that spherical trigonometry plays an important role. Figure 3 shows an arbitrarily tilted surface at P, with normal N, illuminated through an elementary light cone at Q. The flux density at P is, by spherical trigonometry,

$$\frac{H}{\pi}[\cos\xi\cos\theta\sin\theta + \sin\xi\cos\eta\sin^2\theta\cos\varphi + \sin\xi\sin\eta\sin^2\theta\sin\varphi]d\theta d\varphi.$$

If the light cone is of finite size the flux density is

$$D_N = D_x\sin\xi\cos\eta + D_y\sin\xi\sin\eta + D_z\cos\xi, \quad (6)$$

where

$$\left.\begin{aligned} D_x &= \frac{1}{\pi}\int\int H\sin^2\theta\cos\varphi d\theta d\varphi, \\ D_y &= \frac{1}{\pi}\int\int H\sin^2\theta\sin\varphi d\theta d\varphi, \\ D_z &= \frac{1}{\pi}\int\int H\cos\theta\sin\theta d\theta d\varphi. \end{aligned}\right\} \quad (7)$$

Thus the flux density on any tilted surface is easily obtained in terms of the three quantities D_x, D_y, and D_z, which may be considered as components of a flux-density vector **D**.

3. ILLUMINATION FROM UNIFORM SOURCES

Equations (6) and (7) have been applied to the calculation of illumination from sources of various shapes, the most useful of which is probably the rectangular. Figure 4 indicates the shape of figure cut from the unit sphere by a light cone determined by a rectangular window subtending the angles β and γ at point P. If H=const., Eq. (7) gives

$$\left.\begin{aligned} D_x &= \frac{H}{2\pi}[\gamma - \gamma_1\cos\beta], \\ D_y &= \frac{H}{2\pi}[\beta - \beta_1\cos\gamma], \\ D_z &= \frac{H}{2\pi}[\beta_1\sin\gamma + \gamma_1\sin\beta], \end{aligned}\right\} \quad (8)$$

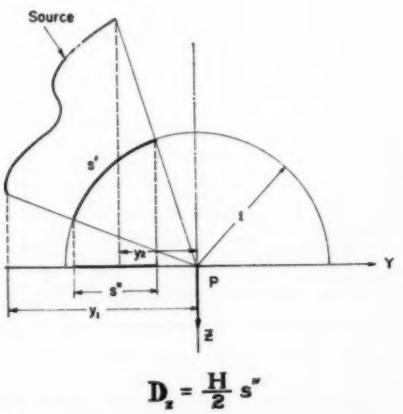

FIG. 2. The two-dimensional problem.

where

$$\tan \beta_1 = \tan \beta \cos \gamma,$$
$$\tan \gamma_1 = \cos \beta \tan \gamma. \tag{9}$$

Thus the flux density is expressed entirely in terms of the two angles β and γ. Results can be computed for easy use and can be plotted as shown in Fig. 5. Another method of presenting the results is shown in Fig. 6. Here each curve gives the complete illumination distribution curve along a perpendicular erected at a corner of the window. The curves thus have more definite significance than those of Fig. 5 and will therefore be found more useful to engineers and architects in the design of fenestrations and luminous architectural elements. Simple extensions give illumination distributions along other lines in the room.[11]

The general triangular source has also been investigated recently and formulas have been derived for the first time.[12] Nomograms have also been worked out to allow engineering calculations with the necessary facility. One may wonder why the triangular source should be investigated, since windows are not ordinarily made in this form. However, the subject is of the greatest practical importance, since it allows the calculation of illumination on tilted surfaces (drafting boards, for instance) the plane of which cuts the rectangular source.[12]

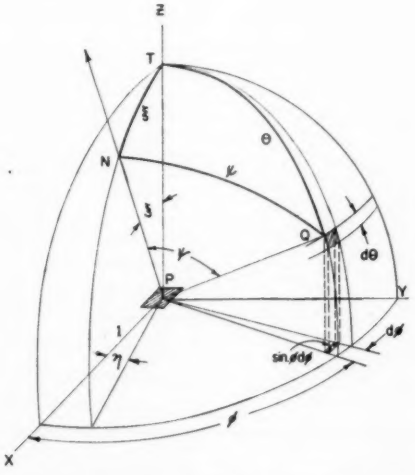

FIG. 3. Coordinate system for illumination calculation.

4. ILLUMINATION FROM NON-UNIFORM SOURCES

Equations (6) and (7) apply also to non-uniform sources, but most applications of this kind are still to be done. One recent application, however, is to the illumination from an overcast sky.[15] Experimental data (Fig. 7) show that a completely overcast sky is far from uniform in helios and has its maximum helios at the zenith and minimum at the horizon. Within the limits of experimental error,

$$H(\theta) = H_0 + H_1 \cos \theta. \tag{10}$$

This formula has been substituted in Eq. (7) and applied to outdoor illumination on any surface tilted through the angle γ from the horizontal.[15] The resulting flux density from sky and ground is

$$D_N = \frac{D_u}{14\pi}\{\pi(3+11\rho) + [11\pi(1-\rho) - 8\gamma]\cos\gamma + 8\sin\gamma\}, \tag{11}$$

where D_u = flux density on an unobstructed horizontal surface, ρ = reflection factor of the ground. Typical curves are shown in Fig. 8.

The distribution of Eq. (10) has also been used in calculating indoor illumination through a rectangular window,[15] giving

$$\left.\begin{aligned} D_x &= \frac{D_u}{14\pi}[(3\gamma+4) - (3\gamma_1+4)\cos\beta \\ &\qquad - 4\cos\gamma(1-\cos\beta)], \\ D_y &= \frac{D_u}{14\pi}[(3\beta+4\zeta) \\ &\qquad - (3\beta_1+4\sin\gamma\sin\beta_1)\cos\gamma], \\ D_z &= \frac{D_u}{14\pi}[3(\beta_1\sin\gamma+\gamma_1\sin\beta) \\ &\qquad + 4(\sin\beta - \cos^2\gamma\sin\beta_1)], \end{aligned}\right\} \tag{12}$$

where $\zeta = \sin\beta\sin\gamma$. Typical curves are shown in Fig. 9. It can be shown that the older assumption of fictitious skies of uniform helios leads to results that are often markedly different from experimental results with overcast skies. The percent error caused by the assumption becomes greater as the distance from the window increases and may easily exceed 50 percent.[15]

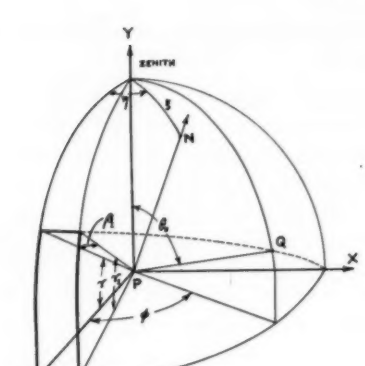

FIG. 4. The rectangular source.

5. ILLUMINATION FROM ARRAYS OF SOURCES

A method of lighting which has become popular since the advent of the fluorescent lamp employs long luminaires (called *troffers*) built into the ceiling (Fig. 10). The illumination distribution from such a system of troffers has been calculated ordinarily by the rather haphazard method of calculating the effect of each source separately and adding the results.[20] Recently, general formulas have been derived.[22] A comparison of calculated values brings out the important conclusion that, for the dimension range used in practice, the troffer system can be imagined replaced by an equivalent uniform ceiling and *the error caused by this approximation does not exceed a few tenths of one percent.*[22] Thus the arduous calculations formerly used can be replaced by the simple curves developed for the uniform rectangular source. The same method has been applied to two-dimensional arrays of ceiling sources and to uniformly spaced windows in the walls.[23]

6. THE LIGHT FIELD

Field theory, which has proved to be such a powerful tool in many branches of physics, has been applied to illumination calculations, notably by Fock and by Gershun.[24] It should be under-

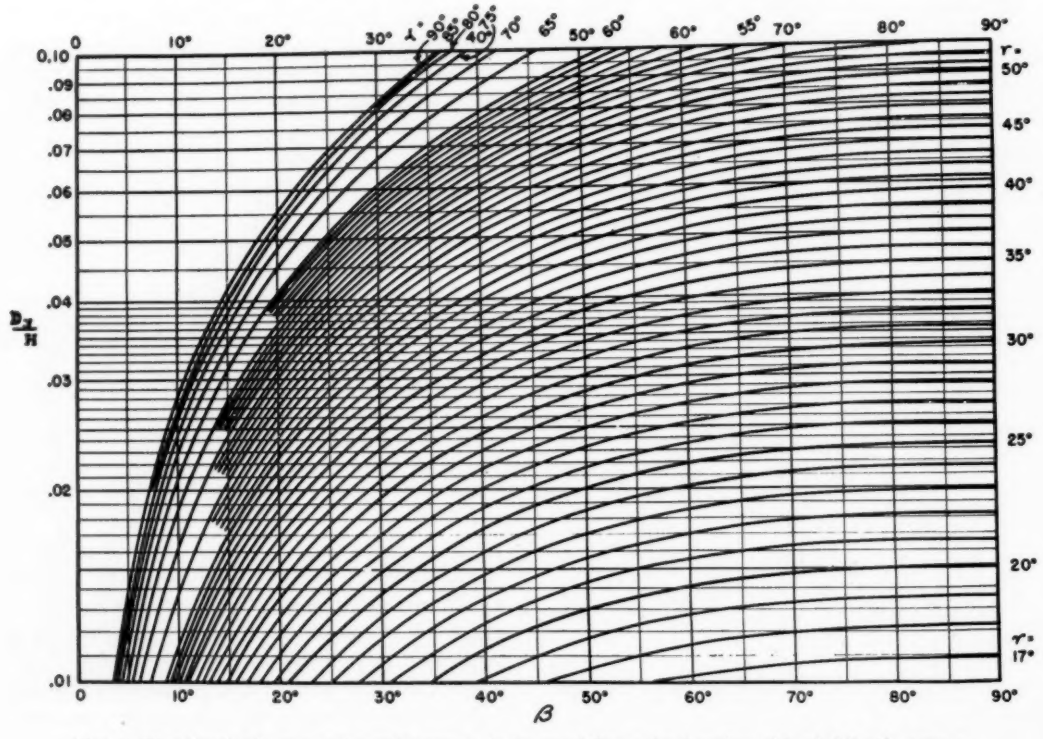

FIG. 5. Flux density from a rectangular source, in terms of the angles β and γ subtended by the source.

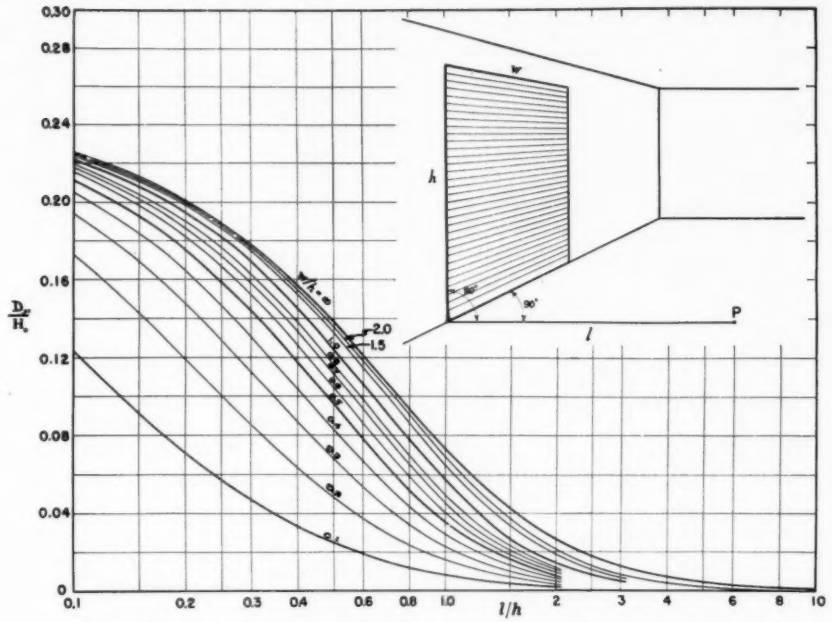

FIG. 6. Flux density from a rectangular window, in terms of window dimensions.

stood that this field theory has no connection with electromagnetic field theory, for we are dealing with a branch of geometrical optics, not physical optics. The theory of the light field is based on the introduction of a flux-density vector **D** similar to the flux-density vectors of electrostatics or magnetostatics. In fact, some illumination problems become identical with well-known electrostatic problems.[29] The light field produced by a uniformly luminous sphere, for instance, is the same mathematically as the electrostatic field from an isolated charged sphere; and the field from a plane of uniform helios is identical with the corresponding electrostatic case.

Thus one can consider a vector field in illumination calculations; and if the media are nondissipative, one can say immediately[25] that

$$\text{div } \mathbf{D} = 0. \tag{13}$$

In the simple cases mentioned above, it is evident

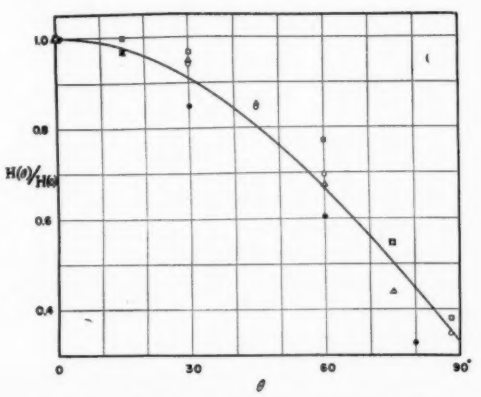

FIG. 7. Helios distribution for an overcast sky.

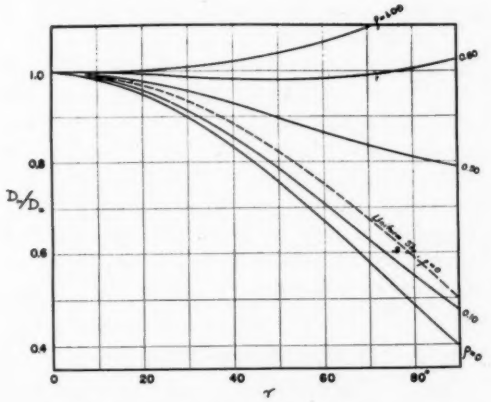

FIG. 8. Flux density on tilted surfaces outdoors.

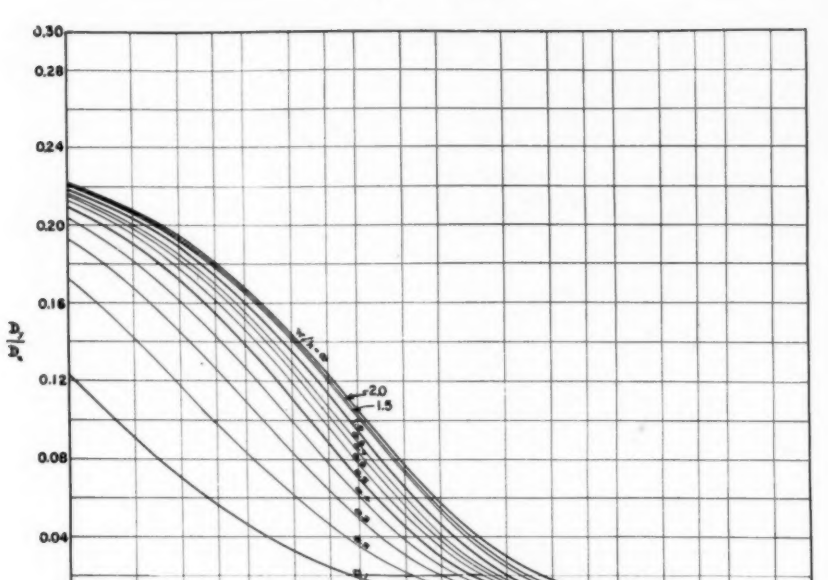

FIG. 9. Flux density from a rectangular window with overcast sky.

also that

$$\text{curl } \mathbf{D} = 0. \tag{14}$$

It is interesting to note, however, that Eq. (14) does not ordinarily apply in the light field. In electrostatics a point charge produces the same field strength in all directions, but an elementary light source has an intensity distribution that is completely arbitrary. This is the fundamental difference between the two fields, so in general the light field is not an irrotational one and no scalar potential exists.[28]

The vector potential has been used in some cases, but without much success. In fact, the idea of the light field, which seemed so promising when it was introduced, has led to no new results recently. One cannot help feeling that the whole scheme is an attempt to force illumination calculations into a mold in which they do not fit.[29] Perhaps the mathematicians can suggest a different kind of field theory which will be more in keeping with the behavior of light.

7. INTERREFLECTIONS

A phase of illumination calculation which has seen considerable recent activity is the subject

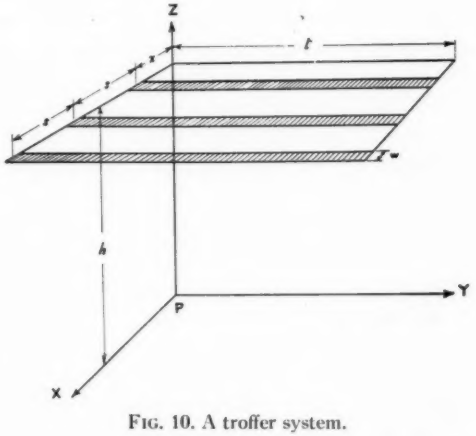

FIG. 10. A troffer system.

of multiple reflections of light in enclosures with perfectly diffusing walls. If the symmetry is sufficient so that the position of a point can be specified in terms of a single variable s, then the helios resulting from all interreflections is written in the integral equation,

$$H(s) = H_0(s) + \rho \int_a^b K(s, t) H(t) dt, \tag{15}$$

where

$H_0(s)$ = helios without interreflections,
ρ = reflection factor of wall,
$K(s, t)$ = kernel of the integral equation, depending on the geometry of the surface.

For example, the kernel for a spherical enclosure of radius a is

$$K(s, t) = 1/4\pi a^2;$$

for a circular cylinder of infinite length,

$$K(s, t) = \tfrac{1}{4} \sin \left| \frac{s-t}{2} \right|.$$

The sphere was solved by elementary methods years ago and the result is the theory of the familiar integrating sphere photometer. Interreflections between infinite parallel plates can also be calculated by elementary methods. Beyond these two simple cases, however, no interreflection problems could be solved except by crude approximations or by measurements made on scale models. In 1928 Buckley transformed this state of affairs by suggesting the use of integral equations;[30] and his work has been carried ahead by a number of investigators.

For the semi-circular cylinder of infinite length,[36] for instance, the calculated variation in helios is shown in Fig. 11. The result is an application of the Hilbert-Schmidt theory of integral equations, which leads to the interesting conclusion[36] that the kernel has an infinite number of eigenvalues, associated with which

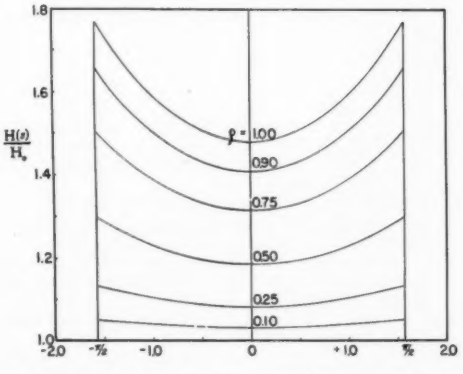

FIG. 11. Helios distribution in a semi-circular cylinder of infinite length.

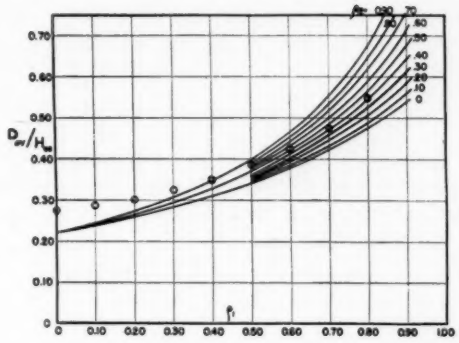

FIG. 12. Average flux density on a horizontal plane. Cubical room, ρ_1 = reflection factor of walls, ρ_2 = reflection factor of ceiling.

is one eigenfunction in the form of a hyperbolic cosine and a set of trigonometric eigenfunctions. The solution of the inhomogeneous equation is written by means of Schmidt's formula, and it is found that for engineering purposes all the terms but the first can be neglected. Thus the curves of Fig. 11 are essentially hyperbolic cosines. Various interreflection problems have also been handled by means of the cinema integraph.[39, 40]

From a practical standpoint, the most important recent development in this field has been the solution of the interreflection problem for the rectangular parallelepiped.[41] It gives for the first time a complete method of calculating the light distribution in rooms and lightwells.[42, 43] An example is given in Fig. 12, which shows the average flux density on a horizontal plane in a cubical room[44] as affected by the reflection factor ρ_1 of the walls and the reflection factor ρ_2 of the ceiling. There is a distinct practical need for the computation and convenient presentation of such results for engineering use. There is also need for the application of the integral equation method to other shapes of enclosures, such as the semi-circular tunnel and various luminaires and lightboxes containing fluorescent lamps.

The foregoing problems were all somewhat idealized so that H could be considered as a function of the single variable s. Magnusson[45, 46] appears to have been the first to apply the two-dimensional integral equation to interreflection problems. To date, analytical solutions have not generally been feasible, though integration by

means of Simpson's rule has given some interesting results. Here is another fruitful field for research.

8. SUMMARY

An attempt has been made to outline the present status of illumination calculations, with particular stress on the advances that have been made during the past five years. The ideal of photometrics as a complete, unified discipline is still far from realization, though recent developments bring the subject closer to that goal. A thorough treatment would include also such subjects as the calculation of light in optical systems and in scattering media. These subjects have not been mentioned in the present paper because they are treated elsewhere.[47, 48]

BIBLIOGRAPHY

(1) J. H. Lambert, *Photometria sive de mensura et gradibus luminis, colorum et umbrae* (1760).
(2) Parry Moon, "The names of physical concepts," Am. J. Phys. **10**, 134 (1942).
(3) Parry Moon, "A system of photometric concepts," J. Opt. Soc. Am. **32**, 348 (1942).
(4) A. C. Stevenson, "On the mathematical and graphical determination of direct daylight factors," Proc. C. I. E. p. 1167 (1931).
(5) J. Dourgnon, "Eléments théoriques de la photométrie," Rev. Gen. de l'Elec. **41**, 619 (1937).
(6) J. Dourgnon, "Quelques remarques sur la photometrie visuelle et la colorimétrie," Bull. Soc. Franç. Elec. **8**, 887 (1938).
(7) F. Benford, "Illumination from extended sources computed by the theory of the integrating sphere," J. Opt. Soc. Am. **30**, 33 (1940).
(8) F. Benford, "Note on illumination characteristics of the camera lens," J. Opt. Soc. Am. **27**, 286 (1937).
(9) P. Satche, "Sur le problème fondamental de la photométrie géométrique," Rev. d'Optique **18**, 20 (1939).
(10) A. Gershun, "A photometric invariant," C. R. (Doklady) de l'Acad. Sci. U. S. S. R. **18**, 31 (1938).
(11) Parry Moon, Discussion, Wartime Lighting Conference, St. Louis, Illum. Eng., Dec. 1942.
(12) D. E. Spencer, "Calculation of illumination from triangular sources," J. Opt. Soc. Am. **32**, 274 (1942).
(13) E. Elvegård and G. Sjöstedt, "The calculation of illumination from sun and sky," Illum. Eng. **35**, 333 (1940).
(14) L. A. Jones and H. R. Condit, "Brightness scale of exterior scenes and the computation of correct photographic exposures," J. Opt. Soc. Am. **31**, 651 (1941).
(15) P. Moon and D. E. Spencer, "Illumination from a non-uniform sky," Illum. Eng. **37** (1942).
(16) H. H. Higbie, "Illumination distribution from surface sources in rooms," Illum. Eng. **31**, 163 (1936).
(17) Cherry, Davis and Boelter, "A mechanical integrator for the determination of the illumination from diffuse surface sources," Illum. Eng. **34**, 1085 (1939).
(18) E. H. Wakefield, "A simple graphical method of finding illumination values from tubular, ribbon, and surface sources," Illum. Eng. **35**, 142 (1940).
(19) B. F. Greenberg, "A device for the determination of illumination," Illum. Eng. **35**, 629 (1940).
(20) H. H. Higbie, "Prediction of illumination at a point from source of any shape," Illum. Eng. **36**, 79 (1941).
(21) W. M. Armstrong, "Nomograms for routine illumination computations," Illum. Eng. **36**, 503 (1941).
(22) D. E. Spencer, "Exact and approximate formulae for illumination from troffers," Illum. Eng. **37** (1942).
(23) D. E. Spencer, "Illumination from arrays of rectangular sources," J. Opt. Soc. Am. **32**, 539 (1942).
(24) A. Gershun, *The Light Field* (Moscow, 1936). English translation by Moon and Timoshenko, J. Math. Phys. **18**, 51 (1939) M. I. T., E. E. Dept. Contr. No. 164 (1939).
(25) A. Gershun, "Sur une théorie du champ lumineux," Rev. Gen. de l'Elec. **44**, 307 (1938).
(26) A. Blondel, "Complément à la critique de la théorie du champ lumineux," Rev. Gen. de l'Elec. **44**, 312 (1938).
(27) G. W. O. Howe, "The field of luminous flux," El. Rev. **123**, 679 (1938).
(28) J. Dourgnon, "Remarques sur l'usage pratique de la photométrie vectorielle," Rev. Gen. de l'Elec. **45**, 437 (1939).
(29) Parry Moon, "Basic principles in illumination calculations," J. Opt. Soc. Am. **29**, 108 (1939).
(30) H. Buckley, "The blackness of blackbodies and the illumination of lightwells," J. Opt. Soc. Am. **18**, 216 (1929).
(31) Z. Yamauti, "On the blackness of cylindrical blackbody," Res. Elec. Lab., Tokyo, No. 378 (1934).
(32) Z. Yamauti, "Etude analytique des "interréflections" dans un cylindre de longeur infinie," Comptes rendus Congrès Int. des Appl. l'Eclairage (Paris, 1937), p. 144; Rev. Gen. de l'Elec. **42**, 293 (1937).
(33) K. Hisano, "Light flux distribution in a rectangular parallelepiped and its simplifying scale," Res. Elec. Lab., Tokyo, No. 394 (1936).
(34) K. Hisano, "Fundamental problems on daylight lighting," Res. Elec. Lab., Tokyo, No. 397 (1936).
(35) W. F. Whitmore, "Interreflections inside an infinite cylinder," J. Math. Phys. **17**, 218 (1939).
(36) Parry Moon, "On interreflections," J. Opt. Soc. Am. **30**, 195 (1940).
(37) R. S. Mabee, "Interreflections between two perpendicular plates," S.M. Thesis, M. I. T., 1940.
(38) E. Singleton, "Some interreflection problems," S.M. Thesis, M. I. T., 1940.
(39) W. R. Hedeman, Jr., "The numerical solution of integral equations on the cinema integraph," Sc.D. Thesis, M. I. T., 1939, pp. 151–200.
(40) W. R. Hedeman, Jr., "The cinema integraph in interreflection problems," J. Math. Phys. **20**, 402 (1941).
(41) Parry Moon, "Interreflections in finite cylinders," J. Opt. Soc. Am. **31**, 223 (1941).
(42) W. T. White, "Calculation of the light distribution in lightwells," J. Opt. Soc. Am. **31**, 308 (1941).
(43) Parry Moon, "Interreflections in lightwells," J. Opt. Soc. Am. **31**, 301 (1941).
(44) Parry Moon, "Interreflections in rooms," J. Opt. Soc. Am. **31**, 374 (1941).
(45) P. Magnusson, "Methods of solving linear inhomogeneous integral equations arising in interreflection problems," Sc.D. Thesis, M. I. T., 1941.
(46) P. Magnusson, "Numerical methods of solving integral equations in two independent variables," J. Math. Phys. (1943).
(47) A. C. Hardy, "Flux calculations in optical systems," invited paper, O. S. A. Annual Meeting, 1942.
(48) S. Q. Duntley, "The mathematics of turbid media," invited paper, O. S. A. Annual Meeting, 1942.